

---

Doctoral

Science

---

2014

## Effect of Nonthermal Plasma on Quality of Fresh Produce

Nrusimhanath Misra

*Technological University Dublin*

Follow this and additional works at: <https://arrow.tudublin.ie/sciendoc>



Part of the [Environmental Health Commons](#), and the [Food Science Commons](#)

---

### Recommended Citation

Misra, N. (2014) *Effect of Nonthermal Plasma on Quality of Fresh Produce*. Doctoral thesis, 2014.

This Theses, Ph.D is brought to you for free and open access by the Science at ARROW@TU Dublin. It has been accepted for inclusion in Doctoral by an authorized administrator of ARROW@TU Dublin. For more information, please contact [arrow.admin@tudublin.ie](mailto:arrow.admin@tudublin.ie), [aisling.coyne@tudublin.ie](mailto:aisling.coyne@tudublin.ie), [vera.kilshaw@tudublin.ie](mailto:vera.kilshaw@tudublin.ie).

# Effect of Nonthermal Plasma on Quality of Fresh Produce



Nrusimha Nath Misra

School of Food Science & Environmental Health

Dublin Institute of Technology

A thesis submitted for the degree of

*PHILOSOPHIAE DOCTOR*

July, 2014

# Effect of Nonthermal Plasma on Quality of Fresh Produce

Nrusimha Nath Misra

School of Food Science & Environmental Health  
Dublin Institute of Technology

*A thesis submitted for the degree of  
PHILOSOPHIAE DOCTOR*

July, 2014

Major Supervisor: Dr P.J. Cullen

Minor Supervisor: Dr Paula Bourke

External Examiner:

Prof (Emeritus) Brian McKenna,  
College of Life Sciences,  
University College Dublin, Ireland

Internal Examiner:

Dr Jesus Maria Frias Celayeta  
School of Food Science & Environmental Health,  
Dublin Institute of Technology, Ireland

## Abstract

Nonthermal technologies have evolved as alternatives to conventional food processing, which lead to poor quality products. Nonthermal plasma (NTP) technology has drawn considerable interest of researchers for decontamination of foods, especially fruits and vegetables. The use of atmospheric pressure NTP technology for the decontamination of fresh fruits and vegetables is an active area researched within the Bio-Plasma Group at Dublin Institute of Technology. The objective of this thesis was to characterise an in-package NTP source and investigate its effects on the physico-chemical quality characteristics of fresh produce.

Electrical diagnostics revealed that the dielectric barrier discharge (DBD) based NTP source operates in filamentary regime and the use of high voltages (up to 80 kV) render stability to the discharge, even at large gaps in the order of the centimetre scale. The optical emission spectroscopy (OES) revealed presence of several excited nitrogen species, and relatively lower levels of singlet oxygen and hydroxyl radicals. The plasma source also generates high amounts of ozone. The discolouration of methylene blue dye in a plasma field suggested that this can be used as a rapid means to evaluate the ozone generation, especially for short treatment durations.

The physico-chemical quality attributes of cherry tomatoes and strawberries were evaluated. Cold plasma treatment did not adversely affect the quality parameters of colour, pH, and texture of cherry tomatoes. A slight increase in respiratory rate following cold plasma treatments was evident for cherry tomatoes and strawberries. The effect of NTP

generated in air on strawberry colour and firmness was insignificant. Use of modified atmosphere gases for plasma treatment of strawberries was also explored and changes in colour and firmness were evident. A time and voltage dependent inactivation of peroxidase enzyme in tomato extracts and whole strawberry fruits was also observed. The enzyme inactivation kinetics was found to follow a sigmoidal logistic model.

The changes in chemical profile of plasma treated strawberries was studied using FTIR and some changes were evident. Further studies were carried out to quantify the changes in anthocyanin and ascorbic acid content. Changes were evident at 80 kV treatment voltages. Head space gas analysis using solid-phase micro-extraction followed by gas chromatography coupled to mass spectrometry (GC-MS) revealed absence of some volatiles in the strawberries. However, the dominant esters responsible for strawberry aroma were retained.

The NTP treatment allowed to rapidly dissipate residues of pesticide on strawberry by significant ( $p < 0.05$ ) levels. The degradation kinetics was modelled using first-order rate equation. Therefore, the technology was concluded to contribute to not only microbiological, but also chemical safety of foods.

Overall, this study suggests that in-package nonthermal plasma treatments can be employed for treatment of fresh foods, without adversely affecting their quality parameters.

# Declaration

I certify that this thesis which I now submit for examination for the award of Doctor of Philosophy, is entirely my own work and has not been taken from the work of others, save and to the extent that such work has been cited and acknowledged within the text of my work.

This thesis was prepared according to the regulations for postgraduate study by research of the Dublin Institute of Technology and has not been submitted in whole or in part for another award in any Institute. The work reported on in this thesis conforms to the principles and requirements of the Institute's guidelines for ethics in research.

The Institute has permission to keep, to lend or to copy this thesis in whole or in part, on condition that any such use of the material of the thesis is duly acknowledged.

Signature:

Date:

*To my family*

## Acknowledgements

- My sincere thanks goes to *Dr PJ Cullen* who gave me the great opportunity to work in his group, giving support and helpful discussions and also the freedom to follow various ideas.
- I wish to express my sincere thanks to *Dr Paula Bourke* for her constant encouragement, support and research strategies.
- Thanks are also due to *Prof Kevin Keener*, Purdue University and *Dr Sonal Patil* for helpful discussions. Special thanks to *Dr Jean-Paul Mosnier*, DCU for his insightful comments during manuscript preparation.
- A "big slice" of thanks goes to *Dr Carl Sullivan*, DIT for helping me pursue my interests in mathematical modelling, besides supporting my 'crazy' research ideas. Thanks to all the academic and technical staff of DIT for their assistance.
- I would like to acknowledge *Prof KSMS Raghavarao*, CSIR-CFTRI, Mysore and *Dr Brijesh Tiwari*, Teagasc, Dublin for their support during my PhD and the excellent cooperation.
- Thanks to *Prof (Emeritus) Brian McKenna*, University College Dublin and *Dr Jesus Frias*, DIT for their critical comments. I really enjoyed the very fruitful and thought provoking discussions with *Dr Jesus Frias*.
- I am grateful to the Irish Research Council (IRC) for awarding the Embark Initiative Fellowship and supporting my research work.
- This acknowledgement will not be complete without the mention of the role played by my research group members (*Dana, Lu, Tamara, Shashi, Carmen, Daniela, Vladimir*) for their friendship and support.



- Finally, I am grateful to my parents and brothers for their unconditional love, affection and support, and for letting me *into the wild*. I am equally grateful to my friends who always supported and encouraged my *wild activities*...!

# Contents

<b>Contents</b>	<b>iv</b>
<b>List of Figures</b>	<b>ix</b>
<b>List of Tables</b>	<b>xii</b>
<b>Nomenclature</b>	<b>xiv</b>
<b>1 Introduction</b>	<b>1</b>
1.1 Overview of the thesis . . . . .	3
<b>2 Review of Literature</b>	<b>8</b>
2.1 Quality of fresh produce . . . . .	8
2.2 Non-thermal Food Processing . . . . .	12
2.3 Fundamentals of Non-thermal Plasma . . . . .	13
2.3.1 Gas breakdown process . . . . .	15
2.3.2 Paschen's Law . . . . .	16
2.4 Nonthermal Plasma Sources . . . . .	17
2.4.1 Microwave Plasma . . . . .	18
2.4.2 Radiofrequency Plasma . . . . .	18
2.4.3 Corona Discharge . . . . .	18
2.4.4 Dielectric barrier discharge (DBD) . . . . .	19
2.4.5 UV Sustained Nonthermal Plasma . . . . .	20
2.4.6 Framework for Classification of NTP Applications . . . . .	20
2.5 Process Variables . . . . .	21
2.6 Plasma chemistry . . . . .	22

---

2.7	Plasma diagnostics . . . . .	23
2.7.1	Electrical Diagnostics . . . . .	23
2.7.2	Optical Diagnostics . . . . .	24
2.7.2.1	Optical Emission Spectroscopy (OES) . . . . .	24
2.7.2.2	Optical Absorption Spectroscopy (OAS) . . . . .	25
2.7.2.3	Mass Spectrometry . . . . .	25
2.8	Non-thermal plasma in food processing . . . . .	26
2.8.1	Treatment of raw fruits and vegetables . . . . .	32
2.8.2	Decontamination of seeds and nuts . . . . .	32
2.8.3	Surface decontamination of eggs . . . . .	34
2.8.4	Decontamination of meat, fish and poultry . . . . .	35
2.8.5	Decontamination of packaging materials . . . . .	36
2.8.6	NTP processing of fruit juices . . . . .	37
2.8.7	Processing of milk and milk products . . . . .	38
2.9	Effect of NTP on quality attributes of food . . . . .	38
2.9.1	Fresh fruits and vegetables . . . . .	38
2.9.2	Eggs . . . . .	40
2.9.3	Meat . . . . .	40
2.10	Effect on pesticide residues . . . . .	41
2.11	Advantages of NTP as a food technology . . . . .	42
<b>3</b>	<b>Materials and Methods</b>	<b>43</b>
3.1	The Nonthermal Plasma source . . . . .	43
3.2	Plasma Diagnostics . . . . .	44
3.2.1	Electrical Diagnostics . . . . .	44
3.2.2	Optical Diagnostics . . . . .	46
3.2.3	Measurement of ozone concentrations . . . . .	47
3.2.4	Dye discolouration for assessment of ozone levels . . . . .	47
3.2.4.1	Reagents and selection of dye concentration . . . . .	47
3.2.4.2	Plasma Treatments . . . . .	47
3.2.4.3	Absorption spectra of dyes . . . . .	48
3.2.4.4	pH measurement . . . . .	48
3.2.4.5	Mathematical Modelling . . . . .	48

---

3.3	Effect of NTP on quality of fresh produce . . . . .	49
3.3.1	Fresh Produce . . . . .	49
3.3.2	Produce density . . . . .	49
3.3.3	Plasma treatments . . . . .	50
3.3.4	Respiration rate . . . . .	51
3.3.5	Produce colour . . . . .	52
3.3.6	Firmness . . . . .	52
3.3.7	Weight loss, visual fungal and pH measurement . . . . .	53
3.4	Enzyme Inactivation Studies . . . . .	53
3.4.1	Reagents . . . . .	53
3.4.2	Plasma Treatment and Sample preparation . . . . .	54
3.4.2.1	Strawberries . . . . .	54
3.4.2.2	Cherry tomatoes . . . . .	54
3.4.3	Enzyme assay . . . . .	55
3.4.4	Peroxidase inactivation kinetics . . . . .	55
3.5	FTIR Spectroscopy & Chemometrics . . . . .	56
3.5.1	Produce . . . . .	56
3.5.2	Plasma treatment . . . . .	56
3.5.3	Sample preparation . . . . .	57
3.5.4	FTIR Analysis . . . . .	57
3.5.5	Data pre-processing . . . . .	57
3.5.6	Multivariate chemometric methods . . . . .	58
3.5.6.1	Correlation heatmap analysis . . . . .	58
3.5.6.2	Principal Component Analysis (PCA) and Hierarchical Clustering on PCs (HC-PC) . . . . .	59
3.6	Bioactive and Volatile profile . . . . .	59
3.6.1	Ascorbic acid content . . . . .	59
3.6.2	Anthocyanin content . . . . .	60
3.6.3	Volatile profile by HS-SPME/GC-MS . . . . .	61
3.7	Pesticide Degradation studies . . . . .	62
3.7.1	Produce . . . . .	62
3.7.2	Reagents . . . . .	62
3.7.3	Exposure of samples to pesticides . . . . .	62

---

3.7.4	Cold plasma treatment . . . . .	63
3.7.5	Analysis of pesticides . . . . .	63
3.7.5.1	Extraction procedure . . . . .	63
3.7.5.2	GC-MS/MS Analysis . . . . .	63
3.7.5.3	Calibration Curve . . . . .	64
3.7.6	Data Analysis . . . . .	64
3.8	Numerical methods and statistical analysis . . . . .	64
<b>4</b>	<b>Plasma diagnostics</b>	<b>66</b>
4.1	Electrical diagnostics . . . . .	66
4.1.1	I-V Characteristics . . . . .	66
4.1.2	Q-V Characteristics . . . . .	68
4.2	Ozone measurement . . . . .	70
4.3	Optical emission spectroscopy . . . . .	71
4.4	Dye discolouration for diagnostics . . . . .	72
4.4.1	Absorbance spectra of dye . . . . .	73
4.4.2	Kinetics of discoloration . . . . .	74
4.5	Change in pH . . . . .	76
4.6	Conclusions . . . . .	77
<b>5</b>	<b>Effect of nonthermal plasma on quality of cherry tomatoes</b>	<b>78</b>
5.1	Apparent density & free volume . . . . .	78
5.2	Respiration rate of cherry tomatoes . . . . .	79
5.3	Weight loss and visual fungal . . . . .	81
5.4	Changes in Instrumental colour . . . . .	83
5.5	Change in pH . . . . .	84
5.6	Fruit firmness . . . . .	85
5.7	Conclusions . . . . .	86
<b>6</b>	<b>Effect of nonthermal plasma on quality of strawberries</b>	<b>87</b>
6.1	Electrical characterisation . . . . .	87
6.2	Ozone concentrations . . . . .	89
6.3	Respiration Rate . . . . .	90
6.4	Strawberry Colour . . . . .	93

---

6.5	Firmness . . . . .	94
6.6	Conclusion . . . . .	94
<b>7</b>	<b>Enzyme Inactivation Studies</b>	<b>96</b>
7.1	Effect of voltage and treatment time . . . . .	96
7.2	First-order kinetic model . . . . .	97
7.3	Model based on Weibull distribution . . . . .	97
7.4	Logistic model . . . . .	99
7.5	Conclusion . . . . .	101
<b>8</b>	<b>Infrared spectroscopy of plasma treated strawberries</b>	<b>103</b>
8.1	Data pre-processing . . . . .	104
8.2	Spectral observations and group assignment . . . . .	104
8.3	Correlation heatmap analysis . . . . .	107
8.4	Principal Component Analysis . . . . .	108
8.5	Hierarchical Clustering on Principal Components (HC-PC) . . . . .	110
8.6	Conclusion . . . . .	112
<b>9</b>	<b>Effect on bioactives and volatiles</b>	<b>113</b>
9.1	Ascorbic acid content . . . . .	113
9.2	Anthocyanin content . . . . .	114
9.3	GC-MS Volatile Fingerprinting . . . . .	116
9.4	Conclusions . . . . .	122
<b>10</b>	<b>Degradation of Pesticides</b>	<b>124</b>
10.1	Ozone Concentration . . . . .	124
10.2	Quantification of pesticide residues and degradation kinetics . . . . .	126
10.3	Mechanism of Degradation . . . . .	127
10.4	Conclusion . . . . .	131
<b>11</b>	<b>Concluding Remarks &amp; Future Recommendations</b>	<b>132</b>
	<b>Publications</b>	<b>136</b>
	<b>References</b>	<b>141</b>

# List of Figures

1.1	Number of publications dealing with plasma technology, plasma-based microbial inactivation in general and with plasma-based microbial inactivation related to food during the last 23 years (Data accessed from web of science on 16 <sup>th</sup> April, 2014). . . . .	3
2.1	An overview of some commonly used quality criteria for fresh fruits and vegetables and their evaluation. . . . .	9
2.2	Classification of Food processing technologies with emphasis on their thermal and non-thermal nature . . . . .	12
2.3	Pictorial representations of the four states of matter. . . . .	14
2.4	Image of the <i>Aurora Australis</i> (non-thermal) and of a cloud to ground lightning strike (thermal) . . . . .	15
2.5	Breakdown potentials in different gases over a wide range of <i>pd</i> values. . . . .	16
2.6	Schematic of corona discharge set-up . . . . .	19
2.7	Schematic of a DBD set-up for in-package plasma . . . . .	20
2.8	Framework for the categorisation of NTP technology . . . . .	21
2.9	Constituents of plasma . . . . .	22
2.10	Survival curves <i>Aspergillus</i> spp. on seed surface . . . . .	33
2.11	TBARS measured in sliced bresaola packed in LLDPE bags and treated with NTP . . . . .	41
3.1	Experimental set-up of dielectric barrier discharge plasma with electrical and optical diagnostics. . . . .	44
3.2	The Q-V Lissajous characteristic curves for a DBD. . . . .	45

---

4.1	The I-V characteristics of the discharge in package. . . . .	67
4.2	The Q-V characteristics of the in-package plasma discharge. . . . .	68
4.3	Evolution of power input to the gas and the breakdown voltage as a function of applied voltage and dielectric thickness. . . . .	69
4.4	Ozone concentration inside package with methylene blue dye. . . . .	70
4.5	Typical Optical Emission Spectrum (OES) of the in-package non- thermal plasma discharge. Operating voltage- 50 kV (RMS). . . . .	72
4.6	Absorption spectra of methylene blue dye treated directly at 30 kV across the electrodes, after 24 h storage. . . . .	73
4.7	Experimental data and fitted lines for degradation kinetics of MB .	74
4.8	Time evolution of pH of MB dye following plasma treatments. . . . .	76
5.1	Respiration rates of control and plasma treated cherry tomatoes at 22°C. . . . .	81
5.2	Weight loss of cherry tomatoes during storage. . . . .	82
5.3	Total Colour Difference between control and treated tomatoes at the end of the storage period. . . . .	83
5.4	pH of control and treated tomatoes. . . . .	84
5.5	Firmness (force at break, N) of control and treated tomatoes. . . . .	85
6.1	(a) The I-V characteristics of discharge in an empty package and (b) package containing strawberries in ambient air. . . . .	88
6.2	Respiration rate of control and plasma treated strawberries in terms of carbon dioxide released and oxygen consumed. Ox and Cd refer to oxygen and carbon dioxide gases respectively; C and P refer to control and plasma treated respectively; G1, G2 same as in Table 6.2.	92
6.3	L*-a*-b* colour parameters of untreated control and ACP treated strawberries, both after 24 h storage. . . . .	93
7.1	Weibull model curve fitting at different voltage levels for POD resid- ual activity . . . . .	99
7.2	Logistic model curve fitting at different voltage levels for POD resid- ual activity. . . . .	100



---

8.1	Average FTIR Spectra & Group Assignment . . . . .	105
8.2	Comparison of FTIR spectra of strawberry with glucose and fructose obtained from NIST database. . . . .	105
8.3	Contour plot of raw spectra for all samples . . . . .	106
8.4	Correlation heatmap of the FTIR spectra . . . . .	107
8.5	PCA of second derivative spectra. . . . .	109
8.6	HC-PC of the raw data. Top: Cluster analysis on entire sample set. Bottom: Cluster analysis on sample set excluding blank samples. . .	111
9.1	Changes in ascorbic acid content of control and NTP treated strawberries (24 h post-treatment). . . . .	114
9.2	Anthocyanin content of control and plasma treated strawberries (24 h post-treatment). . . . .	115
9.3	Overlaid raw GC-MS chromatograms of the control and plasma treated strawberries. . . . .	117
9.4	PCA of the volatiles identified by SPME/GC-MS . . . . .	121
10.1	Chromatogram showing retention times of the pesticides. . . . .	126
10.2	Pesticide degradation Kinetics. . . . .	127
10.3	Proposed reaction products for Cyprodinil. . . . .	129
10.4	Proposed degradation pathway of Fludioxonil . . . . .	130

# List of Tables

2.1	Parameters used in the quality assessment of fresh fruits and vegetables. . . . .	10
2.2	Chemical classes of compounds in cultivated strawberry fruits . . .	11
2.3	Recent findings in the area of NTP inactivation of microorganisms .	27
4.1	Parameters of methylene blue degradation kinetics model . . . . .	75
5.1	Free volume of the package(s) and weight of cherry tomatoes . . . .	79
5.2	Regression coefficients of gas dynamics model . . . . .	80
5.3	The CIE-L*-a*-b* values of fresh, control and treated group of tomatoes. . . . .	83
6.1	Discharge electrical parameters derived from Q-V measurements. . .	88
6.2	Regression coefficients $K_1$ and $K_2(h)$ of the two parameter equations fitted to experimental data for O <sub>2</sub> consumption and CO <sub>2</sub> evolution for strawberries. . . . .	91
7.1	Results on the parameters of the models fitted to inactivation kinetics of POD enzyme. . . . .	98
9.1	HS-SPME-GC-MS analysis of volatile compounds in control and plasma treated strawberries. . . . .	118
10.1	Summary of the pesticides studied. . . . .	125
10.2	Model parameters for pesticide degradation based on first-order kinetics. . . . .	128

# Nomenclature

## Greek Symbols

$\alpha$  scale factor

$\gamma$  shape parameter

$\rho$  density, kg/m<sup>3</sup>

$\pi$   $\simeq 3.14\dots$

## Subscripts

0 initial

*adj* adjusted

*cell* discharge cell

*d* dielectric

*e* Napier's constant

*exp* experimental

*gap* inter electrode gap

*min* minimum

*org* original

*p* peak

*ref* reference

### **Acronyms**

**r** correlation coefficient

*A* absorbance

*C* capacitance

*C*<sup>\*</sup> chroma

*d* distance

*h*<sup>\*</sup> hue

*K*<sub>*p*</sub> rate constant

*P* power

*p* pressure

*Q* charge

*RA* residual activity

*RMSE* root mean square error

*t* time

*TI* Tomato index

*W* weight

*V* voltage

# Chapter 1

## Introduction

Consumer demands for high-quality foods with "fresh-like" and additive free characteristics that require minimum effort and time for preparation have led to the development and rise of minimally processed foods. But minimally processed fresh products have a relatively short shelf-life, due to increased metabolism and microbial spoilage. Physiological and biochemical changes in such products occur at a faster rate than in intact fruits resulting in the rapid onset of enzymatic browning. Fresh fruits and vegetables in recent times are often associated with microbial safety concerns. Several large scale food-borne illness outbreaks have been recorded within past few years. For example, recently, fresh, whole cantaloupes from Colorado-based Jensen Farms in USA were linked to a multistate outbreak of *Listeria monocytogenes* infections (listeriosis) from August through October 2011 [FDA \[2012\]](#). Yet another incident arose within Europe, where *Escherichia coli* O104:H4 bacteria caused a serious outbreak of food-borne illness focused in northern Germany in May through June 2011 [[Kennedy, 2012](#)].

Ensuring safe and quality food has become a more challenging task today than at any point of time in history. New risks are being encountered because of changing characteristics of the relevant micro-organisms, changing production methodologies, changes in the environment and the ecology, and an increase in the global trade of food stuffs [[Havelaar et al., 2010](#)]. As consumer demands and food safety issues have changed, so have the food processing technologies to ensure food safety [[Gould, 2001](#)]. Moreover, there are multiple issues relating to the

quality of thermally processed foods such as nutritional losses and adverse effects on organoleptic quality. Modern food processing technologies on one hand deal with further development of traditional methods, e.g. high-temperature short time (HTST) heating or vacuum cooking, while on the other hand with technologies that have been adopted from different industry-branches and adapted to food processing, e.g. extrusion, microwave-technology or high pressure-treatment.

Consumer demands and short comings of the existing technologies triggered the need for the development of "non-thermal" approaches to food processing [Sampedro et al., 2005]. Non-thermal technologies are preservation treatments that are effective at ambient or sub-lethal temperatures, thereby minimizing negative thermal effects on nutritional and quality parameters of food [Tiwari et al., 2009b]. These include the application of gamma irradiation, beta irradiation (electron beam), power ultrasound, ozonation, pulsed light, UV treatment, pulsed electric field (PEF), high hydrostatic pressure etc. However, some of these commercially viable methods are limited in practice due to associated adverse perceptions (e.g. gamma irradiation and high energy electron beams) or high initial investments required and/or other constraints. Purely physical techniques, such as high hydrostatic pressure, are chemically safe but require complex or expensive equipment [Rastogi et al., 2007], affect the quality of the product [Kruk et al., 2011] and are generally incompatible with online treatments. Only few approaches are suitable for treatment of solid foods, in particular fruit and vegetables. Very recently Nonthermal Plasma (NTP) has been added to the existing list of non-thermal processes for the decontamination of fresh produce [Critzler et al., 2007; Lee et al., 2006; Niemira and Sites, 2008].

Technologies like UV treatment, ozonation, power ultrasound, and pulsed light are commonly designated as Advanced Oxidation Processes (AOP). The use of pulsed UV light as a means of microbial inactivation is a mature technology that has commercial application in surface disinfection of packaging materials, but demonstrates limitations due to shadowing effects in food products [Gomez-Lopez et al., 2007]. Indeed, it is fair to say that there is currently no ideal method to achieve sterilization at ambient temperature. NTP or cold plasma technology, which has recently drawn considerable attention of food scientists and researchers [Basaran et al., 2008; Selcuk et al., 2008; Vleugels et al., 2005], has shown potential

for solid foods. This is evident from Figure 1.1 which shows the increase in the number of scientific publications concerning developments in NTP science and its applications towards, decontamination, in general, and foods in particular.

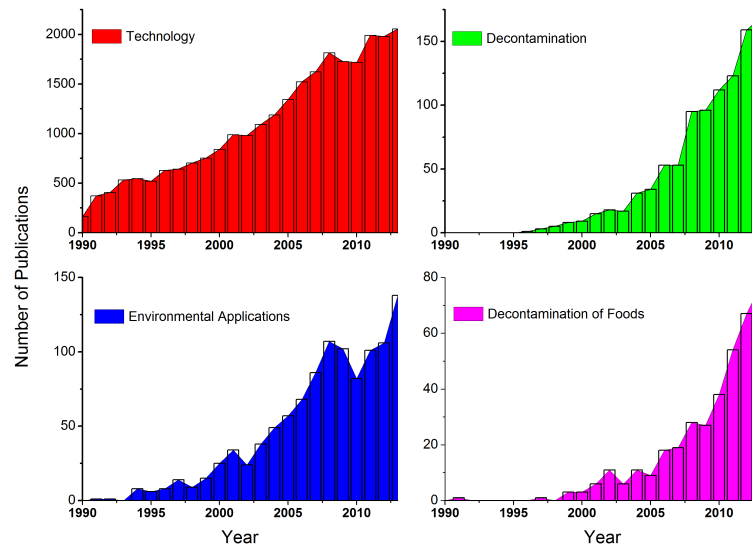


Figure 1.1: Number of publications dealing with plasma technology, plasma-based microbial inactivation in general and with plasma-based microbial inactivation related to food during the last 23 years (Data accessed from web of science on 16<sup>th</sup> April, 2014).

## 1.1 Overview of the thesis

The major benefits of nonthermal plasma technology are that it is a dry process, effective at low temperatures, requiring low energy input. The use of atmospheric pressure NTP technology for the decontamination of fresh fruits and vegetables is an active area researched within the BioPlasma Group at Dublin Institute of Technology. The group focuses on three major issues, the inactivation of food-borne pathogens, the changes to food quality, and properties of food packaging materials. The characterisation of the in-package NTP source and the effects of NTP treatments on the physico-chemical quality characteristics of fresh produce form the subject matter of this thesis. The structure of this thesis is outlined

below:

- In order to build or customise a plasma source for the decontamination or treatment of foods and/or optimise its performance, it is necessary to develop a sound understanding of the nonthermal plasma technology. The fundamentals of nonthermal plasma technology- its physics and chemistry, the plasma sources and diagnostics of plasma have been reviewed in **Chapter 2**. A summary of the scientific reports regarding food-borne pathogen inactivation with NTP and the effects on food quality are provided here. There is a paucity of data in the literature on the possible changes in food quality parameters induced by non-thermal plasma treatments. A clear research gap, especially in the context of quality changes in non-thermal plasma treated fresh produce has been identified. In order to fill this gap, the main focus of this thesis is to study the effect of in-package plasma treatments on quality characteristics of selected fresh produce (cherry tomatoes and strawberries).
- The materials and methods employed for the experiments, and the details of the data analysis procedures are described in detail in **Chapter 3**.
- To understand the behaviour of a plasma source and to explain the cause of any observed changes in foods or the effect on micro-organisms and/or for the optimisation of a plasma process, an understanding of the characteristics of the source is required. Therefore, the first objective of this work includes characterisation of the DBD plasma source, both electrically and optically. The electrical characterisation aims at identifying the regime in which NTP source operates- arc, filamentary or glow and the Q-V Lissajous parameters of the DBD. The optical characterisation includes the use of optical emission spectroscopy. In addition, chemical methods for characterisation of the reactive species generated by plasma are also exploited. For the optimisation of the process, a cheaper and simpler method for assessment of the non-thermal plasma effects is desirable. In order to address this requirement, methylene blue dye was selected as a model indicator for the in-package plasma treatment. Methylene blue is commonly used as a redox indicator in analytical chemistry. The relation between process variables and the discolouration of dye is mathematically modelled. **Chapter 4** presents the



results of electrical, optical and chemical diagnostics of the dielectric barrier discharge (DBD) plasma set-up. In addition, the dye discolouration studies as a means to diagnose the efficacy of the plasma source are also presented here.

- The changes in the quality parameters of cold plasma treated cherry tomatoes are presented in **Chapter 5**. The quality parameters reported include the evaluation of fruit colour, firmness, weight loss, pH change and respiration rate over a storage period of 13 days. The plasma treatments for this study were conducted using a plasma source powered from a 60 kV transformer. The nature of this plasma source (floating potential configuration) did not allow measurements of electrical parameters in the laboratory.
- **Chapter 6** presents the results of quality studies on nonthermal plasma treated strawberries. The quality parameters reported for strawberries include the evaluation of fruit colour, firmness and respiration rate. When designing the experiments for this chapter it was noted that most studies to date regarding cold plasma decontamination of plant produce report on the use of a noble gases such as argon [Baier et al., 2013; Bermúdez-Aguirre et al., 2013] or common diatomic gases such as nitrogen [Fernandez et al., 2013], oxygen [Klockow and Keener, 2009] and/or air [Critzler et al., 2007; Klockow and Keener, 2009; Niemira and Sites, 2008]. In the food industries, however, it is a common practice to use various gas mixtures in food packages for extension of shelf-life and quality, also known as modified atmosphere packaging (MAP). Modified atmosphere refers to any atmosphere different from normal air (20-21% O<sub>2</sub>, 78-79% N<sub>2</sub>, 0.03% CO<sub>2</sub>, and trace gases) [Elhadi, 2009]. There are no studies in literature reporting attainment of cold plasma state in MAP gases for treatment of fresh produce. Therefore, in order to explore the possible potential benefits, in addition to air, experiments have also been conducted with two common MAP gases, 65% O<sub>2</sub> + 16% N<sub>2</sub> + 19% CO<sub>2</sub> ( $\pm 1\%$ ) and 90% N<sub>2</sub> + 10% O<sub>2</sub> ( $\pm 1\%$ ) for in-package plasma treatment of strawberries. Besides the quality studies, the electrical characterisation of the plasma discharge in the three gases in presence and absence of strawberries is also presented.

- Based on the results obtained from quality studies in air and MAP gases (**Chapter 6**), it was observed that the fruit quality is retained well with air plasma compared to MAP gases. Therefore all further studies in the thesis were carried out using air as the inducer gas for the nonthermal plasma.
- Unlike research for food-borne pathogen inactivation, no studies have been conducted to this end to evaluate the effect of DBD plasma on enzymes from fruit or vegetable sources. Therefore, (i) evaluation of the effects of atmospheric pressure DBD based NTP process variables on the activity of peroxidase enzyme and (ii) modelling the kinetics of enzyme activity is also an objective of this work. **Chapter 7** presents the results and discussion for inactivation of enzymes using NTP and its mathematical modelling. The treatments were carried out for crude enzyme extracts of tomato and whole fruits of strawberry, to evaluate the tomato peroxidase and strawberry peroxidase activity.
- In order to obtain information about the chemical changes in plasma treated strawberries, the use of Fourier transform infrared (FTIR) spectroscopy and chemometrics was explored, as presented in **Chapter 8**. While FTIR spectroscopy and chemometrics allowed to conclude that there were chemical changes among control and plasma treated strawberries, it did not provide information about the functional groups that were changes actually occurred.
- In order to explore the chemical changes occurring in the strawberries following plasma treatments, two most important bioactives, namely ascorbic acid and anthocyanin were selected and their concentrations quantified by liquid chromatographic methods. Furthermore, the changes in the volatile profile of the plasma treated strawberries was also quantified using head space sampling and gas chromatography- mass spectrometry. The effect of nonthermal plasma on the bioactive and volatile profile of the strawberries is presented in **Chapter 9**.
- Pesticide residues on fresh produce are chemical contaminants and pose health risks when present in concentrations higher than those permitted by the regulatory bodies. Hence, a further objective of this thesis includes exploring the

feasibility of employing NTP treatments for dissipation of pesticide residues. The rapid dissipation of pesticide residues (viz. azoxystrobin, cyprodinil, fludioxonil and pyriproxyfen) on strawberries using NTP was also evaluated as an exploratory part of this work and the results are summarised in **Chapter 10**. Herein, the kinetics of pesticide degradation is modelled using a first-order rate equation and a mechanism for degradation of fludioxonil is proposed.

- In **Chapter 11**, a summary of the main results, the conclusions drawn and suggestions for future work are enlisted.

# Chapter 2

## Review of Literature

### 2.1 Quality of fresh produce

Food quality is a 'multi-faceted concept' for which consumers use both quality attributes and quality cues to form their assessment of perceived quality [Ophuis and Trijp, 1995]. Quality cues are observable product characteristics that can be intrinsic (e.g. appearance, colour, shape, size, structure) or extrinsic (e.g. price, brand, nutritional information, production information, country of origin). For the assessment of food quality, food scientists and engineers employ both subjective and objective methods. The former rely on quality perception by a group of individuals based on their senses, while the latter is based on use of instrumental methods for quantification of quality parameters. The quality parameters for fresh produce have been summarised in Figure 2.1, and broadly classify the parameters into physical, chemical and microbiological. In the context of fresh produce industry, an integration of handling steps from farm to retail is critical to the final quality. Apart from the nutritional viewpoint, the important physico-chemical parameters that are often employed for judging the quality of fresh fruits and vegetables include colour, texture/firmness, weight loss, pH, acidity, and respiration rate. These parameters have been summarised in Table 2.1. The respiration rate of fresh produce is an important factor in quality preservation. Respiration involves the oxidation of energy-rich organic molecules of the cells (such as starch, sugar and organic acids) to simpler molecules ( $\text{CO}_2$  and  $\text{H}_2\text{O}$ ), with the simultaneous

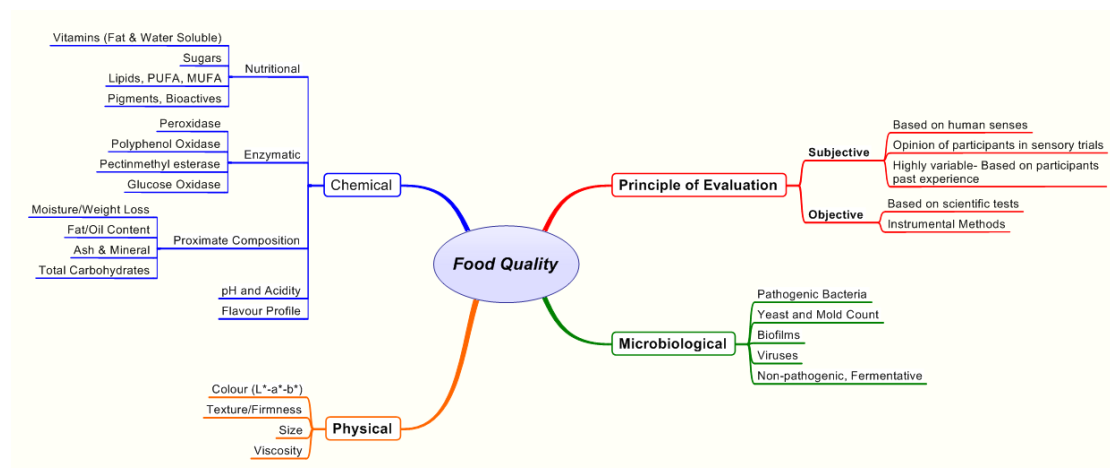


Figure 2.1: An overview of some commonly used quality criteria for fresh fruits and vegetables and their evaluation.

production of energy (in the form of ATP and heat) and other molecules. This energy is used by the cell for synthetic reactions. The rate of respiration is often a good index of the storage life of horticultural products- the higher the rate, the shorter the life; the lower the rate, the longer the life [Robertson, 2012]. Around 3-5% of the post-harvest weight loss of produce is accounted for by the escape of CO<sub>2</sub> from the cells. Storage conditions slow the physiological processes associated with ripening [Akbulak et al., 2007]. Improper control of the gas compositions in packaged fresh produce may lead to undesirable results such as anaerobic respiration, accelerated physiological decay, and shortened shelf life. The climacteric stage of most climacteric fruits generally coincides with changes associated with ripening such as colour changes, softening and increased tissue permeability [Robertson, 2012]. Diffusion of gases across the fruit boundary and loss of water vapours from the fruit occur either through aqueous/waxy layers of the epidermis or through gaseous pores [Kader and Saltveit, 2003].

The chemical and biochemical quality of fruits and vegetables includes their proximate composition, enzymatic activity, nutritional quality (including bioactives such as antioxidants, phenolics, natural pigments, organic acids), and also volatile flavour compounds. The important chemical classes of quality parameters have been summarised in Table 2.2 using Strawberry, a soft fruit, as an example.

Table 2.1: Parameters used in the quality assessment of fresh fruits and vegetables. Compiled from various sources [Clydesdale, 1993; Rico et al., 2007; Tzortzakis, 2007].

Parameter	Importance	Examples of changes	Measurement
<b>Colour</b>	Colour of fresh produce originates from natural plant pigments and is considered to have a key role in food choice, food preference and acceptability, and may even influence taste thresholds, sweetness perception and pleasantness.	Chlorophyll degradation and browning in lettuce, and carotene degradation, whiteness and browning in carrot.	Colour is measured using colorimeters, which record the amount of light reflected and expressed in units of colour space (L*-a*-b* values).
<b>Texture</b>	Fresh produce are often desired for their crispy/crunchy/juicy/ soft and easy-to-chew and swallow characteristics.	Produce loses its texture due to the activity of the enzymes such as pectin methylesterase (PME) and/or cell structure breakdown, and cell leakage.	Penetrometers measure the force required to penetrate a given depth into the produce, while texture profile analysers give complete texture profile.
<b>Acidity &amp; pH</b>	Organic acids play an important role in the sugar to acid ratio, which affects the flavour. Citric and malic acids are the most abundant in fruits.	The malic acid content of apples and pears decreases faster than the citric acid during maturation.	Acidity is usually measured by titration and expressed as equivalent citric acid for fruits and vegetables. A pH meter is used for measuring pH of the produce.
<b>Respiration</b>	Respiration involves the oxidation of energy-rich organic molecules of the cells (such as starch, sugar and organic acids) to simpler molecules (CO <sub>2</sub> and H <sub>2</sub> O), with the simultaneous production of energy (in the form of ATP and heat) and other molecules. The rate of respiration is often a good index of the storage life.	Improper control of the gas composition in packaged produce leads to undesirable anaerobic respiration, accelerated physiological decay, and shortened shelf life.	Gas analysers are used for measuring the oxygen and carbon-dioxide levels, from which respiration rate is calculated.
<b>Transpiration &amp; Weight Loss</b>	When respiring, the produce also releases water, which escapes from the produce: $C_6H_{12}O_6 + 6O_2 \rightarrow 6CO_2 + 6H_2O + \text{energy}$	~3-5% of the weight loss in produce is accounted by the escape of CO <sub>2</sub> from the cells.	Weight loss is expressed as percentage of initial weight of sample.

Table 2.2: Chemical classes of compounds in cultivated strawberry fruits, which dictate nutritional quality [Nielsen and Leufven, 2008; Pelayo et al., 2003; Vandriessche et al., 2013b; Zhang et al., 2011].

Chemical Class	Examples from Strawberry
Sugars and sugar alcohols	1-methyl- $\alpha$ -d-galactopyranoside, 1-methyl- $\alpha$ -d-galactopyranoside, glycerol, 2,6-di-methyl- $\alpha$ -d-galactopyranoside, 6-o-nonyl-glucitol, ribose, glucose, fructose, fructose, $\beta$ -d-glucopyranose, galactose, sorbit, gluco-hexodialdose, threitol, turanose, turanose, turanose, sucrose, turanose, palatinose
Dietary fibre and polysaccharides	pectins, gums, mucilages, cellulose, lignin, hemicellulose, starch
Amino Acids	serine, arginine, glutamic acid, histidine, aspartic acid, glycine, threonine, alanine, cystine, tyrosine, valine, methionine, lysine, isoleucine leucine, phenylalanine, and proline
Pigments	pelargonidin-3-o- $\beta$ -glucopyranoside, cyanidin-3-o- $\beta$ -glucopyranoside, peonidin-3-o- $\beta$ -glucopyranoside, malvidin--3-o- $\beta$ -glucopyranoside; all the above mentioned pigments are anthocyanins
Fatty Acids	n-hexadecanoic acid, 9, 12-(z, z)- octadecadienoic acid, octadecanoic acid, propanoic acid, 2,3,4-trihydroxybutyric acid, octadecanoic acid , n-hexadecanoic acid
Organic Acids	phosphoric acid, butanedioic acid, malic acid, 2-hydroxybutanoic acid, 5-hydroxymethyl-2-furoic acid, ethanedioic acid, arabinonic acid, xylonic acid, monoamidoethylmalonic acid, gluconic acid, pentonic acid, mannonic acid, 2-keto-d-gluconic acid, citric acid, 2-deoxyerythro-pentonic acid, d-glycero-l-manno-heptonic acid, 2-hydroxyethylsulfonic acid, gulonic acid, palmitic acid, 3,4,5-trihydroxypentanoic acid, allonic acid
Enzymes	polyphenol oxidase (ppo), peroxidase (pod), pectin methylesterase (pme), lipases
Minerals	calcium, magnesium, phosphorous, pottasium, sodium, zinc, copper, fluoride, iron, selenium, manganese

## 2.2 Non-thermal Food Processing

Non-thermal technologies can be defined as preservation treatments that are effective at ambient or sub-lethal temperatures, thereby minimizing negative thermal effects on nutritional and quality parameters of foods. According to [Min and Zhang \[2005\]](#), non-thermal processes are food preservation methods to inactivate spoilage and pathogenic microorganisms at temperatures below those used for thermal pasteurization, without significant changes to flavour, colour, taste, nutrients, and functionalities. Novel non-thermal processing technologies for food preservation have the potential to address the demands of the consumer and deliver high-quality processed foods with an extended shelf-life that are additive-free and have not been subjected to extensive heat treatment. Because of the relatively mild conditions of most non-thermal processes compared with heat pasteurization, consumers are often satisfied by the more fresh-like characteristics, minimized degradation of nutrients, and the perception of high quality.

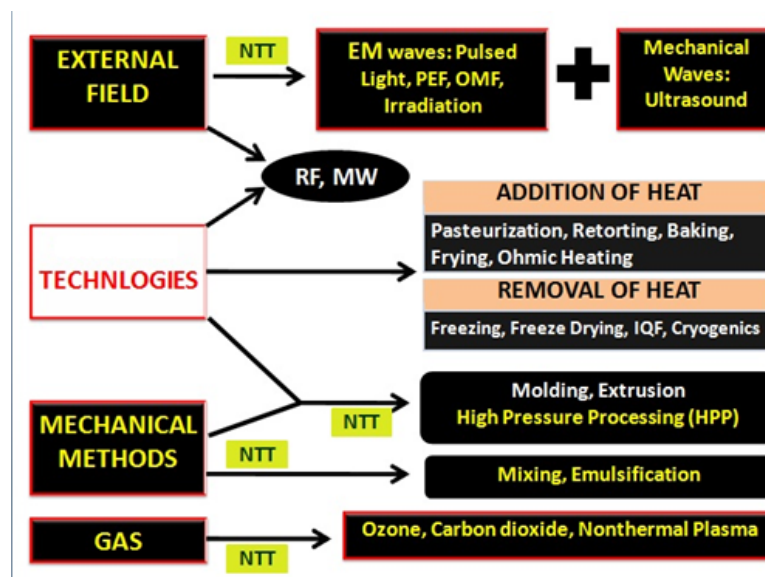


Figure 2.2: Classification of Food processing technologies with emphasis on their thermal and non-thermal nature. (EM = Electromagnetic, RF = Radio Frequency, MW = Microwaves, IQF = Individual Quick Freezing, NTT = Non-thermal Technologies, PEF = Pulsed Electric Fields, OMF = Oscillating Magnetic Fields). It may be noted that this is neither a universal classification framework, nor does it include all the food processing technologies.



The non-thermal food technologies currently known include, high pressure processing (HPP), irradiation, ultrasound, antimicrobials, membrane technology, ozonation and electrical methods such as pulsed electric fields (PEF), light pulses, oscillating magnetic fields (OMF), and very recently, nonthermal plasma. Figure 2.2 gives a broad classification of the various food processing technologies with emphasis on their thermal or non-thermal nature. The research and developments in non-thermal or cold processing technologies are mainly with the aim that undesirable micro-organisms, allergens and enzymes should be inactivated without damage to nutritional and sensory properties resulting normally from thermal treatment. To extend the use of non-thermal processing within the food industry, combinations of these technologies with traditional or emerging food preservation techniques have also been extensively studied. Combinations of HPP, PEF, ultrasonication with heat, different pH, antimicrobials, modified atmospheric packaging (MAP) etc have been researched and the results reported in the literature are mostly additive/synergistic, nevertheless, there are exceptions [Raso and Barbosa-Cánovas, 2003].

## 2.3 Fundamentals of Non-thermal Plasma

In 1922, the American scientist Irving Langmuir proposed that the electrons, ions and neutrals in an ionized gas could be considered as corpuscular material entrained in some kind of fluid medium and termed this entraining medium plasma, similar to the plasma (meaning formed or molded in Greek), introduced by the Czech physiologist Jan Evangelista Purkinje to denote the clear fluid which remains after removal of all the corpuscular material in blood. However, it emerged that there was no fluid medium entraining the electrons, ions, and neutrals in an ionized gas [Bellan, 2006], nevertheless the name prevailed.

The term plasma in its present context refers to a partially or wholly ionized gas composed essentially of photons, ions and free electrons as well as atoms in their fundamental or excited states possessing a net neutral charge. The plasma possesses a net neutral charge because the number of positive charge carriers is equal to the number of negative ones [Kudra and Mujumdar, 2009]. Electrons

and photons are usually designated as light species in contrast to the rest of the constituents designated as heavy species. Due to its unique properties plasma is often referred to as the fourth state of matter according to a scheme expressing an increase in the energy level from solid to liquid to gas and ultimately to plasma (Figure 2.3). Thus, any source of energy which can ionise a gas can be employed for generation of plasma.

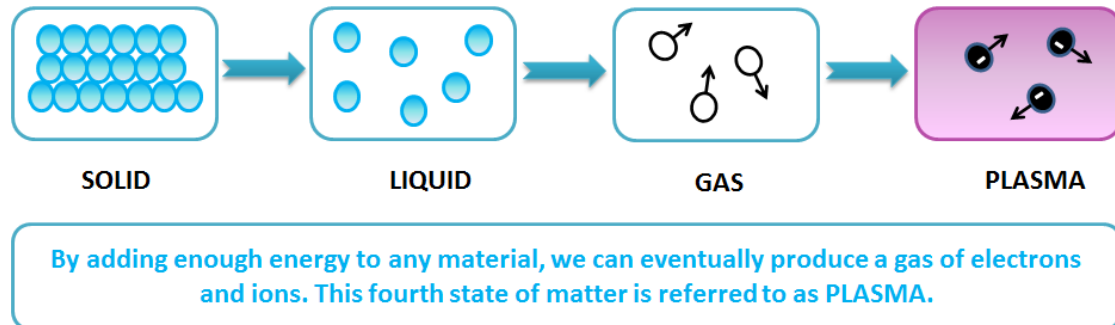


Figure 2.3: Pictorial representations of the four states of matter.

Two classes of plasma, namely thermal and NTP can be distinguished on the basis of conditions in which they are generated. Some examples of nonthermal and thermal plasma observed in nature include the *Aurora Borealis* (northern lights), *Aurora Australis* (southern lights) and all cloud to ground thunder strikes (Figure 2.4). This classification of plasma is based on the relative energetic levels of electrons and heavy species of the plasma.

NTP (near ambient temperatures of 30-60 °C) is obtained at atmospheric or reduced pressures (vacuum) and requires less power input. NTPs are characterised by an electron temperature much above that of the gas (macroscopic temperature) and consequently do not present a local thermodynamic equilibrium. NTP can be generated by an electric discharge in a gas at lower pressure or using microwaves. Typical illustrations for plasma generation at atmospheric pressure include corona discharge, Dielectric Barrier Discharge (DBD), Radio-Frequency Plasma (RFP) and the gliding arc discharge. In contrast, thermal plasmas are generated at higher pressures, require high power, and an almost thermal equilibrium exists between the electrons and the heavy species. In electrical discharge plasmas, electrons are usually first to receive the energy from an electric field and then distribute



Figure 2.4: On the left is an image of the *Aurora Australis* (non-thermal; Photo by Joseph M. Acaba, Astronaut, NASA) and on the right is an image of a cloud to ground lightning strike (thermal).

it between other components of plasma. Electrons accumulate the energy from the electric discharges following collisions and then they transfer a small fraction of this energy to the heavy particles. The reason for the transfer of only a small fraction of energy is that electrons are much lighter than heavy species.

### 2.3.1 Gas breakdown process

When an electric field is absent in atmospheric air under ambient conditions, the atoms, molecules, electrons and ions are in a state of equilibrium. This means that the rate of creation of charged particles is approximately balanced by the rate of recombination. When an electric field is applied across the gas, a small current is developed due to the already existing free electrons and ions. However, this current lacks the ability to disturb the equilibrium and the ion, electron mobilities are nearly constant. However, when the electric field and current density are increased, the equilibrium is disturbed by the formation of ions and electrons. The current continuously increases with the rise in voltage until a breakdown voltage is reached. For a dielectric barrier discharge (discussed later in section 2.4.4), the magnitude of breakdown voltage depends on the state variables of the gas, electrode gap, dielectric material and secondary electron emission coefficient.

### 2.3.2 Paschen's Law

Paschen discovered the relationship among the breakdown voltage, gas pressure and gap distance between the parallel plates in 1889. In his work, it is proved that the breakdown voltage of parallel plates reactor is a function of pressure and gap distance. For a uniform electric field, this can be written in the mathematical form as

$$V_t = f(pd) \quad (2.1)$$

where,  $p$  is the pressure and  $d$  is the gap distance. This represents the experimental relationship known as Paschen's law.

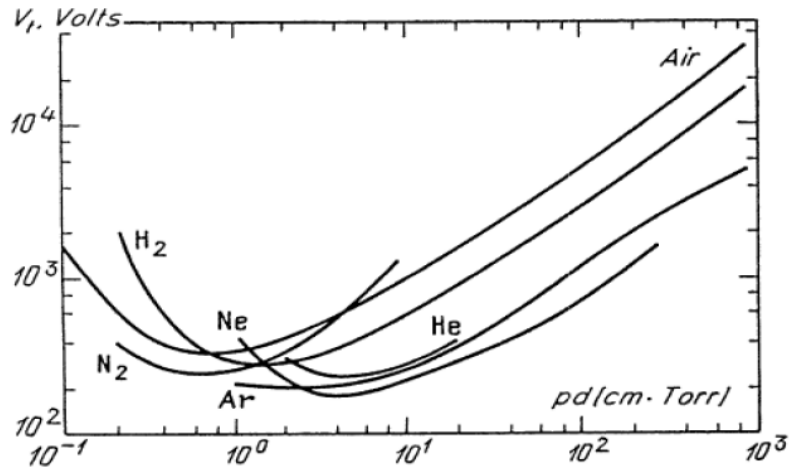


Figure 2.5: Breakdown potentials in different gases over a wide range of  $pd$  values.

The graphical curves of breakdown voltage  $V_t$  versus  $pd$  for different gases and electrode material have a unique minimum value. The smallest value of breakdown is called as the minimum sparking or breakdown potential. It has a value of several hundred volts. The graph shows some experimental curves of breakdown voltage  $V_t$  versus  $pd$ . There is huge impact on the breakdown voltage in the case of mixture of two different gases. For example, a small impurity of argon in neon atoms enhances the ionization due to Penning effect. The curves in Figure 2.5 displays the change in breakdown voltage for the specified gases. When moving towards the right on

a Paschen curve, it may be noted that the threshold value of  $V_t$  initially reduces and then increases with increase in  $pd$ . Beyond the minimum  $V_t$ , the breakdown voltage is consistently increased with  $pd$  (slightly slower). This type of behaviour emerges because in case of large gaps and elevated pressures, the electrons can produce the numerous ionizing collisions even at very reduced electric field. On the contrary, the occurrence of collisions is very small on the left-hand branch at lower  $pd$ . The ionization is possible in case of strong electric field to achieve the required amplification. The breakdown rises rapidly as  $pd$  falls. It means that a sufficient ionisation is not present at very smaller  $pd$ , regardless of the electric field strength.

## 2.4 Nonthermal Plasma Sources

As mentioned earlier, plasma can be formed in any neutral gas by providing sufficient energy capable of causing ionisation of the gas. Thus the source of energy is very high temperature from flames or arcs in case of thermal plasma and electrical energy or electromagnetic waves in case of most NTPs. The technologies used to obtain NTP, thus, vary from use of radiofrequency waves, to capacitive or inductive coupling methods, to dielectric barrier discharges. Formerly, plasma treatments were carried out under vacuum conditions, but researchers have now developed atmospheric pressure plasma sources, resulting in reduced cost, increased treatment speed, and industrial applicability [Yoon and Ryu, 2007; Yun et al., 2010]. The ability to generate non-thermal plasma discharges at atmospheric pressure makes the decontamination process easier and less expensive [Kim et al., 2011]. Plasma generation at atmospheric pressure is of interest, both technically and commercially to the food industries because this does not require extreme conditions. However, until very recently, most of the cold plasma devices available commercially were developed for research and aimed at biomedical applications. Therefore, for food applications, these devices must be customised or tailor made.

### 2.4.1 Microwave Plasma

These plasma systems are based on high frequency microwave discharges (in the order of GHz) in a gas. Microwave plasma technology permits dense non-equilibrium plasmas to be generated at pressures up to 35-52 Pa and at power levels reaching 1 MW. The key advantage of high-frequency fields is a stabilising effect on the plasma and generation of streamerless plasmas in molecular gases [Bárdoš and Baránková, 2010]. Duo-Plasmaline<sup>®</sup> is a linearly extended plasma source excited using microwaves of 2.45 GHz at a pressure  $\leq 1000$  Pa [Petasch et al., 1997] and several other plasma treatment systems have evolved based on this principle. The Plasmodul<sup>®</sup> is a microwave sustained low pressure plasma reactor with a modular concept based on the Duo-Plasmaline<sup>®</sup> principle which provides easy up-scaling for industrial applications [Schulz et al., 2003]. This type of microwave excited plasma sources are well suited for large area plasma treatment [Petasch et al., 1997] and could be employed for surface treatment of foods or processing surfaces at industrial scale.

### 2.4.2 Radiofrequency Plasma

These are capacitive discharges produced more often in noble gases such as helium or argon by the application of RF power (e.g., 13.56 MHz) to one powered electrode, with a grounded electrode held at a small separation. Low frequency RF ( $\leq 100$  kHz) electric field is also used to generate glow discharge between two metal electrodes. A practical example of glow discharge includes fluorescent lamps.

### 2.4.3 Corona Discharge

Corona refers to a weak luminous discharge, which is generated at atmospheric pressure near sharp points, edges, or thin wires using large electric fields (see Figure 2.6). Coronas are thus inherently non-uniform discharges that develop in the high field region near the sharp electrode spreading out towards the planar electrode. This phenomenon of local breakdown is called corona discharge. Corona discharges have been widely used in ozone generators and particle precipitators.

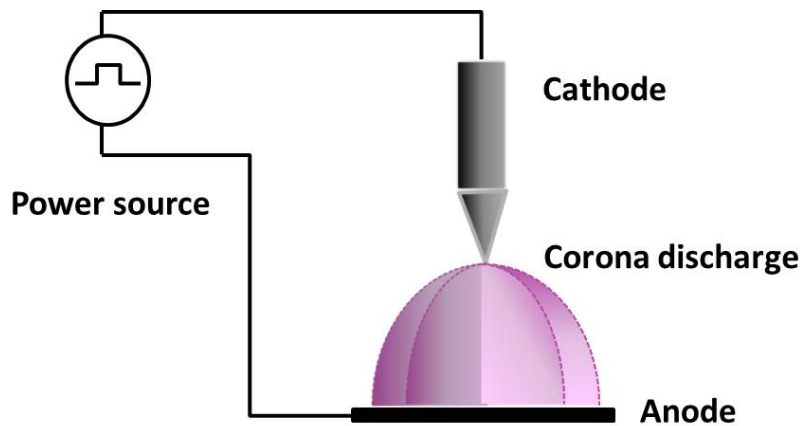


Figure 2.6: Schematic of corona discharge set-up

#### 2.4.4 Dielectric barrier discharge (DBD)

In DBD, plasma is generated between two electrodes, separated by one or more dielectric barriers (see Figure 2.7). The main characteristic of DBDs is the presence of a dielectric material between the discharge gap and one of the two electrodes. When the potential across the gap reaches the breakdown voltage the dielectric acts as a stabilizing material leading to the formation of a large number of micro-discharges. Thus, the dielectric material inhibits the glow-to-arc transition in a DBD. In recent times, DBD plasmas in air, helium and several gas mixtures have been employed for in-package ionisation and treatment of fresh produce. In-package ionisation is a dry, non-thermal process which can extend shelf-life of packaged foods by reducing spoilage organisms inside the package [Klockow and Keener, 2009]. Depending on the gas mixture, dielectric surface properties, and operating conditions, vastly different modes ranging from filamentary to completely diffuse barrier discharges, can be achieved [Kogelschatz, 2002]. The barrier glow discharge generated between two parallel electrodes is yet another type of DBD operating at higher frequencies and is often called One-Atmosphere Uniform Glow Discharge Plasma (OAUGDP). In a possible industrial scale set-up, food may be conveyed through the DBD to achieve microbial decontamination.

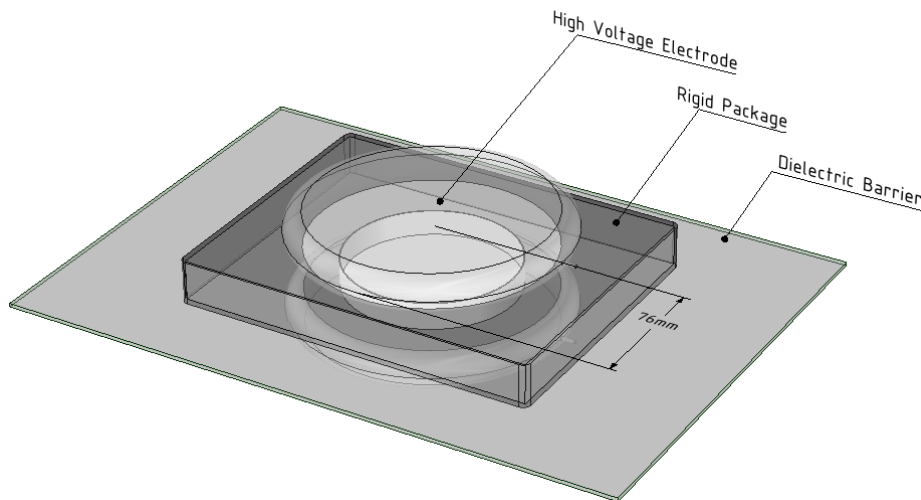


Figure 2.7: Schematic of a dielectric barrier discharge set-up for in-package plasma treatment.

### 2.4.5 UV Sustained Nonthermal Plasma

*Biozone Scientific* has developed a new process for the generation of cold oxygen plasma (COP) by subjecting air to high-energy deep-UV light with an effective radiation spectrum between 180 nm and 270 nm. This non-thermal gas plasma is composed of several species including negative and positive ions, free radical molecules, electron, UV-photons and ozone [Terrier et al., 2009].

### 2.4.6 Framework for Classification of NTP Applications

Despite the various technologies to generate NTP, in general from an application standpoint, these can be classified into three modes of operation viz. electrode contact, direct treatment and remote treatment (see Figure 2.8) [Niemira, 2012]. A detailed discussion on various cold plasma sources has been provided by Bárdoš and Baránková [2010] and Bárdoš and Baránková [2008]. The versatile feature of most plasma systems is the freedom to select a gas or gas mixture. Improvements in the existing plasma systems and newer equipment directed for treatment of food systems are likely to draw attention from researchers and engineers in near future.



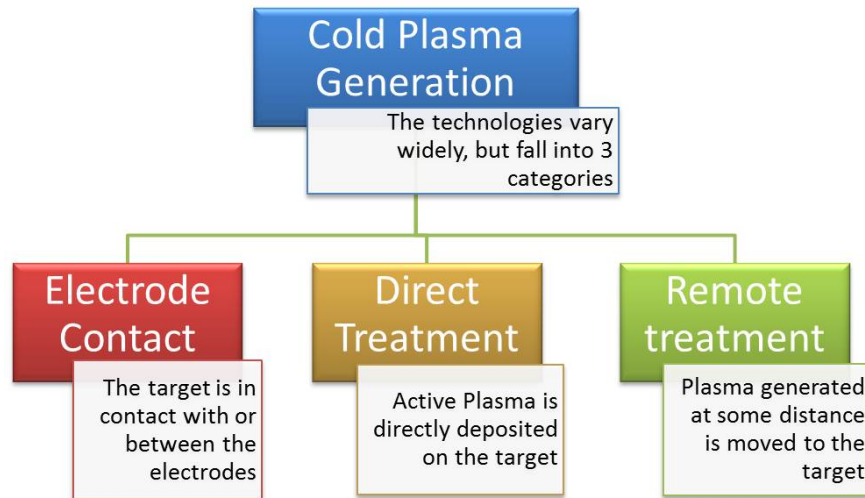


Figure 2.8: Framework for the categorisation of NTP technology based on mode of operation.

## 2.5 Process Variables

The concentrations in which the plasma agents occur in plasma depend greatly on the device set-up (reactor geometry), operating conditions (gas pressure, type, flow, frequency and power of plasma excitation) and gas composition which affect their efficacy in a process when employed. For example, the destructive efficiency of various gas plasma sources and temperatures on *Bacillus* spp. spores were compared by Hury et al. [1998]. This group demonstrated that oxygen-based plasma is more efficient than pure argon plasma. Gases commonly employed for atmospheric pressure plasma operations include helium, argon, sulphur hexafluoride ( $\text{SF}_6$ ), nitrogen/ $\text{CO}_2$  mixtures and air. The selection of operating gas largely dictates the process cost.

Another deciding criterion is whether the substrate to be sterilised is in direct contact with the plasma (*Direct Exposure*) or located remote from it (*Remote Exposure*) [Boudam et al., 2006; Laroussi, 2005; Moisan et al., 2001]. If exposed remotely, the quantum of heat transmitted to a sample is reduced, the charged particles do not play a role since they recombine before reaching the sample, and

many of the short-lived neutral reactive species also do not reach the sample. Since the components of the plasma are reactive and self-quenching, with a relatively short half-life, decreased time of flight would be expected to be one of the major factors in antimicrobial efficacy in this case [Niemira and Sites, 2008].

By varying the process parameters involved in plasma generation, a multitude of mechanisms can be actuated which may act individually or synergistically. Nevertheless, the details of interaction of the different plasma agents with the different components of bacterial cells or spores are currently very limited. The interactions which occur between plasma agents and biological materials, ultimately leading to sterilization are still under investigation.

## 2.6 Plasma chemistry

The behaviour of plasma is largely determined by the plasma chemistry. Plasma chemistry can be highly complex with a large number of different constituting species (Figure 2.9) at any given point of time. For example plasma chemistry in air is believed to be made up of more than 75 species and almost 500 reactions [Gordillo-Vazquez, 2008]. In air, chemical reactions are mainly initiated by the impact of electrons with oxygen and nitrogen. It is a general belief that dissociation is much easier than ionization and this is the reason for higher radical densities than ion densities in plasma. However, the reality is that dissociation is typically only a factor of 310 more frequent than ionization and the radical densities are higher due to slower transport rather than more effective production [Schram, 2002].

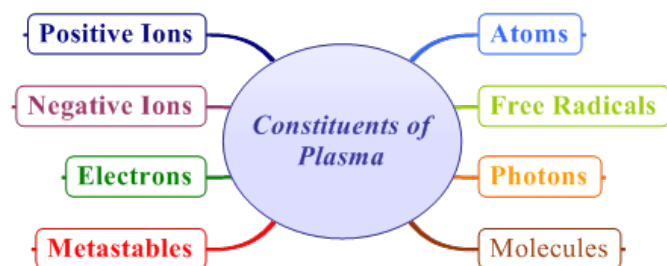


Figure 2.9: Constituents of plasma

The main types of reactions occurring in volume plasma are divided into homogenous and heterogenous reactions. Homogenous reactions occur between species in the gaseous phase as a result of inelastic collisions between electrons and heavy species or collisions between heavy species; whereas, heterogenous reactions occur between the plasma species and the solid surface immersed or in contact with the plasma.

In nonthermal plasma discharges containing oxygen, oxygen molecules are first dissociated by electrons to form oxygen atoms which subsequently react with  $O_2$  to form ozone ( $O_3$ ). In fact, mechanisms for  $O_3$  generation in oxygen plasmas involve more than 50 chemical reactions and at least 10 species [Lee et al., 2004]. Of greatest practical interest are reactions leading to the destruction and formation of NO and its further oxidation products. At much longer times in a humid air system, there is a build-up of ozone and the higher oxides and hydrides of nitrogen, which are the final products of the discharge [Herron and Green, 2001]. The reactions leading to the formation of various charged and neutral species in a humid air discharge are summarised in Sieck et al. [2000], [Gordillo-Vazquez, 2008] and Herron and Green [2001].

## 2.7 Plasma diagnostics

All the studies reported in this thesis were carried out using a DBD. Considering this, the descriptions in following section(s) have been limited to the context of a DBD or where applicable, plasma sources of oecumenical nature.

### 2.7.1 Electrical Diagnostics

The electrical diagnostics of plasma discharges often involve measurement of charge, voltage across electrodes, discharge current, frequency, resonance, and mode of operation (arc, filamentary, or glow discharge). In atmospheric air, the breakdown electric field is  $\sim 30$  kV/cm and the peak value of the discharge current is of the order of milliamperes [Kogelschatz, 2003]. In general, most electrical characterisation techniques rely on equivalent electrical models of the plasma set-up. An electrical

model is a convenient and simple approach, as the discharge plasma is usually regarded as an equivalent electrical circuit representing the relationship between the reactor configuration and electrical parameters [Zhang et al., 2010]. For example, the Q-V measurements first devised by Manley [1943] employs a capacitor in series with the DBD. Assuming the parallel plate DBD to be purely capacitive in nature, this approach relies on the fact that the charge remains same when two capacitors are connected in series, for measuring the total charge, total power input and capacitances in the circuit using Lissajous figures [Falkenstein and Coogan, 1997; Zhang et al., 2010]. Similarly, the voltage drop across a non-inductive resistor in series with the ground electrode of a DBD can also be employed for measuring the discharge current [Chiper et al., 2011]. Such measurements require high voltage probes and high resolution oscilloscopes. Fast Fourier Transform (FFT) of the time-domain voltage and/or current is another practice for obtaining the harmonic patterns in discharge [Ragni et al., 2010].

### 2.7.2 Optical Diagnostics

Understanding the plasma chemistry has remained a challenge for plasma chemists and physicists for many decades due to the underlying complexity. In attempts to understanding the plasma chemistry, a number of non-intrusive techniques have developed over time and these have been reviewed by Hershkowitz and Breun [1997] and Herman [2003], and discussed in detail by Konuma [1992]. The optical diagnostics commonly employed include optical emission spectroscopy (OES), optical absorption spectroscopy (OAS), Fourier Transform Infrared (FTIR) Spectroscopy, and Laser Induced Fluorescence [Gottscho and Miller, 1984]. The latter two are common in polymer and electronics industries. Optical diagnostic is a powerful tool for the non-invasive measurement of the plasma properties in complex reactive discharges [Liu et al., 2012].

#### 2.7.2.1 Optical Emission Spectroscopy (OES)

A fraction of the energy transferred to the gas in a plasma discharge is responsible for excitement of several chemical species to higher energy states by collisions with energetic electrons, and subsequently the relaxation is accompanied by emission

of a photon. The excited species can therefore be detected using the UV-Vis-IR emission spectra of the discharge. In OES, the spectrum of the (light) radiation emitted by the plasma is collected using an optical fiber, sliced (by means of a diffraction grating) and its intensity measured as function of the wavelength using a detector (photomultiplier tube or charge coupled device (CCD)). The identification of plasma species requires knowledge of the emission lines of plasma species, which often can be obtained from National Institute of Standards and Technology [?] atomic spectra database and several published works [Gaydon and Pearse, 1976; Laux et al., 2003; Meiners, 2010]. If information about line shapes is known, then OES can be employed for calculating the rotational and vibrational temperature of electrons. Such computation should however be used with caveats that all photons may not strike the collector window coupled to the optical fiber.

### 2.7.2.2 Optical Absorption Spectroscopy (OAS)

In OAS, the light absorbed by the excited species is measured as a function of the wavelength. OAS is used to probe highly excited molecules because these states are long lived, yet do not decay via emission of a visible photon, which rules out identification by OES [Stillahn et al., 2008]. The set-up for this technique comprises of a lamp (typically emitting in UV-Vis and/or infrared region from a deuterium/tungsten lamp(s)), light from which passes through the reactors plasma zone to enter into an optical fibre, which sends the transmitted light to the spectrometer.

### 2.7.2.3 Mass Spectrometry

Optical techniques such as OES, OAS and FTIR spectroscopy are in-situ techniques, while mass spectrometry (MS) of plasma belongs to an ex-situ class of plasma diagnostics, as it samples out a fraction of the plasma volume for identification of the chemical species in plasma [Gottscho and Miller, 1984]. A mass spectrometer could be regarded as a mass resolved ion energy analyser and is useful in detecting neutral as well as ion species [Pokorný et al., 2013] and measuring the ion energy distribution (IED) in plasma discharges [Liu et al., 2012]. Quadrupole MSs are the most common instruments used in plasma diagnostics.

## 2.8 Non-thermal plasma in food processing

The non-thermal plasma technology is an emerging disinfection method that offers a complementary or non-thermal alternative approach for reducing the microbial populations on food produce surfaces and packaging materials. The combination of highly energetic plasma species with a non-thermal treatment makes NTP particularly suited for decontamination in food processing settings [Yu et al., 2006]. NTP has a myriad of potential applications for the food industry including the dry disinfection of foods (like meat, poultry, fish and freshly harvested horticultural produce), granular and particulate foods (dried milk, herbs and spices) and sprouted seeds. There is significant scope for NTP sterilization of particulate foods, particularly after the ban of ethylene oxide gases. This technology has also been successfully applied for the sterilization of packaging material [Deilmann et al., 2008] and also their functional modification for imparting desired properties [Gülec et al., 2006; Ozdemir et al., 1999]. NTP has been proved effective for reducing microbial population on the surface of materials, such as glass, metals, fabrics, and agar, with wide range of microorganisms including vegetative forms, spores, fungi, viruses and parasites, etc. These studies have been summarised in Table 2.3. Although most of the previous work on bacterial inactivation has been conducted with bacteria deposited on the surface of abiotic materials such as membrane filters and glass slides, data on the disinfection of foodstuffs is steadily accumulating [Noriega et al., 2011].

Table 2.3: Recent findings in the area of NTP for inactivation of microorganisms and spores.

Organism	Plasma conditions	Substrate	Salient result	References
<i>Escherichia coli</i> , <i>Staphylococcus aureus</i>	Atmospheric plasma corona discharge, with high voltage (20kV) DC power supply	On agar plates	Changes of pH levels from alkaline to acid, upon plasma application to bacteria in water, does not play a predominant role in cell death.	<a href="#">Korachi et al. [2010]</a>
<i>Staphylococcus aureus</i>	DC cold- atmospheric pressure plasma microjet with compressed air as the working gas	Aqueous suspen- sions of the organism	First 10 min treatment led to insignificant inactivation. After 16 min <i>S. aureus</i> was completely inactivated. Effective inactivation of <i>S. aureus</i> was found to start after the pH values decreased to about 4.5.	<a href="#">Liu et al. [2010]</a>
<i>Bacillus atrophaeus</i> , <i>Geobacillus</i> <i>sterothermophilus</i> , <i>Clostridium sporogenes</i> , <i>Kocuria rhizophila</i> , <i>Staphylococcus aureus</i> , <i>Aspergillus niger</i>	Low- pressure inductively-coupled plasma (ICP) with different mixtures of gases	Glass substrates and silicon wafers coated with the organ- ism by spraying.	All the organisms were found to be reduced by at least 4 orders of magnitude under optimized low- pressure argon plasma. Efficiency of inactivation was variable for different strains of a given species.	<a href="#">Von Keudell et al. [2010]</a>
<i>Bacillus subtilis</i>	Oxygen and nitrogen treated using 8 Duo- Plasmalines driven by microwaves power	Microscopic slides stacked with spores	Plasma treatment of the spores caused release of DPA, generat- ion of auxotrophic mutants, reduction in Kat X activity and damage to DNA. A biphasic model for the inactivation kinetics was proposed.	<a href="#">Roth et al. [2010]</a>

Organism	Plasma conditions	Substrate	Salient result	References
<i>Escherichia coli</i> , <i>Bacillus subtilis</i> , <i>Candida albicans</i> , <i>Staphylococcus aureus</i>	High-frequency capacitive discharge (0.4 torr) and barrier discharge (0.4-0.5 torr) in air excited at commercial frequency of 5.28 MHz	Glass plate and petri dish	The most probable sterilization agents of the plasma generated were established to be "hot" and "cold" OH radicals the excited electrically neutral N <sub>2</sub> and O <sub>2</sub> molecules, and the UV plasma radiation.	<a href="#">Azharonok et al. [2009]</a>
Influenza viruses (RSV, hPIV-3 and A (H5N2) )	Air subjected to high-energy deep-UV light using Biozone scientific COP generator	Air	More than 99.8% reduction of influenza virus A (H5N2).	<a href="#">Terrier et al. [2009]</a>
<i>Escherichia coli</i> KCTC1039, <i>Bacillus subtilis</i>	Helium and Oxygen based electric discharge plasma produced at 13.56 MHz (RF)	Dried cells, endospore suspension on a cover-glass	Treated cells had severe cytoplasmic deformations and leakage of bacterial chromosome. UV from the plasma only slightly affected the viability of the spores.	<a href="#">Hong et al. [2009]</a>
<i>Deinococcus radiodurans</i>	Dielectric Barrier Discharge (DBD)	Cells dried in laminar flow hood; cells suspended in distilled water	4 log reduction of CFU count in 15 s of the extremophile organism suspended in distilled water. This was attributed to the fact that plasma compromises the integrity of the cell membrane of the organism.	<a href="#">Cooper et al. [2009]</a>
<i>Escherichia coli</i> type 1, <i>Saccharomyces cerevisiae</i> , <i>Gluconobacter liquefaciens</i> , <i>Listeria monocytogenes</i>	Cold atmospheric plasma plume generated by an AC voltage of 8 kV at 30 kHz	Inoculated membrane filters; inoculated fruit surfaces	Efficacy of inactivation was markedly reduced for microorganisms on the cut surfaces than on filters due to the migration of microorganisms from the exterior of the fruit tissue to its interior and not quenching of reactive plasma species.	<a href="#">Perni et al. [2008a]</a>



Organism	Plasma conditions	Substrate	Salient result	References
<i>Escherichia coli</i> O157:H7, <i>Salmonella Stanley</i>	Gliding Arc plasma	On agar plates and inoculated onto surfaces of Golden Delicious apples	Bacterial inactivation was shown to be a function of flow rate and duration of exposure.	<a href="#">Niemira and Sites [2008]</a>
<i>Aspergillus parasiticus</i> and Aflatoxins	Air gases and SF <sub>6</sub> plasma using total applied power of approximately 300 W	Hazelnuts, Peanuts, Pistachio nuts	SF <sub>6</sub> plasma was more effective with a 5-log decrease in fungal population for the same duration as air plasma. 20 min air plasma treatment resulted in a 50% reduction in total aflatoxins (AFB1, AFB2, AFG1, and AFG2), while only a 20% with SF <sub>6</sub> plasma treatment. No significant organoleptic changes were observed.	<a href="#">Basaran et al. [2008]</a>
<i>Escherichia coli</i> , <i>Saccharomyces cerevisiae</i> , <i>Pantoea agglomerans</i> <i>Gluconacetobacter liquefaciens</i>	Atmospheric NTP using an AC voltage (variable 12kV and 16kV)	Pericarps of mangoes and melons	<i>S. cerevisiae</i> was the most resistant amongst all test organisms. An increase in the applied voltage led to more efficient production of reactive plasma species (oxygen atoms) which was attributed for better inactivation.	<a href="#">Perni et al. [2008b]</a>
<i>Escherichia coli</i> O157:H7, <i>Salmonella sp.</i>	One atmosphere uniform glow discharge plasma (OAugDP) operated at 9 kV power and 6 kHz frequency	Apples, Cantaloupe and Lettuce	Inactivation was observed in all the cases. Extent of log reduction varied with the organisms.	<a href="#">Critzler et al. [2007]</a>
<i>Escherichia coli</i>	Air in a Dielectric discharge chamber	Raw almonds	Up to 5 log reduction observed	<a href="#">Deng et al. [2009]</a>

Organism	Plasma conditions	Substrate	Salient result	References
<i>Escherichia coli</i> NCTC 9001, <i>Campylobacter jejuni</i> ATCC 33560, <i>Campylobacter coli</i> ATCC 33559, <i>Listeria monocytogenes</i> NCTC 9863, <i>Salmonella enterica</i> Enteritidis ATCC 4931, <i>Salmonella enterica</i> Typhimurium ATCC 14028, <i>Bacillus cereus</i> NCTC 11145 endospores.	Pulsed plasma gas discharge (PPGD) using high-voltage pulses (with 40-kV DC capacitor) in a coaxial treatment chamber. Different treatment gases viz. N <sub>2</sub> , CO <sub>2</sub> , O <sub>2</sub> and air sparged	Poultry wash water at 4 °C	Rapid reductions in microbial numbers (by $\leq 8 \log$ CFU/ml). Use of O <sub>2</sub> alone produced the greatest reductions. In general gram negative test bacteria were more susceptible.	<a href="#">Rowan et al. [2007]</a>
<i>Aspergillus niger</i> , <i>Bacillus atrophaeus</i> , <i>Bacillus pumilus</i> , <i>Clostridium botulinum</i> type A, <i>Clostridium sporogenes</i> , <i>Demococcus radiodurans</i> , <i>Escherichia coli</i> , <i>Staphylococcus aureus</i> , <i>Salmonella mons</i>	Cascaded dielectric barrier discharge in air	PET foils	Highest count reduction was observed for the vegetative cells with at least 6.6 log <sub>10</sub> with in 1 s. <i>Aspergillus niger</i> was the most resistant test strain with an inactivation rate of about 5 log <sub>10</sub> in 5 s.	<a href="#">Muranyi et al. [2007]</a>
Biofilms produced by <i>Chromobacterium violaceum</i>	RF high pressure cold plasma jet using Atomflo 250 reactor with 100 W RF power supply using He and N <sub>2</sub> gas	Biofilms produced in 96-well polystyrene micro-plates	A 10 min plasma treatment was able to kill almost 100% of the cells. A complex, biphasic model of inactivation was observed.	<a href="#">Abramzon et al. [2006]</a>

Organism	Plasma conditions	Substrate	Salient result	References
<i>Bacillus subtilis</i> spores	Dielectric-barrier discharge (DBD) with pure He or He-O <sub>2</sub> mixture.	Polycarbonate membranes, supported by a layer of technical no.3 agar in a petridish.	Spore inactivation was mostly induced by the reactive oxygen species with the heat, UV photons, electric field and charged particles; all making minor contributions. Atmospheric-helium plasma was more effective than atmospheric He-O <sub>2</sub> mixture plasma.	Deng et al. [2006]
<i>Escherichia coli</i> K12	Atmospheric plasma plume generated using He gas with a peak voltage of 6 kV	<i>E. coli</i> cells deposited on surface of membrane filters	SEM revealed severe loss in structural integrity of plasma-treated cells. Survival of <i>E. coli</i> cells was found to depend on the cell surface density, as it affects plasma penetration depth. Physiological state of cells (i.e. phase of growth) affects their resistance to plasma inactivation.	Yu et al. [2006]

### 2.8.1 Treatment of raw fruits and vegetables

Microorganisms can be found on raw and minimally processed produce at populations ranging from  $10^3$  to  $10^9$  CFU/g. Although washing produce in water may remove some soil and other debris, it cannot be relied upon to completely remove microorganisms and also may result in cross-contamination of food preparation surfaces [Nguyen-the and Carlin, 1994]. Chlorine wash is the most prevalent method for the preliminary decontamination of fresh produce at an industrial scale, primarily due to its relatively low cost, efficacy, availability and ease of operation [Connolly et al., 2010]. Commercially, only around 100 to 200 ppm chlorine is used for sanitation purposes. However, chlorine derivatives are not considered safe compounds since they react with organic material to form reactive by-products such as chloramines and trihalomethanes. In a number of European countries, including the Netherlands, Sweden, Germany and Belgium, the use of chlorine on minimally processed vegetable products is prohibited [José and Vanetti, 2012; Rico et al., 2007]. Unlike chlorine, which selectively destroys certain enzymes in bacteria, ozone (the prominent anti-microbial species formed in most NTP with oxygen as a component) acts as a general protoplasmic oxidant [Khadre et al., 2001; Sykes, 1965].

Niemira and Sites [2008] significantly reduced the viable populations of *Salmonella* spp. and *E. coli* 0157:H7 inoculated on apple surfaces using cold plasma generated from a gliding arc. A 2.9 to 3.7  $\log_{10}$  CFU/ml and 3.4 to 3.6  $\log_{10}$  CFU/ml reduction of *Salmonella stanley* and *E. coli*, respectively was observed. The authors reported the highest flow rate of the air (discharge medium) i.e. 40 litres/min, to be most effective. Recent important findings related to plasma based inactivation of microflora associated with fresh fruits and vegetables are included in Table 2.3.

### 2.8.2 Decontamination of seeds and nuts

The main entry of mycotoxins into the human and animal food chain is from agricultural products such as cereal grains and oilseeds or products derived from these [Jiménez et al., 1991]. Low-pressure cold plasma with sulphur hexafluoride

( $SF_6$ ) treatment for 10 min has been found to result in approximately a 5-log decrease in fungal populations on the surface of hazelnuts, peanuts, and pistachio nuts [Basaran et al., 2008]. In addition, with similar treatments for 20 min using air plasma a 50% reduction in total aflatoxins (AFB1, AFB2, AFG1, and AFG2) has been reported [Basaran et al., 2008].

Decontamination of tomato seeds, wheat (*Triticum durum*), bean, chickpea, soybean, barley, oat, rye, lentil (*Lens culinaris*) and corn, contaminated with *Aspergillus parasiticus* 798 and *Penicillium* spp. to less than 1% of initial count have also been reported in literature, with treatment times ranging from 30 s to 30 min [Selcuk et al., 2008] (Figure 2.10). These effects were obtained using a custom designed batch type low pressure cold plasma (LPCP) prototype unit operating under vacuum, in air and  $SF_6$  gases. It is worth noting that seeds remain viable post-treatment. Deng et al. [2007] reported effective reductions of

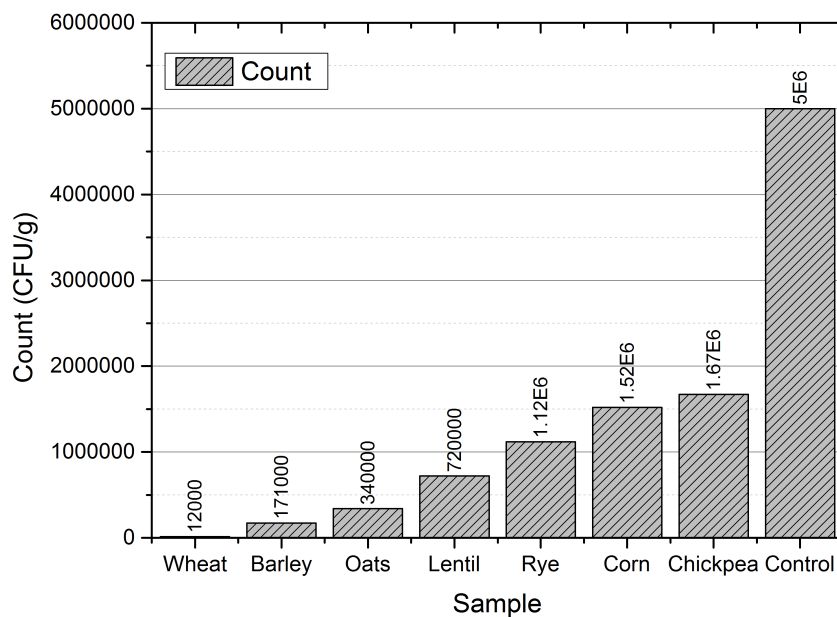


Figure 2.10: Survival curves of  $SF_6$  low pressure cold plasma exposed *Aspergillus* spp. on various seed surface (Selcuk et al. 2008).

*E. coli* on almond of almost 5-log after 30-sec treatment at 30 kV and 2000 Hz using a DBD plasma. Enhanced inactivation of *E. coli* inoculated on almonds was associated with increasing voltage and frequency input to the DBD system in this

research. Niemira [2012] also reported a decrease in the count of *Salmonella* and *Escherichia coli* O157:H7 on almonds treated using a jet plasma operating with air and nitrogen feed gases.

### 2.8.3 Surface decontamination of eggs

*Salmonella* spp. is a well-recognised hazard for egg consumers and a need for alternative methods of decontaminations has been highlighted by Davies and Breslin [2003]. Vertical transmission of *Salmonella* and *Campylobacter* from infected breeders to their offspring through contamination of the eggs is one possibility of how pathogens spread throughout flocks and/or are present inside eggs [Newell and Fearnley, 2003; Snelling et al., 2005]. *Salmonella* has been shown to be present in eggs [Berchieri Jr et al., 2001] and as such contaminated eggs are also a major food safety risk. In *Campylobacter* spp this has been shown but is not thought to be the major route of transmission [Doyle and Erickson, 2006].

Several non-thermal approaches for the surface decontamination of eggs, such as pulsed light technology [Hierro et al., 2009], ozone, UV radiation [Fuhrmann et al., 2010; Rodriguez-Romoand and Yousef, 2005] and electrolyzed water [Cao et al., 2009] have already been researched. These attempts are in extension to the failure of conventional techniques in efficient cleaning of the surface of eggs. Ragni et al. [2010] reported on the efficacy of resistive barrier discharge (RBD) plasma for decontamination of shell eggs. They identified a maximum reduction of  $\sim 2.5$  Log CFU/eggshell in *Salmonella enteritidis* levels following a 60-90 min of treatment at 35% RH. Efficacy was enhanced at a higher RH level of 65%, where maximum reductions of 3.8 and 4.5 Log CFU/eggshell were achieved after 90 min of exposure. Similar observations were made for *Salmonella typhimurium* with an overall reduction of 3.5 Log CFU/eggshell, after 90 min of treatment. The enhanced effects of increased RH on the efficiency of the treatments have been explained on the basis of presence of oxygen species as detected in the discharge emission spectra. These results are at par with the UV and ozone treatments of eggs reported earlier [Rodriguez-Romoand and Yousef, 2005].

Donner and Keener [2011] evaluated the use of dielectric barrier discharges for in-package ozonation to reduce *Salmonella enteritidis* on raw, shell eggs. After a 24-hour storage period, they observed 3 log<sub>10</sub> reductions. Their results demonstrate the effectiveness of in-package ozonation treatment from a dielectric barrier discharge plasma for reducing *Salmonella enteritidis* on raw, shell eggs without significant effects on measured egg quality parameters over time.

#### 2.8.4 Decontamination of meat, fish and poultry

Surface contamination of ready to eat (RTE) meat may occur during processing as *L. monocytogenes* can persist in the processing environment and be transferred to product from equipment such as slicers [Berzins et al., 2010]. In products where the contamination is primarily localised to the surface, the prevalence and level of *L. monocytogenes* may be lowered via surface decontamination. Rød et al. [2012] investigated the application of cold atmospheric pressure plasma for decontamination of a sliced ready-to-eat (RTE) meat product (bresaola) inoculated with *Listeria innocua*. This group treated the inoculated samples at 15.5, 31, and 62 W for 2-60 s inside sealed linear-low-density-polyethylene bags containing 30% oxygen and 70% argon. The treatments resulted in a reduction of *L. innocua* ranging from 0.8±0.4 to 1.6±0.5 log cfu/g with no significant effects of time and intensity while multiple treatments at 15.5 and 62 W of 20 s with a 10 min intervals increased the reduction of *L. innocua*. Moon et al. [2009] treated pork skin using a plasma source powered by a 13.56 MHz radio frequency (RF) supply through an impedance matching network powered between 20 and 150 W. The sterilization efficiency of plasma (1 min treatment time) against *E. coli* inoculated on pork surface was comparable with that of a conventional UV sterilizer (30 sec treatment).

Kim et al. [2011] studied the effect of atmospheric pressure plasma (at 75, 100, and 125 W of input power for 60 and 90 s) on the inactivation of *L. monocytogenes* (KCTC 3596), *E. coli* (KCTC 1682), and *S. typhimurium* (KCTC 1925) inoculated onto sliced bacon. They used two gas compositions; helium (10 l/min) and a mixture of helium and oxygen, (10 l/min and 10 sccm, respectively) for the plasma generation. The authors reported that plasma with helium only reduced

inoculated pathogens by about 1-2 log<sub>10</sub> cycles, while the helium/oxygen gas mixture exhibited microbial reduction of about 2-3 log<sub>10</sub>. Based on log reduction data, microscopic and colorimetric studies, [Kim et al. \[2011\]](#) concluded that APP treatment was effective for the inactivation of the three pathogens used in their study. [Lee et al. \[2011\]](#) also reported a reduction of *L. monocytogenes* inoculated onto ham by 1.94 to 6.52 log units for 2 min treatments with APP jets of He, He + O<sub>2</sub>, N<sub>2</sub>, or N<sub>2</sub> + O<sub>2</sub> feed gases.

In a study of cold plasma treatment of cold smoked salmon, [Chiper et al. \[2011\]](#) employed a DBD operating at atmospheric pressure in 100% argon and (93% argon+ 7% CO<sub>2</sub>) gas mixture with a potential difference of 13 kV (peak to peak) across the electrodes. They observed ~3 log<sub>10</sub> CFU reduction after 60-120s treatment for *Photobacterium phosphoreum* and an insignificant effect on the inactivation of *Listeria monocytogenes* or *Lactobacillus sakei*.

Poultry carcasses are commonly contaminated with enteric pathogens such as *Salmonella* sp., *Campylobacter* sp. and *Listeria monocytogenes* [[Murphy et al., 2004](#)]. NTP treatment of cooked chicken breast using plasma jet was investigated by [Lee et al. \[2011\]](#), who observed 1.37 to 4.73 log reductions of *L. monocytogenes* after 2 min treatment with He, N<sub>2</sub>, and their mixtures with O<sub>2</sub> gas. [Noriega et al. \[2011\]](#) employed a cold atmospheric plasma pen (CAP-Pen) for decontamination of chicken and reported > 3 log reductions of *L. innocua* on membrane filters after 10 s treatment, 1 log reduction on chicken skin after 8 min treatment, and > 3 log reductions treatment on chicken muscle after 4 min under optimal conditions. Recently [Dirks et al. \[2012\]](#) demonstrated the feasibility of NTP as an intervention to reduce foodborne pathogens: *Salmonella enterica* and *Campylobacter jejuni* on raw poultry surfaces.

### 2.8.5 Decontamination of packaging materials

Most regulatory guidelines specify microbiological requirements for food packaging and in many cases the packaging process is an important control point in hazard analysis critical control point (HACCP) [[Mittendorfer et al., 2002](#)]. NTP has the potential to replace or complement popular chemical based sterilisation methods for food packaging materials in industries. From a food industry point of view,



current commercial applications of cold plasma are primarily limited to packaging industry and include sterilisation of anti-fouling and printable surfaces and permeability reduction of polymers for carbon dioxide and oxygen [Basaran et al., 2008; Schneider et al., 2005]. Packaging materials such as plastic bottles, lids and films can be rapidly sterilised using NTP without adversely affecting their properties or leaving any residues.

Plasma deposition of heat sensitive materials such as vitamins, antioxidants and antimicrobials into the packaging material may be sought as potential alternative in the emerging field of antimicrobial and active packaging. Fernández-Gutierrez et al. [2010] have demonstrated the application of NTP for deposition of vanillin film over red delicious apples. The antimicrobial nature of vanillin against bacteria, yeasts and fungi well documented in literature [Cerrutti and Alzamora, 1996; Fitzgerald et al., 2004].

### 2.8.6 NTP processing of fruit juices

Changes in consumer preferences towards healthier and minimally processed beverages has led to increased research interest in non-thermal processing technologies in order to manufacture safe and fresh-like products, with enhanced retention of organoleptic quality [Palgan et al., 2011]. Recent studies indicate that atmospheric NTP technology has potential significance for commercial level orange juice treatments, considering the fact that only a 5 log reduction is required for pasteurization of liquid foods. Shi et al. [2011] employed a DBD to effectively reduce the population of *Staphylococcus aureus*, *Escherichia coli* and *Candida albicans* inoculated in orange juice by  $>5 \log_{10}$  after 12, 8, and 25 s treatments respectively at peak voltage of 30 kV. This research group demonstrated the ability of NTP to extend the shelf life of freshly squeezed orange juice. Prior to this, Montenegro et al. [2002] employed direct current corona discharges obtained using a pulsating 0-15 kV DC power supply to generate NTP in liquid media. They reported a reduction in the number of *Escherichia coli* O157:H7 in apple juice by more than 5 log CFU/mL in 40 s. It is a well-recognised fact that the resultant ionisation that occurs during plasma discharge activity allows substantial levels of ozone to be formed and to

dissolve in liquids [Espie et al., 2001].

### 2.8.7 Processing of milk and milk products

Milk and milk products have long been associated with infectious diseases including campylobacteriosis, salmonellosis, yersinosis, listeriosis, tuberculosis, brucellosis, staphylococcal enterotoxin poisoning, streptococcal poisoning and *Escherichia coli* O157:H7 infection [Gurol et al., 2012; Sampedro et al., 2005]. In this respect, non-thermal food processing has played an important role in improving food quality by maintaining its microbiological safety and quality profile while only minimally affecting its sensory and health-related properties [Sobrino-López and Martín-Belloso, 2010]. Pulsed electric field (PEF) processing has already been extensively researched and to some extent commercialised for treatment of milk. The first attempt to decontaminate milk using cold plasma generated from a corona discharge (9 kV of AC power supply) has been made by Gurol et al. [2012]. This group has reported *E. coli* count reduction from 7.78 log CFU/ml to 3.63 log CFU/ml after 20 min treatment in whole milk and an average 54% reduction after 3 min treatment irrespective of fat content. Thus, it appears that cold plasma generated under controlled conditions has potential to decontaminate milk.

Milk products including sliced cheese are often associated with food-borne listeriosis. Recently the effects of atmospheric NTP on the inactivation of 3-strain cocktail of *L. monocytogenes* in sliced cheese have been examined by Song et al. [2009]. This group reported ~6 log reduction in the viable population of *L. monocytogenes* after 120s treatment at 125W power using radiofrequency plasma (13.65 MHz) operating in helium gas. Further, the microbial log reduction was enhanced with increased input power and plasma exposure time.

## 2.9 Effect of NTP on quality attributes of food

### 2.9.1 Fresh fruits and vegetables

Niemira and Sites [2008] employed cold plasma generated in a gliding arc to inac-

tivate micro-organisms inoculated on golden delicious apples. They observed no gross changes in colour or texture within 1 to 2 hour of treatment. Contact angle (CA) measurements for nonthermal oxygen plasma treated lambs lettuce have shown increased wettability of adaxial leaf surfaces after plasma exposure [Grzegorzewski et al., 2010]. Further, in the case of lettuce a successive degradation of epicuticular waxes and cutin of the plants epidermis was indicated by means of FTIR (ATR) and scanning electron microscopy (SEM).

Studies on the effect of non-thermal plasma on food components are scarce in literature. Based on experiments using low pressure oxygen plasma it has been observed that a time and structure dependent degradation can be observed for different selected model flavonoids adsorbed on solid surfaces, which was attributed to plasma-immanent reactive species such as O ( $^3P$ ), O<sub>2</sub> ( $^1\Delta_g$  and  $^1\Sigma_g^+$ ), O<sub>3</sub>, or OH radicals [Grzegorzewski, 2010]. It has been observed in lambs lettuce that pure compounds show a time-dependent degradation (flavonoids) or remain unchanged (phenolic acids) after exposure to oxygen plasma [Grzegorzewski et al., 2010]. Also, for the same model plant based food, a significant increase of protocatechuic acid, luteolin, and disometin has been recorded after 120 s of treatment, independent of the applied plasma driving voltage. The effect of the UV and radical species of plasma on the lipids and other sensitive constituents of the foods such as vitamins C and E (which are naturally occurring in most fruits and vegetables and many foods) still remains ambiguous. Suitability of plasma technology for treatment of high fat/ lipid containing and other sensitive foods (where chemical changes may be induced) is doubted. Products that have high lipid content would likely be affected by oxidation, resulting in formation of hydroxyl acids, keto acids, short-chain fatty acids and aldehydes etc. that cause off-flavours and odours. For these reasons meat products may not be ideal substrates for treatment with plasma [Critzler et al., 2007]. For a full evaluation, additional issues concerning food quality must be considered and these include changes in nutrient content colour and textural qualities, toxic residues and other chemical changes [Vleugels et al., 2005].

### 2.9.2 Eggs

Ragni et al. [2010] investigated the efficacy of resistive barrier discharge (RBD) plasma for decontamination of shell egg surfaces. An important aspect of this study is that plasma treatment did not lead to any compromise of the cuticle quality, generally considered as the first mode of defence against microbial invasion. This was evidenced from the scanning electron microscopy (SEM) and dye uptake studies.

### 2.9.3 Meat

Rød et al. [2012] investigated the application of cold atmospheric pressure plasma for decontamination of a sliced ready-to-eat (RTE) meat product (bresaola) inoculated with *Listeria innocua*. They reported that concentrations of thiobarbituric acid reactive substances (TBARS) increased with power and storage time and were significantly higher than those of the control samples after 1 and 14 days of storage at 5 °C (Figure 2.11). However, the levels were low (from 0.1 to 0.4 mg/kg) and beneath the sensory threshold level. Surface colour changes included loss of redness of ~ 40% and 70% after 1 and 14 days of storage, respectively, regardless of plasma treatment. The results of this study indicated that cold plasma may be applicable in surface decontamination of pre-packed RTE food products. However, oxidation may constitute an issue in some products.

Moon et al. [2009] successfully decontaminated pork skin using a plasma source powered by a 13.56 MHz radio frequency (RF) supply powered at 20-150 W. They quantified the colour change using a colorimeter and observed no thermal damage from the plasma treatment in the L<sup>\*</sup>-, a<sup>\*</sup>-, and b<sup>\*</sup>- values compared to the control sample, suggesting the usefulness of the atmospheric pressure glow discharge as a living tissue treatment tool that does not cause any thermal damage.

In yet another study, using a direct treatment with a working gas containing only 1% oxygen no reduction in a<sup>\*</sup>-values has been observed in cold atmospheric pressure plasma (at 75, 100, and 125 W of input power for 60 and 90 s) treated sliced bacon by Kim et al. [2011] indicating that the plasma treatment per se did not influence colour markedly. This group also reported that surface tissues of treated samples did not show any significant changes or damage based on micro-

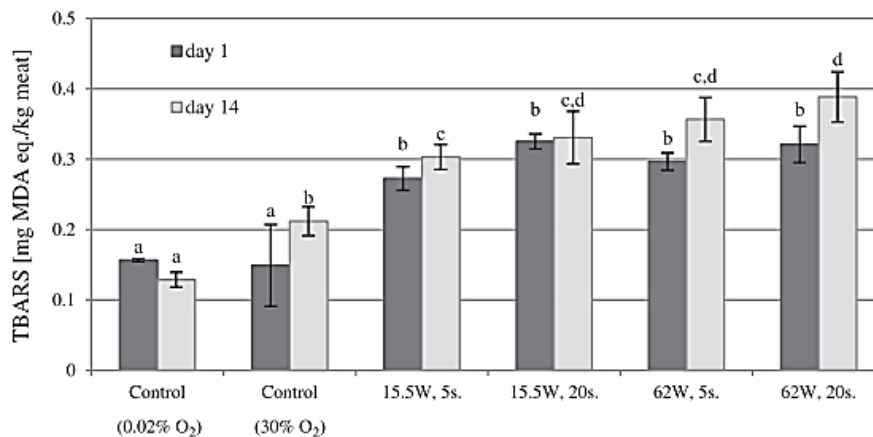


Figure 2.11: Average TBARS measured in sliced bresaola packed in LLDPE bags and treated with cold atmospheric pressure plasma at 15.5 and 62 W for 0 (control), 5 and 20 s as well as untreated bresaola stored in original unopened commercial packages (0.02% O<sub>2</sub>). Samples were stored at refrigerated temperature for 1 and 14 days. Results are given as mg of malonaldehyde equivalents per kg of meat.

scopic observation (60 ×). However, moisture evaporation from the surface of the treated samples was confirmed by the authors. No differences in the pH levels of bacon after NTP treatment with different gas compositions, at different input power levels, and for various exposure times were reported by the group.

## 2.10 Effect on pesticide residues

The use of pesticides in modern agricultural practices has enabled the stabilisation of crop production patterns globally. Nevertheless, the environmental and health problems associated with the use of pesticides at such a global scale cannot be overlooked. A constant search for new pesticides is on-going to combat the resistance developed in pests against the traditional pesticides. For example, fungicides, such as azoxystrobin, cyprodinil and fludioxonil are relatively new pesticides that have been introduced on the market [Garau et al., 2002]. However, the fact that agricultural products cannot be sold if they contain pesticides exceeding the residual limit implicates the need for development of methods to effectively eliminate residual pesticides in harvested crops [Iizuka et al., 2013; Yamaguchi,

2006].

Non-thermal plasma (NTP) is relatively very novel technology for the decontamination of fresh foods and meat. A limited number of studies have demonstrated the successful degradation of pesticides by NTP. The degradation of Dichlorvos and Omethoate organophosphorus pesticides sprayed onto maize samples, using an inductively coupled radio-frequency NTP source operating in oxygen was demonstrated by Bai et al. [2009]. Recently, Bai et al. [2010] also demonstrated the successful degradation of dichlorvos pesticides on glass slides using the same inductively coupled plasma (ICP) source. In an earlier study, Kim et al. [2007] reported the decomposition of paraoxon and parathion with an atmospheric pressure, radio-frequency plasma generated in Ar and Ar/O<sub>2</sub> mixture. However, there have been no studies regarding in-package NTP aided pesticide degradation on strawberries. Pesticides on strawberries pose health risk when present in concentrations higher than those permitted, as they are often consumed without washing or some kind of processing.

## 2.11 Advantages of NTP as a food technology

Based on the scientific, non-scientific and patent literature, the advantages of non-thermal plasma treatment for food preservation can be summarised as follows-

1. NTP offers high microbial inactivation efficiency at low temperatures (generally  $< 70^{\circ}\text{C}$ );
2. Most plasma sources allow just in time production of the acting agents;
3. NTP causes low impact on the internal product matrix;
4. The application of the technology is free of water or solvents;
5. NTP leaves no residues, given sufficient time is provided for the recombination reactions to proceed;
6. The technology is energy efficient.

# Chapter 3

## Materials and Methods

### 3.1 The Nonthermal Plasma source

The experiments reported within this thesis were carried out using one of the two dielectric barrier discharge plasma systems, namely the DIT-60 and the DIT-120. Both the systems work on the same principle described earlier in section 2.4.4. A schematic of the experimental set-up employed for the work is presented in Figure 3.1.

The DBD system comprises of two circular aluminium plate electrodes (outer diameter = 158 mm) over polypropylene (PP) dielectric layers (of 2 mm thickness) between which a PP package containing the food sample is placed. The electrodes had a contact surface area of 249.64 cm<sup>2</sup>. For the DIT-120, the high voltage step-up transformer (Phenix Technologies, Inc., USA) powered at 230 V, 50 Hz delivers a high voltage output in the range 0-120 kV rms. On the other hand, the DIT-60 is capable of delivering output in the range of 0-60 kV rms.

Two different rigid PP packages having dimensions of 310 mm×230 mm×40 mm and 310 mm×230 mm×22 mm were used for the quality studies. The PP layer of the package also served as a dielectric material. Rigid polyethylene terephthalate (PET) packages having dimensions of 150 mm × 150 mm × 35 mm were employed for all other studies. The rigid packages with produce were sealed inside polymeric film of 50 μm thickness (Cryovac B2630 or Cryovac BB3050) with very low gas transmission rates, in order to prevent leakage of the plasma-generated reactive

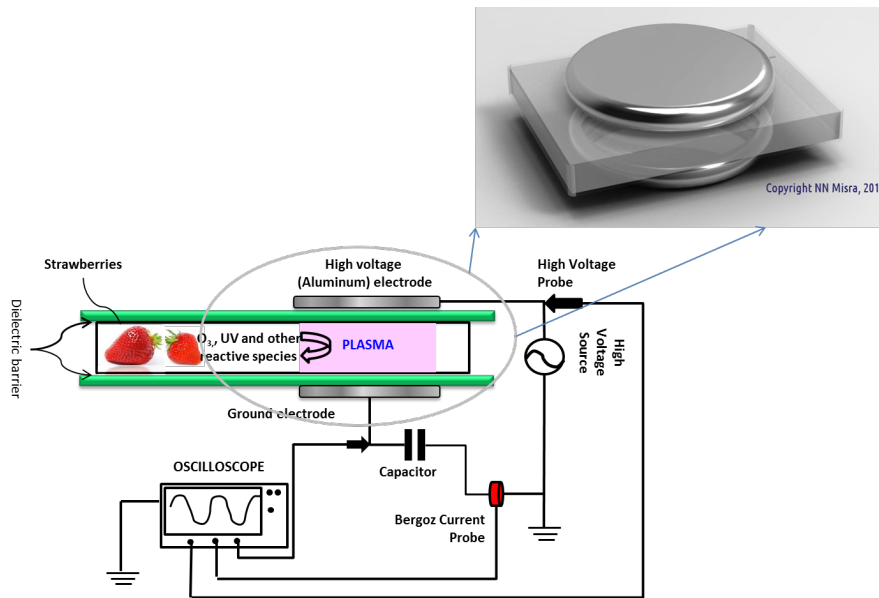


Figure 3.1: Experimental set-up of dielectric barrier discharge plasma with electrical and optical diagnostics.

species, during and post-treatments. This film served as an additional layer of dielectric. The atmospheric air conditions at the time of treatments were recorded using a humidity-temperature probe connected to a data logger (Testo 176T2, Testo Ltd., UK).

## 3.2 Plasma Diagnostics

### 3.2.1 Electrical Diagnostics

The voltage applied to the electrodes was monitored using a high voltage probe (North Star PVM-6) coupled to a 10:1 voltage divider to allow recording of the full voltage waveforms on an Agilent InfiniVision 2000 X-Series Oscilloscope (Agilent Technologies Inc., USA). The discharge characteristics were monitored using Q-V measurements by connecting a capacitor  $C_0 = 8.8 \text{ nF}$  in series on the ground side of the discharge. The voltage drop across the capacitor was recorded using a 1000:1 high voltage probe (Testec-Electronik TT-HVP 15kV), while a current transformer probe (Bergoz CT-E1.0S) was used to measure the current waveforms. The charge



on the capacitor versus the applied voltage was plotted to obtain Lissajous figures from which the capacitance of the discharge gap, the capacitance of the dielectric, the total power delivered to the plasma, the transferred charge and discharge-on time (duration of the discharge per half cycle) were calculated, respectively.

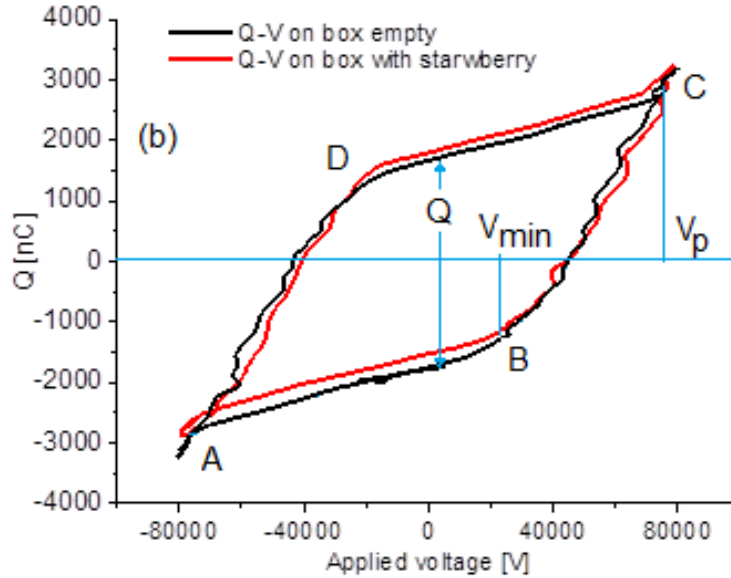


Figure 3.2: The Q-V Lissajous characteristic curves for a DBD.

The current-voltage (I-V) waveforms were used to assess the regime in which the DBD is operating. The electrical performances of the discharge were derived from the  $Q-V$  measurements according to the method developed by [Manley \[1943\]](#), [Falkenstein and Coogan \[1997\]](#) and [Zhang et al. \[2010\]](#) where  $C_d$  is the dielectric capacitance,  $C_{gap}$  is the capacitance of the discharge gap,  $P$  is the discharge power,  $\Delta Q$  is the total charge transported over a cycle and  $\Delta t$  is the duration of the discharges per half voltage cycle. The capacitances are calculated from the slopes of the  $Q-V$  parallelogram obtained as Lissajous figure with  $C_d$  and  $C_{cell}$  (total capacitance of the discharge cell) indicated in Figure 3.2 while  $C_{gap}$  is given by

$$C_{gap} = \frac{C_d \cdot C_{cell}}{C_d - C_{cell}} \quad (3.1)$$

The transported charge is calculated as

$$\Delta Q = 2.C_0.\Delta V \quad (3.2)$$

and

$$\Delta t = \frac{1}{2\pi f} \left[ \frac{\pi}{2} - \sin^{-1} \left( \frac{V_p}{V_{min}} \right) \right] \quad (3.3)$$

with  $C_0$  the measurement capacitor,  $f$  the frequency (50 Hz) and  $V_{min}$  the breakdown voltage,  $V_p$  the peak voltage and  $Q$  is the charge. The discharge power is calculated as the product of the area of the Lissajous charge-voltage loop and the frequency of applied voltage.

### 3.2.2 Optical Diagnostics

The energy transferred to the plasma produces various gaseous species in excited states. Some of these species can be identified based on the characteristic optical emission spectra (OES) of the plasma. Optical emission spectra of the discharge emissions within packages were acquired at 1.5 nm resolution with a computer controlled Stellarnet EPP 2000C-25 spectrometer, in which light from the plasma is coupled via an optical fibre. The diffraction grating in the spectrometer had a radius of curvature of 40 mm, 590 grooves per mm and an entrance slit width of 25  $\mu\text{m}$ . The fibre had a numerical aperture of 0.22 with optimum performance in the ultraviolet and visible portion of the spectrum. The spectrometer operates in the wavelength range 190 nm to 850 nm. The spectra are evaluated qualitatively to identify the active species generated by the discharge. For the experiments on discolouration of methylene blue, an Ocean Optics spectrometer (HR2000+) was used. The HC1 variable blaze diffraction grating coupled with a 25 $\mu\text{m}$  gave an optimal wavelength resolution of 1.1 nm. The spectrometer operated in the wavelength range 200 nm to 1050 nm. For all experiments, emission spectra and corresponding noise spectra were recorded using integration times of 500 ms and averaged over 10 measurements. All spectra were corrected for noise levels by subtracting the noise background. Emission line and peak identification was based on National Institute of Standards and Technology [2012] atomic spectra database and published works [Connolly et al., 2013; Herron and Green, 2001; Meiners,

2010].

### **3.2.3 Measurement of ozone concentrations**

Ozone concentrations within the package were measured, immediately following NTP treatments, using Gastec short-term ozone detection tubes (Product No. 18M, Gastec, Japan). These tubes contain a reagent which changes colour after coming in contact with the specified gas and are calibrated for specific sampling volumes. 10 mL of gas were pulled out of the package, through the tube, using a gas pump (Gastec, Japan) and a hypodermic needle. To avoid leakage of the gas, a silicone septum with adhesive was used at the point of gas sampling.

### **3.2.4 Dye discolouration for assessment of ozone levels**

#### **3.2.4.1 Reagents and selection of dye concentration**

Analytical-grade methylene blue (0.5%) obtained from Sigma-Aldrich, Ireland was used for all experiments. This dye was selected after an initial screening of various dyes including methylene blue, methyl orange and bromothymol blue for their sensitivity to the plasma treatments. Several dilutions of MB were prepared and their absorption spectra recorded to determine the most suitable concentration whose absorption maximum was within the measurement range of a UV-Vis spectrophotometer (Shimadzu UV 1800, Shimadzu Scientific Instruments). Based on spectral data of dilutions, a concentration of 0.001% MB was selected for all studies.

#### **3.2.4.2 Plasma Treatments**

For the treatment of methylene blue dye, 10 mL aliquot of MB dye solution was added to petri plates (60 mm diameter  $\times$  15 mm height, Sigma-Aldrich, Ireland) and placed inside the rigid polypropylene packages, which served as the reaction chamber. The dyes levelled to approximately 5 mm height inside the petri plate. Each box contained two such petri plates- one inside the field (meaning directly in the inter-electrode space) for direct exposure and another outside the field for indirect exposure. The working gas was air at atmospheric pressure. Treatment times of 0 s (Control), 15, 30, 45, 60, 90 and 120 s, at 30, 40 and 50 kV rms

across the electrodes were performed. After processing, boxes were stored at room temperature (16 °C) for 24 h.

### 3.2.4.3 Absorption spectra of dyes

The dyes were sampled into 1 cm path length cuvettes and their visible absorption spectra were obtained using a spectrophotometer (Shimadzu UV 1800, Shimadzu Scientific Instruments). Degradation efficiency was defined as percentage decrease of absorbance according to equation 3.4

$$Degradation[\%] = \left[ \frac{A_0 - A}{A_0} \right] \times 100 \quad (3.4)$$

where  $A_0$  is the absorbance of untreated dye solution (0 s treatment) and  $A$  is the absorbance after the plasma treatment at wavelength of maximum absorption ( $\lambda_{max}$ ).

### 3.2.4.4 pH measurement

The pH of all dye samples were measured before and after 24 h storage using a calibrated glass electrode ORION pH meter (model 420A, Thermo Fisher Scientific Inc.) at ambient temperature (16 °C).

### 3.2.4.5 Mathematical Modelling

Based on visual inspection of the experimental data, it was noted that the kinetics of degradation followed a sigmoidal pattern. Considering this, two empirical models, the Gompertz model and the First-Order kinetics model were evaluated for modelling the experimental data on dye degradation. The first-order model is given by equation 3.5

$$A_t = A_{max} - A_{max} \cdot e^{-kt}, A_{max} \leq 100 \quad (3.5)$$

where,  $A_t$  is the % degradation at any time,  $t(s)$ ,  $A_{max}$  is the maximum degradation,  $k$  is the rate constant ( $s^{-1}$ ). The Gompertz model is given by equation

## 3.6

$$A_t = A_{max} \exp(-e^{-K(t-t_c)}), A_{max} \leq 100 \quad (3.6)$$

where,  $A_t$  is the % degradation at any time,  $t$ (s),  $A_{max}$  is the maximum degradation,  $K$  is the rate parameter ( $s^{-1}$ ) and  $t_c$ (s) is the critical time.

### 3.3 Effect of NTP on quality of fresh produce

#### 3.3.1 Fresh Produce

Two different products, namely cherry tomatoes (*Solanum lycopersium*) and strawberries (*Fragaria annanasa*) were selected for studying the effect of NTP on their quality. Whole fresh cherry tomatoes (Class I, origin- Egypt, average diameter  $2.6 \pm 0.6$  cm) and fresh strawberries (var. Elsanta, Co. Meath, Ireland) were purchased from a local wholesale agricultural produce market (Smithfield, Dublin) and stored under refrigerated conditions for 1 hour prior to the experiments. Elsanta is the most important strawberry variety in central and north Europe, and therefore of high commercial interest [Gössinger et al., 2009]. Tomatoes and strawberries were divided into two groups- one group was used as control, while the other for in-package plasma treatment. The tomatoes had a pH of  $4.25 \pm 0.10$ , and a soluble solid content of  $4.2 \pm 0.2$  ° Brix, as measured with a hand-held refractometer (Bellingham and Stanley Ltd., UK). The Strawberries used had a pH of  $3.92 \pm 0.09$ , as measured with a calibrated glass electrode ORION pH metre (model 420A, Thermo Fisher Scientific Inc.), and a soluble solid content of  $8.6 \pm 0.2$  °Brix, as measured with a hand-held refractometer (Bellingham and Stanley Ltd., UK). The colour of the strawberries were  $L^* = 47.86 \pm 2.33$ ,  $a^* = 42.49 \pm 1.60$  and  $b^* = 26.63 \pm 2.15$ , recorded using a colorimeter (Colour Quest XE Hunter Lab, Northants, U.K.).

#### 3.3.2 Produce density

To estimate the volume filled by the tomatoes and strawberries inside the package, their apparent density was determined. For cherry tomatoes, the weight was obtained using a precision balance (Sartorius, Germany) and the volume by the

method based on Archimedes principle. The tomatoes were fixed with a thin, straight and hard copper wire and introduced into a beaker filled with a known mass (kg) of water. The temperature of water was recorded using a thermometer to be  $15 \pm 0.2$  °C. The resulting force measured as weight with the balance corresponds to buoyancy of the cherry tomatoes and equals the volume of the water displaced by the tomatoes. The apparent density was determined using the following equation-

$$\rho = \frac{W_{Tomato}}{W_{water}} \quad (3.7)$$

where  $\rho$  is the apparent density,  $W_{Tomato}$  is the weight of the tomato and  $W_{water}$  is the weight of volume of water displaced by the tomato (equal to weight of the tomato). The apparent density of the tomatoes was estimated to be  $1.026 \pm 0.003$  g/cm<sup>3</sup> based on water displacement measurements for 10 samples. This value is in agreement with that reported by [Stertz et al. \[2005\]](#) for organically grown Brazilian cherry tomato variety.

The apparent density of the strawberries was also determined by the volume displacement method using toluene instead of water, to avoid floating [[AOAC, 1998](#)]. The choice of toluene was also based on the fact that it interacts to a lesser extent with the fruit [[Ferrando and Spiess, 2003](#)] and can efficiently fill the shallow dips of strawberries due to its low surface tension. The temperature of the liquid was registered using a thermometer to be  $20.0 \pm 0.2$  °C. The mean apparent density of the strawberry samples was found to be  $0.938 \pm 0.004$  g/cm<sup>3</sup> and was used in the calculations for respiration rate.

### 3.3.3 Plasma treatments

Flexible packages made from high barrier Cryovac B2630 film of size 34 cm × 33 cm were used to pack  $107 \pm 3$  g of tomatoes (10 tomatoes in each package). The average thickness of the film (gauge) was 48 μm. The oxygen and carbon dioxide transmission rates for this film were 4.5 cm<sup>3</sup> (STP)/ (m<sup>2</sup>-24 h-atm) and 66 cm<sup>3</sup> (STP)/(m<sup>2</sup>-24 h-atm) at 0% RH, 4 °C. The water vapour transmission rate of the film was 0.45 g/(100 in<sup>2</sup>-24h) at 100% relative humidity and 37 °C. The bags were filled to approximately 3.5 L with air using a laboratory electric pump. The at-

atmospheric conditions at the time of treatment were  $22 \pm 1$  °C and  $45 \pm 4\%$  relative humidity. The low gas permeability of the packaging films allowed retention of the active plasma species without leakage. A single value of 30 kV RMS voltage and four different treatment times, 30 s, 60 s, 180 s and 300 s were selected for the experiments, while each experiment was performed at least in duplicate. Treatments were carried out by indirect mode, meaning that the tomatoes were placed away from the inter-electrode zone thereby ensuring homogeneous discharge. When indirectly treated, the charged particles and short-lived transient-state species do not affect the sample under treatment, as they recombine before reaching it. This leaves only stable reactive species to act on the samples. The control and treated packages were stored under accelerated conditions at  $20 \pm 2$  °C and  $60 \pm 5\%$  RH conditions in an environmental chamber (MLR-350HT, Sanyo Electric Biomedical Co. Ltd., Japan).

For treatment of strawberries, the sealed, rigid polypropylene package with berries was placed in the inter-dielectric space. The strawberries itself were however, not located in the inter-electrode space (indirect treatment). Treatments were carried out at ambient temperatures of 25 °C. The strawberry samples were subjected to ACP treatment for 5 minute and subsequently stored for 24 h at 10 °C and 90% RH.

### 3.3.4 Respiration rate

The change in gas composition ( $O_2$  and  $CO_2$ ) inside each package was monitored over time using a gas analyser (Systech Instruments, UK) for the packaged cherry tomatoes. After 24 h of storage the treated strawberries were carefully moved into a gas jar (2.365 L volume) inside a sterile incubation chamber, flushed with the respective gases at the inflow rate of 2.5 L/min for 3 min, sealed to air tight conditions and stored at 10 °C and 90% relative humidity (RH). Gas sampling was performed with a hypodermic needle inserted through an adhesive septum previously fixed to the bags, at a flow rate of 150 mL/min for 10 s. The instrument is based on electrochemical sensor to record  $O_2$  concentration, and uses a mini-IR spectrophotometer to record  $CO_2$  concentrations (accuracy: 0.1% v/v  $O_2$ ; 2% v/v  $CO_2$ ). Initial experiments showed that sampling had no significant influence on

gas concentration in the packages or respirometer, as the total volume was much greater than the volume sampled by the instrument during the experiment.

### 3.3.5 Produce colour

For cherry tomatoes, colour was quantified using L\*-a\*-b\* colorimetry (using Colour Quest XE Hunter Lab, Northants, U.K.) after 14 days of storage, while for strawberries it was measured after the 24 h storage period. The colour measurement was performed on (along four symmetrical sections) each cherry tomato and strawberry, and average values reported. The instrument was calibrated using white ( $L^* = 93.97$ ,  $a^* = 0.88$  and  $b^* = 1.21$ ) and green ( $L^* = 56.23$ ,  $a^* = 21.85$ ,  $b^* = 8.31$ ) standard tiles. The  $L^*$  parameter (lightness index scale) ranges from 0 (black) to 100 (white). Parameter  $a^*$  measures the degree of red (+a) or green (-a\*) colour and the  $b^*$  parameter measures the degree of yellow (+b) or blue (-b\*) colour. The CIE  $L^*$ ,  $a^*$ ,  $b^*$  parameters were used to report the total colour difference as

$$TCD = \sqrt{L^{*2} + a^{*2} + b^{*2}} \quad (3.8)$$

The hue angle ( $h^*$ ) and chroma ( $C^*$ ) were calculated as

$$h^* = \tan^{-1} \left( \frac{b^*}{a^*} \right) \quad (3.9)$$

$$C^* = \sqrt{b^{*2} + a^{*2}} \quad (3.10)$$

The tomato colour index (TI) was calculated using the formula [Arias et al., 2000]

$$TI = \left( \frac{a^*}{b^*} \right) \quad (3.11)$$

### 3.3.6 Firmness

The firmness of control and treated samples was analysed using an Instron texture analyser (Instron 4302 Universal Testing Machine, Canton MA, USA). For cherry tomatoes, the texturometer was mounted with a 500 N load cell and equipped with



a 2 mm flat head stainless steel cylindrical probe which punctures the sample at a download speed of 200 mm/min and a distance of 10 mm [Heredia et al., 2007]. A single whole tomato was placed on the stage for each measurement. The maximum force (N) required to puncture the sample was used as an indication of firmness. The firmness of 3 tomatoes from each package was measured individually and an average firmness value was reported. For strawberries, the force necessary to cause a deformation of 3 mm with a speed of 0.2 mm/s in four strawberries was recorded using an the texture analyser, with a 3.5-mm-diameter flat-faced cylindrical probe. This test measures fruit firmness based on the resistance of the flesh to deformation by the probe [Nunes et al., 2005]. Data were analysed by using Bluehill software.

#### **3.3.7 Weight loss, visual fungal and pH measurement**

Quality parameters of weight loss and visual fungal of cherry tomatoes were monitored for up to two weeks of storage. Weight loss was expressed as a percentage of initial weight of the sample. For visual fungal, the quality of cherry tomatoes was visually assessed on a daily basis by examining for signs of growth of filamentous hyphae or black spots of botrytis. The pH of the cherry tomatoes was determined by using a handheld pH-meter with spear electrode (Eutech Instruments, Thermo Fisher Scientific Inc., Netherlands). Tomato pH was measured in triplicates before packaging, and of control and treated groups at the end of the storage period.

## **3.4 Enzyme Inactivation Studies**

### **3.4.1 Reagents**

Monosodium phosphate, disodium phosphate, p-phenylenediamine, sodium chloride, triton X-100 and hydrogen peroxide were obtained from Sigma-Aldrich, Ireland. Poly(vinylpyrrolidone) (PVPP) was obtained from Fischer Scientific, USA. All the chemicals that were used in the extraction and assay of the enzymes were of analytical grade or higher degree of purity.

## 3.4.2 Plasma Treatment and Sample preparation

### 3.4.2.1 Strawberries

Whole packaged strawberries were used for NTP treatments. Samples were treated at three voltage level of 30, 40 and 50 kV for 1-5 minutes of treatment time. After DBD plasma treatments, samples were stored for 24 hours at room temperature before enzyme extraction. Following treatment, enzyme extraction was done using the method of [Terefe et al. \[2010\]](#). The extraction solution was made in 0.2 M sodium phosphate buffer (pH=6.5) consisting of 4% (w/v) poly(vinylpyrrolidone) (PVPP), 1% (v/v) triton X-100 and 1 M NaCl (Sigma Aldrich, Ireland). Strawberry samples were homogenized with the extraction solution (1:1) and centrifuged (Sanio MSE Mistral 3000ii, UK) at 14,000g and 4 °C, for 30 min. The supernatant was used as the crude enzyme extract for POD assay.

### 3.4.2.2 Cherry tomatoes

Crude enzyme was extracted from cherry tomatoes, following the method used by [Hemeda and Klein, 1990](#) with slight modifications and used for plasma treatments. Tomatoes were washed and cut into small pieces and blended at high speed for 1 minute with 20% (w/v) water addition at 4 °C. The homogenate was stirred for 15 min and then centrifuged at a relative centrifugal force of 13000 g for 30 min at 4 °C with a centrifuge (Sanio MSE Mistral 3000ii, UK). Supernatant solutions were collected and then filtered through Whatman No. 4 paper. The filtered solution constituted the enzyme extract and it was kept frozen at -18 °C until plasma treatments, which were carried out within 48 h of the extract preparation [\[Ercan and Soysal, 2011\]](#). The plasma treatment of the crude enzyme extraction was carried out in petri plates (60 mm diameter × 15 mm height) placed inside the DBD. Treatments were carried out at 30, 40 and 50 kV for 1-5 minute. Each experiment was run in two replicates (15 mL extract per run) and all measurements were performed at least in duplicate.

### 3.4.3 Enzyme assay

POD activity was measured using the method described by [Cano et al. \[1997\]](#). POD activity was assayed spectrophotometrically by placing 2.7 mL of 0.05 M sodium phosphate buffer (pH = 6.5), 0.2 ml of p-phenylenediamine (10 g/kg) as H-donor, 0.1 ml of hydrogen peroxide (15 g/kg) as oxidant and 0.1 ml of enzymatic extract in a 1 cm path cuvette. The oxidation of p-phenylenediamine was measured at 485 nm and 25 °C using a Shimadzu UV 1800 spectrophotometer (Shimadzu Scientific Instruments) for 10 min in kinetic mode. POD activity was determined by measuring the initial rate of the reaction computed from the linear portion of the plotted curve. One unit of POD activity was defined as a change in absorbance at 485 nm  $\text{min}^{-1} \text{ml}^{-1}$  of enzymatic extract.

### 3.4.4 Peroxidase inactivation kinetics

The percentage of residual POD activity (RA) was defined by equation [3.12](#):

$$RA = \frac{A_t}{A_0} \cdot 100 \quad (3.12)$$

where  $A_t$  and  $A_{max}$  were the enzyme activities of treated and untreated samples, respectively.  $A_t$  and  $A_0$  were determined immediately after plasma treatment to avoid any effect of storage time. Experimental data was modelled using a first-order inactivation model (equation [3.13](#)).

$$RA = RA_0 \cdot e^{-K_p \cdot t} \quad (3.13)$$

The inactivation rate constant  $K_p$  was obtained by least squares non-linear regression. The inactivation rate constant  $K_p$  can also be obtained from the slope of the regression of  $\ln(RA)$  compared with treatment time ( $t$ , min). Weibull distribution (equation [3.14](#)), was also fitted for investigation of the inactivation kinetics.

$$RA = RA_0 \cdot e^{-\left(\frac{t}{\alpha}\right)^\gamma} \quad (3.14)$$

where,  $RA(\%)$  is the residual activity of POD at time  $t$ ,  $RA_0 (\%)$  is the residual activity without any treatment (100%),  $t$  is the treatment time (min),  $\alpha$  is the

scale factor ( $\min$ ) and  $\gamma$  is the shape parameter (dimensionless) which indicates concavity or convexity of the curve. It is to be noted that Weibull model was first employed to describe destruction kinetics of microorganisms, but has also been used for studying enzyme inactivation kinetics [Elez-Martínez et al., 2006] for other nonthermal technologies.

In addition to first order and Weibull models, a three parameter logistic model, presented in equation 3.15, was also evaluated, considering the visual shape of data.

$$RA = \frac{(100 - A_{min})}{1 + \left(\frac{t}{t_{50}}\right)^p} + A_{min} \quad (3.15)$$

where,  $A_{min}$  ( $=0$ ) is the minimum value attained by the logistic function,  $t_{50}$  is the time for half maximal activity and  $p$  is the power term. This equation represents a sigmoidal type of inactivation curve.

## 3.5 FTIR Spectroscopy & Chemometrics

### 3.5.1 Produce

Fresh strawberries (*Fragaria × ananasa*, var. Elsanta, Class I) were purchased from the local wholesale fruit market (Dublin, Ireland) and stored under refrigerated conditions for  $\sim 1$  h before carrying out the experiments.

### 3.5.2 Plasma treatment

Two discreet voltages viz. 60 and 80 kV (RMS) at 50 Hz frequency were applied across the electrodes for these experiments. The rigid PET package had dimensions of 150 mm  $\times$  150 mm  $\times$  35 mm. Packages with strawberry samples were sealed inside polymeric film of 50  $\mu$ m thickness (Cryovac BB3050, SealedAir, UK) with very low gas transmission rates. All treatments were conducted in air. The atmospheric air condition at the time of packaging and treatment was  $42 \pm 1\%$  relative humidity (RH) and  $25 \pm 2$  °C, as measured using a humidity-temperature probe connected to a data logger (Testo 176 T2, Testo Ltd., UK). The strawberry

samples were subjected to nonthermal plasma treatment for 1 and 5 minutes and subsequently stored for 24 h at 10 °C and 90% RH.

### 3.5.3 Sample preparation

The control and treated group of strawberries were chopped and frozen for 24 h at -80 °C in a cryogenic fridge (Model 906, Thermo Scientific Forma, -86 Ultralow Freezer). Subsequently, they were freeze-dried for a period of 24 h and then manually ground into fine powder using a mortar and pestle. A 3% w/w dilution of the ground samples was prepared by mixing 9 mg of the sample with 281 mg of dry potassium bromide (KBr, Sigma-Aldrich, Ireland). Pellets were prepared by exerting a pressure of 100 kg/cm<sup>2</sup> for approximately 1 minute in a pellet press (Specac, United Kingdom).

### 3.5.4 FTIR Analysis

The IR spectra were recorded using a Nicolet Avatar 360 FTIR E.S.P. (Thermo Scientific, Waltham, MA, USA) over the frequency range 4000-400 cm<sup>-1</sup> by co-adding 64 interferograms. Two scans of each pellet were collected in transmittance units at 2 cm<sup>-1</sup> resolution at room temperature using OMNIC software (version ESP 5.2). These spectra were subtracted against background air spectrum. After every scan, a new reference air background spectrum was taken. To account for variations that could result from pellet thickness and uniformity, different pellets were prepared from the same sample and their spectra pooled (spectra were nearly identical). The sample measurements were replicated for four individual samples of each treatment class.

### 3.5.5 Data pre-processing

The wavenumber vs. transmittance spectra were first converted to absorbance spectra for further mathematical treatment. The spectral data was corrected for artefacts and undesirable scatter effect by multiplicative scatter correction (MSC), a data transformation method. This involved two steps [[Rinnan et al., 2009](#)]-

1. Estimation of the correction coefficients (additive and multiplicative contributions)

$$Y_{org} = b_0 + b_{ref,1} \cdot Y_{ref} + e \quad (3.16)$$

2. Correction of the recorded spectrum

$$Y_{corr} = \frac{(Y_{org} - b_0)}{b_{ref,1}} = \frac{Y_{ref} + e}{b_{ref,1}} \quad (3.17)$$

where,  $Y_{org}$  is one original sample spectra measured by the instrument,  $Y_{ref}$  is a reference spectrum used for pre-processing of the entire dataset,  $e$  is the un-modeled part of  $Y_{org}$ ,  $Y_{corr}$  is the corrected spectra,  $b_0$  and  $b_{ref,1}$  are scalar parameters, which differ for each sample. The average spectrum of the entire dataset was used as the reference spectrum. MSC was performed using the R statistical software (<http://www.r-project.org/>).

### 3.5.6 Multivariate chemometric methods

Pre-processed spectra or pre-processed second derivative spectra were exported as text files for file format modification on Microsoft Excel for statistical treatment on R 3.0.2. Second derivative spectra were systematically used to improve the infrared band resolution and thus enhance the discrimination of vibrators contributing to the shape of raw FTIR spectra [Céline et al., 2014].

#### 3.5.6.1 Correlation heatmap analysis

Correlations in the wavelength space were computed to compare the scaled second derivative spectra. This method has the advantage of relying only on the shape of the spectra and not on the absolute magnitude of the responses. The dot product correlation coefficient ( $r$ ) is given by

$$r = \frac{\sum X_i Y_i}{\sum X_i^2 Y_i^2} \quad (3.18)$$

where,  $X_i$  and  $Y_i$  are the ordinate values of the two spectra being compared at wavelength  $i$ , the summations being performed over the whole or a selected part of the spectra [Li Yoon et al., 1999]. Correlation heat map analysis was performed using the R statistical software (<http://www.r-project.org/>) with *spatstat*, *RColorBrewer* and *gplots* packages.

### 3.5.6.2 Principal Component Analysis (PCA) and Hierarchical Clustering on PCs (HC-PC)

PCA was performed on the second derivative spectrum to visualise the high dimensional spectral data. The PCA loadings plot was used to identify the frequency range where maximum changes were perceivable. Hierarchical clustering on principal components (HC-PC) of the spectral data matrix was also performed using the R statistical software (<http://www.r-project.org/>) with *FactoMineR* package [Lê et al., 2008].

## 3.6 Bioactive and Volatile profile

For the bioactive and volatile profiling experiments, the cold plasma treated strawberry samples were frozen in a cryogenic freezer and stored at  $-80\text{ }^{\circ}\text{C}$  before subsequent analysis.

### 3.6.1 Ascorbic acid content

The ascorbic acid content in strawberries was analysed by HPLC with a slight modification of the method described by Uckoo et al. [2013]. Briefly, the strawberry samples were homogenised at 24000 rpm using an UltraTurrax T-25 Tissue homogeniser. 1 g of the homogenate was diluted with 1 mL of 3% metaphosphoric acid, in a centrifuge tube and mixed for 15 min. The diluted sample was centrifuged at 10,000 rpm for 10 minutes and the clear supernatant was filtered through  $0.45\text{ }\mu\text{m}$  membrane filter.  $10\text{ }\mu\text{L}$  was injected into the HPLC for analysis.

The HPLC system consisted of a Waters 600 Satellite connected to a Waters UV-tuneable absorbance detector and Waters autosampler (Waters, Ireland). The mobile phase consisted of isocratic 3 mM phosphoric acid in water maintained at

a flow rate of 1 mL/min. Ascorbic acid was separated on a C-18, Phenomenex Gemini-Nx series column (Phenomenex, U.K.), 5  $\mu\text{m}$  particle size, 110Å pore size (250 mm  $\times$  4.6 mm). Peak separation of ascorbic acid was monitored at  $\lambda=254$  nm. Five concentrations of ascorbic acid standard in 6% metaphosphoric acid in the range 10-100  $\mu\text{g}/\text{mL}$  were injected, and the peak area and height were determined. Chromatographic data was collected and processed using Empower2 software (Waters, Ireland).

### 3.6.2 Anthocyanin content

For extraction, the strawberry samples were homogenised at 24000 rpm using an UltraTurrax T-25 tissue homogeniser. 5 g of the homogenised strawberry puree was mixed with 10 mL of 7:3 acetone: water mixture (with 0.1% Acetic acid) and sonicated for 10 min. Following sonication, the mixture was centrifuged for 10 min at 1500g, 4 °C and the supernatant collected. 10 mL of acidified methanol (0.1% acetic acid) was added to the residue, sonicated for 10 min, followed by centrifugation for 10 min at 1500 g (4 °C) and the supernatant was collected. The supernatants obtained were pooled and dried under a constant nitrogen flow to 1 mL. The volume was made up to 10 mL using water and methanol mixture (1:1 with 0.1 % acetic acid). The extract was injected after filtration through 0.45  $\mu\text{m}$  PTFE syringe filter (Phenomenex, U.K) and placed in an autosampler vial.

The HPLC system consisted of a Waters 600 Satellite connected to a Waters UV-tunable absorbance detector and Waters autosampler (Waters, Ireland). Separation was carried out on a C-18, Phenomenex Gemini-Nx column (Phenomenex, U.K.), 5  $\mu\text{m}$  particle size (250 mm  $\times$  4.6 mm). For HPLC, the mobile phase was a solution comprising of a mixture of acetonitrile (83 mL), methanol (33 mL) and acetic acid (170 mL) which were mixed with trichloroacetic acid (0.65 g) which was previously dispersed in water and made to a final volume of 1 L with distilled water. The sample loop was 20  $\mu\text{L}$  with an isocratic flow rate of 1 mL/min and the total run time was less than 10 min. Detection was carried out at 520 nm. For quantification, external calibration curves for pelargonidin-3-glucoside (P3G) were prepared at concentrations ranging between 25  $\mu\text{g}/\text{mL}$  to 100  $\mu\text{g}/\text{mL}$ . Chromatographic data was collected and processed using Empower2 software (Waters,



Ireland).

### 3.6.3 Volatile profile by HS-SPME/GC-MS

The extraction of volatiles from the strawberry samples was performed according to the method described by [Vandendriessche et al. \[2013a\]](#) with some modifications. The frozen strawberry samples were allowed to thaw to about 5-10 °C, followed by crushing in a mortar and pestle and homogenisation at 18000 rpm using an UltraTurrax T-25 tissue homogeniser. For aroma analysis, 5 g of strawberry puree was transferred into a 20 mL glass headspace vial, flushed with helium gas and sealed using crimp-top caps with silicone septa seals. Prior to solid phase micro-extraction (SPME), the strawberry samples were incubated for 10 min at a temperature of 35 °C. Headspace (HS) volatiles were extracted by exposing a 100 µm PDMS (polydimethylsiloxane) coated SPME fibre to the vial headspace for 10 min at a temperature of 35 °C.

A Varian 3800 GC (JVA Analytical Ltd., Ireland) with a 2200 Varian ion trap MS was used to analyze the samples. SPME fibre injections were made splitless for the entire GC runtime with the GC injection port temperature held at 250 °C. Grade 5.0 helium, filtered through a Gas Clean GC/MS filter (Varian), was used as the carrier gas at a constant flow rate of 1.5 mL/min. Volatile compounds were adsorbed by a fused-silica capillary column (CP-Sil 8, JVA Analytical Ltd., Ireland) with a length of 30 m, an inner diameter of 0.25 mm and a 0.25 µm film thickness. The initial column oven temperature was set at 35 °C and held at this temperature for 5 min. The temperature was then increased to 75 °C at a rate of 10 °C/min, then ramped to a final temperature of 250 °C at a rate of 5 °C/min and held isothermal for 15 min. MS analysis of the eluted compounds was then carried out using the technique of electron impact ionization. The electron ion source energy used was 70 eV and the mass range chosen was from 35 m/z to 350 m/z. Data were collected using the Varian software. Volatile compounds present in strawberries were tentatively identified basing on computer matching against commercial (NIST 2008) libraries and on our own spectral library of pure substances and literature data. The aim of the present work being comparison of different treatments, absolute quantification was not strictly necessary and therefore peak

areas were used for analysis.

## 3.7 Pesticide Degradation studies

### 3.7.1 Produce

Fresh strawberries (*Fragaria ananasa*, var. Elsanta) were purchased from the local wholesale fruit market (Dublin, Ireland) and stored under refrigerated conditions for  $\sim 1$  h before carrying out the experiments. The strawberries were screened for the presence of pesticides and those selected were found to be absent for the studied pesticides.

### 3.7.2 Reagents

Acetone ( $\geq 99.9\%$  capillary GC-grade), Dichloromethane ( $\leq 0.0005\%$  non-volatile matter), Petroleum Ether, Ethyl Acetate ( $\leq 0.0005\%$  non-volatile matter) and Sodium Sulphate (anhydrous) were all obtained from Sigma-Aldrich, Ireland. Azoxystrobin, Cyprodinil, Fludioxonil and Pyriproxyfen standards were also obtained from Sigma-Aldrich, Ireland.

### 3.7.3 Exposure of samples to pesticides

A cocktail of all the four pesticide standards was prepared in ethyl acetate at 100 ppm concentration i.e. 25 ppm of each. Initial quality control runs in our laboratory have shown that the selected pesticides do not react with each other. To ensure a homogeneous distribution of pesticides on the fruit surface, we adopted the method of immersion into the pesticide solution for 15 s. The dipped pesticides were allowed to air-dry under dark conditions, inside a laminar flow hood for 1 h, followed by a second dip for 15 s and repeated drying. This method allowed an effective transfer of pesticides to the strawberry at levels of  $\sim 2$  ppm.

### 3.7.4 Cold plasma treatment

Three discreet voltages viz. 60, 70 and 80 kV (RMS) at 50 Hz frequency were applied across the electrodes for these experiments. The rigid PET package had dimensions of 150 mm × 150 mm × 35 mm. The atmospheric air conditions at the time of packaging and treatment was 42±1% relative humidity (RH) and 25±2 °C, as measured using a humidity-temperature probe connected to a data logger (Testo 176 T2, Testo Ltd., UK). The strawberry samples were subjected to ACP treatment for 60, 120, 180, 240, and 300 s and subsequently stored for 24 h at 10 °C and 90% RH.

### 3.7.5 Analysis of pesticides

#### 3.7.5.1 Extraction procedure

A number of methods currently exist for the extraction and analysis of multi-residue pesticides from a variety of food matrices. We employed the mini-Luke (multi-residue) method using acetone, dichloromethane and petroleum ether mixture (1:1:1) for the extraction of pesticide residues. Briefly, ca. 15 g of homogenised strawberry sample was blended (T25 Ultra-Turrax, Ika Works Inc., USA) with 30±1 mL of acetone, followed by addition of 30±1 mL of Dichloromethane and 30±1 mL of Petroleum ether and further blending. 30±1 g of sodium sulphate ( $Na_2SO_4$ ) was then added and blended for 30 s to salt out the polar pesticides. This mixture was then centrifuged for 5 min at 3500 rpm and the organic phase collected. Subsequently 60 mL of the organic phase was concentrated in a rotary evaporator to ca. 2 mL with an intermediate step involving addition of 10 mL ethyl acetate. Appropriate dilutions were performed before loading on the auto sampler.

#### 3.7.5.2 GC-MS/MS Analysis

Gas chromatography coupled to mass spectrometry (GC-MS/MS) is widely used in the analysis of pesticides that are highly volatile [Likas et al., 2007]. An Agilent 7890N GC coupled with Agilent 7000A triple quadrupole MS was employed for the analysis of pesticides, with ionization achieved by electron impact at 70 eV

in multiple reaction monitoring (MRM) mode. The capillary column used was an Agilent 190915-433 capillary column (30 m × 0.25 mm I.D. × 0.25 μm thickness) with HP-5MSI (5% Phenyl Methylpolysiloxane) stationary phase. The operating conditions were: injection port temperature, 250 °C; interface temperature, 280 °C; column oven temperature, 100 °C for 5 min, ramped at 20 °C/min to 180 °C, followed by 5 °C/min to 280 °C for 10 min; helium carrier gas (flow rate of 1.0 mL/min); 2 μL injection volume. The split/splitless injector was operated in the split-less mode. Sample injection was automated with the use of an Agilent 7693 auto sampler.

### 3.7.5.3 Calibration Curve

A five point calibration curve was constructed for each pesticide covering a range of 10-250.0 ng/mL. The resulting correlation coefficients were higher than 0.991 in all cases. Quantifications of pesticides based on peak area data were conducted using these curves.

### 3.7.6 Data Analysis

GC-MS/MS data were acquired with Agilent MassHunter Workstation acquisition software and analysed using Agilent MassHunter Workstation Qual software (ver. B.05.000 SP02/Build 5.0.291.4, Agilent Technologies). Spectral deconvolution was performed on open-source AMDIS software provided by NIST. The significance of differences among treatments was evaluated using Tukey's multiple comparison test at significance levels of  $p \leq 0.05$  (SPSS ver 19, SPSS Inc., Chicago, IL).

## 3.8 Numerical methods and statistical analysis

Multiple comparison analysis by Tukey method was used to analyse the significance of differences between different treatments using SPSS statistical package (SPSS ver 19, SPSS Inc., Chicago, IL). Means were considered significant at  $p \leq 0.05$ . For model fitting and parameter elucidation, programs were written in MatLab Version 7.0 (The MathWorks, MA, USA). Model fitting was done by nonlinear regression routines using Levenberg-Marquardt algorithm. For the evaluation of

the fitting capacity of the models, the statistical criterion of the adjusted coefficient of multiple determinations ( $R_{adj}^2$ ) and the root mean squared error RMSE have been used.

$$RMSE = \sqrt{\frac{\sum_{i=1}^{n_t} [y_{exp}(t_i) - y(t, p)]^2}{n_t - n_p}} \quad (3.19)$$

where  $y_{exp}(t_i)$  denotes the experimental observations,  $y(t, p)$  the predicted values,  $n_t$  the total number of data points,  $n_p$  the number of estimated model parameters.

$$R_{adj}^2 = 1 - \left( \frac{n_t - 1}{n_t - n_p} \right) \cdot \left( \frac{SSE}{SSTO} \right) \quad (3.20)$$

Herein, SSTO is the total sum of squared errors and SSE the sum of squared errors.

# Chapter 4

## Plasma diagnostics

To optimise the performance of the system it is necessary to develop a method to rapidly characterise the levels and action of ozone (and other species) generated inside the package. In order to achieve this, methylene blue (MB) dye was selected as model indicator for in-package treatment. MB is commonly used as redox indicator in analytical chemistry. It is worthwhile noting that MB is also a potential environmental pollutant released from textile industries [Chen, 2000] and is an ideal simulant for colorant in food industry effluents. Thus, the impacts of this work could be twofold- (i) A method for assessment of in-package ozone generation from the dielectric barrier discharge configuration using methylene blue dyes as an indicator; (ii) Establishment of the ability and evaluation of the efficacy of degradation of pollutant dyes inside a closed reactor using dielectric barrier discharge as an advanced oxidation process (AOP).

### 4.1 Electrical diagnostics

#### 4.1.1 I-V Characteristics

The current-voltage waveforms for the discharges within packages at different voltage levels are shown in Figure 4.1. The waveforms shown in Figure 4.1 reveal that the applied voltage is near sinusoidal, while the total current is composed of the displacement current superposed by numerous current pulses per half-cycle of the applied voltage. The discharge in the air can be characterized as operating in a

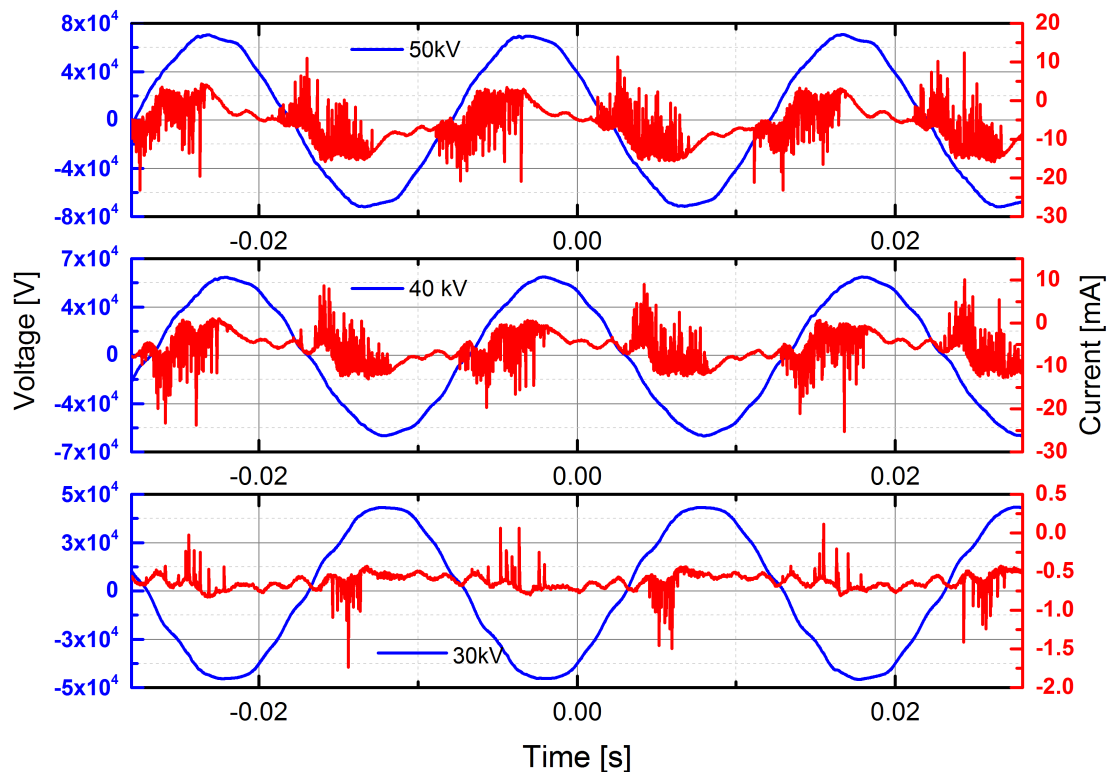


Figure 4.1: The I-V characteristics of the discharge in package.

typical filamentary regime with a microdischarge zone in each half-cycle of the applied voltage, which is organized by numerous streamer clusters at different durations up to the maximum of the applied voltage. This pattern can be observed for all operating situations under consideration (shown in Figure 4.1 are 30, 40 and 50 kV). The use of high voltages permit the generation of a stable discharge, even at large gaps in the centimetre range (2.2 cm to 4 cm). The dielectric is the key factor for the proper operation of the discharge. It limits the charge transported in the discharge, i.e. limits the current flow to the system, and distributes the discharge over the entire electrode area [Dojcinovic et al., 2011].

A note on the barrier discharge phenomena is appropriate at this point. As the high voltage electrode experiences the increase in voltage, so does the gas in the gap between the electrodes. As a consequence, any free electrons in the gap are accelerated, thus acquiring enough energy to cause ionisation. This results in a cascade effect, which exponentially increases the number of electrons in the gap.

Electrons created via electron impact ionization rush toward one of the dielectric plates, in the opposite direction to the electric field. An equal number of ions are also generated during electron impact ionization (the plasma is electrically neutral). The ions rush toward the opposite dielectric plate in the same direction as the electric field. As a result, surface charge with opposite sign accumulates on both dielectric plates. This causes the electric field to become shielded from the gas filled gap. In fact, the electric field across the gap cannot exceed the breakdown electric field, which is highly dependent on the gas and background pressure. The breakdown electric field is also a function of the surface properties of the dielectric material. Surface charge accumulation temporarily terminates the discharge until the field reverses direction and the process repeats in the opposing direction.

#### 4.1.2 Q-V Characteristics

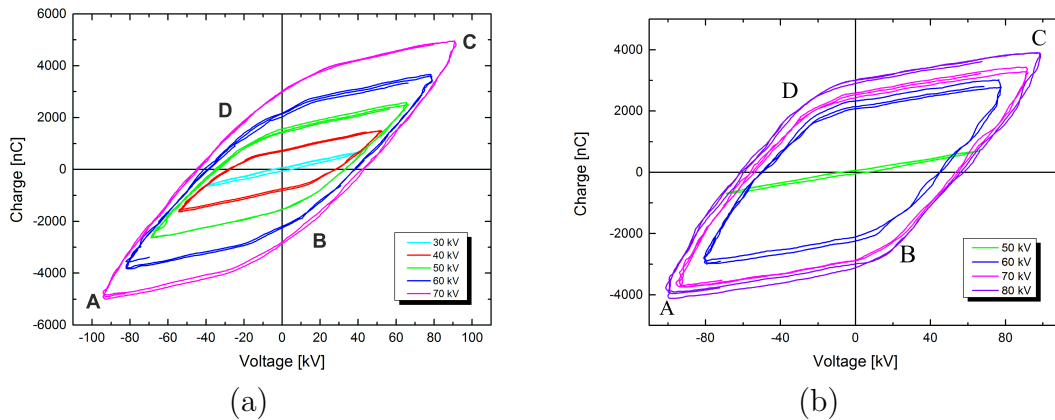


Figure 4.2: The Q-V characteristics of the in-package plasma discharge with (a) 10 mm dielectric at 22 mm gap, and (b) 10 mm dielectric at 42 mm gap.

The charge-voltage (Q-V) characteristics of the discharges at applied voltages are superimposed in Figure 4.2, which represent closed loop Lissajous diagrams, resembling a parallelogram. The resemblance with parallelogram shape indicates that the basic series capacitance model is applicable to our DBD in the experimental conditions used. The slight deviation from an ideal parallelogram shape is typically attributed to the resistive behaviour of the discharge [Zhang et al., 2010]. The sides marked A-B and C-D in the Lissajous figure represent the period



when the discharge is idle while B-C and D-A, its journey through the breakdown, transferring charges through the gap. The slopes yielding the value of the total capacitance are comparatively shallow at lower voltages and the associated error in the slope measurement is estimated to be  $\pm 10\%$  in all cases. Following the very basic nature of a capacitor, the charge transported clearly increases with increase in applied voltage (Figure 4.2). The electrical performances of the discharge derived from the Q-V measurements according to the method developed by Manley [1943], and Falkenstein and Coogan [1997] are shown in Figure 4.3. The discharge

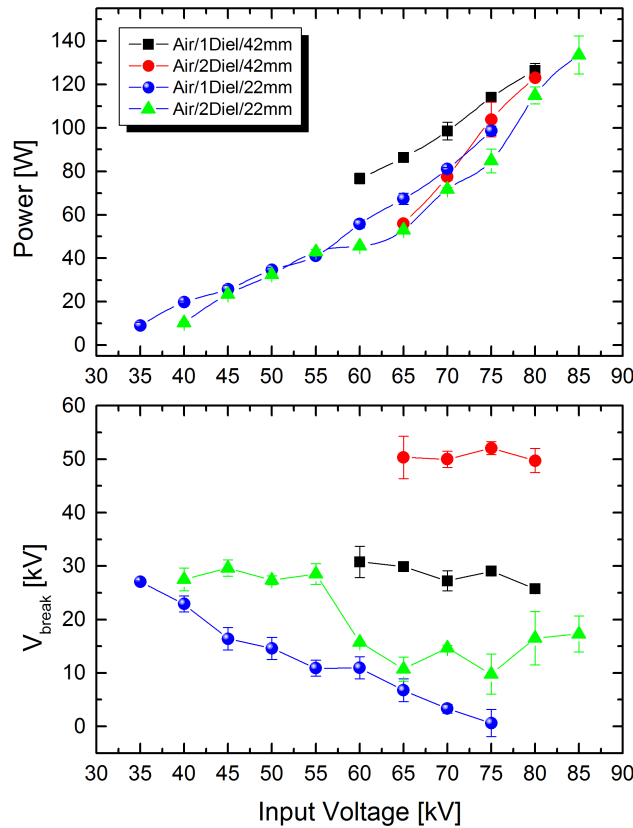


Figure 4.3: Evolution of power input to the gas and the breakdown voltage as a function of applied voltage and dielectric thickness. Legend: 1Diel refers to a single dielectric barrier of 10 mm thickness for driving electrode, while 2Diel refers to an additional dielectric of 10 mm thickness for the driven electrode.

power is calculated as the product of the area of the Lissajous charge-voltage loop and the frequency of applied voltage. An increase in total power input with in-

creases in voltage can be noticed. A single dielectric barrier allows higher power input to the discharge compared to two barriers. However, use of two barriers is recommended for further increasing power inputs while operating over wider input voltage ranges. Within the operating conditions chosen, the power typically varies between 10 to 150 W. A decrease in the breakdown voltage with increase in applied voltage can also be observed. However, the breakdown voltage increases with increase in total dielectric thickness, irrespective of gap width. The discharge features during treatment of produce are discussed in the respective chapters.

## 4.2 Ozone measurement

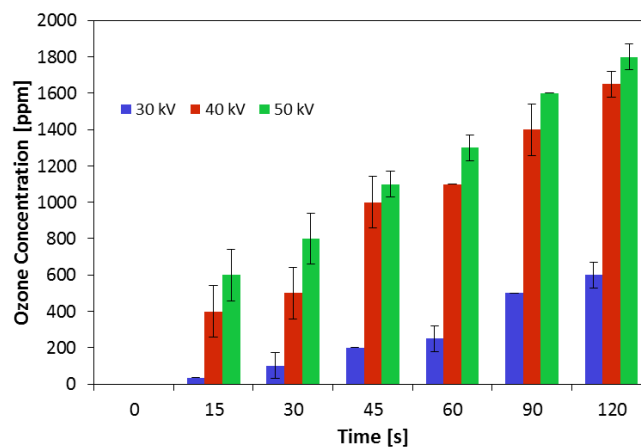


Figure 4.4: Ozone concentration inside package with methylene blue dye.

When high voltage is applied across the electrodes, the electric field generated produces the phenomenon known as DBD [Amjad et al., 2012; Kogelschatz, 2003; Kogelschatz et al., 1997]. These discharges cause the bombardment of electrons on oxygen molecules, breaking it to a single O atom inside the discharge gap, which then combines with oxygen molecule ( $O_2$ ) to form ozone gas ( $O_3$ ) [Amjad et al., 2012]. Considering the fact that ozone is a powerful oxidant with a redox potential of 2.07 and has many established commercial and industrial applications, ozone levels were specifically measured in this study. DBD is generally recognized as one of the most efficient method to produce ozone [Alonso et al., 2005]. In

this study, concentration of ozone inside the package increased steadily with the duration of ionization as shown in Figure 4.4.

The in-package ozone concentration also increased rapidly in tandem with increasing applied voltage levels. This correlated well with the increased charge transported at higher voltages, which permits increased number of collisions with oxygen for ozone formation. The DBD plasma in air is a source of a wide range of reactive species, created both in the gas and in the liquid phase where the dye is treated. This discharge is able to produce  $O_3$ ,  $H_2O_2$ , OH and other active species. Ozone is mainly produced from air or oxygen by electrical discharges. Beside ozone, electrical discharges in humid air also produce a variety of chemically active species, such as  $O\cdot$ ,  $\cdot OH$ ,  $N\cdot$ ,  $HO_2\cdot$ ,  $N_2^*$ ,  $N^*$ ,  $OH^-$ ,  $O_2^-$ ,  $O^-$ ,  $O_2^+$ ,  $N_2^+$ ,  $N^+$ , and  $O^+$  [Dojcinovic et al., 2011]. The ozone and other active species produced in the gas phase can subsequently dissolve into the aqueous phase (of produce or liquid solutions), where they react with the substrate. The ozone concentrations recorded during each specific study is provided in respective chapters for ease of comprehension.

### 4.3 Optical emission spectroscopy

The energy transferred to the plasma produces various gaseous species in excited states. Some of these species can be identified based on the characteristic optical emission spectra (OES) of the plasma [Chiper et al., 2004]. Accordingly, the existent species in the gas phase were investigated by OES during DBD discharge in this study. Figure 4.5 presents the optical emission spectra in a window of 280 to 1100 nm for the non-thermal plasma in air, operating at 50 kV (RMS) under direct treatment, indirect treatment and for an empty package. Similar trend were observed for other voltages (data not shown). The emission measurements were taken within the first few seconds of the initiation of discharge. Most of the distinct peaks obtained in the near UV region corresponded to strong emissions from  $N_2(C - B)$  second positive system [Gaydon and Pearse, 1976]. Many peaks associated with optical transitions of O atom are observed at low intensities (inset in Figure 4.5): 725.4 nm from  $O(5s^3S \rightarrow 3p^3P)$ , 777.4 nm from  $O(2s^22p^33p^5P \rightarrow 2s^22p^33s^5S)$ , and 749.76 nm from  $O(2s^22p^2(^3P)3d \rightarrow 2s^22p^2(^3P)4p)$ . The relatively lower in-

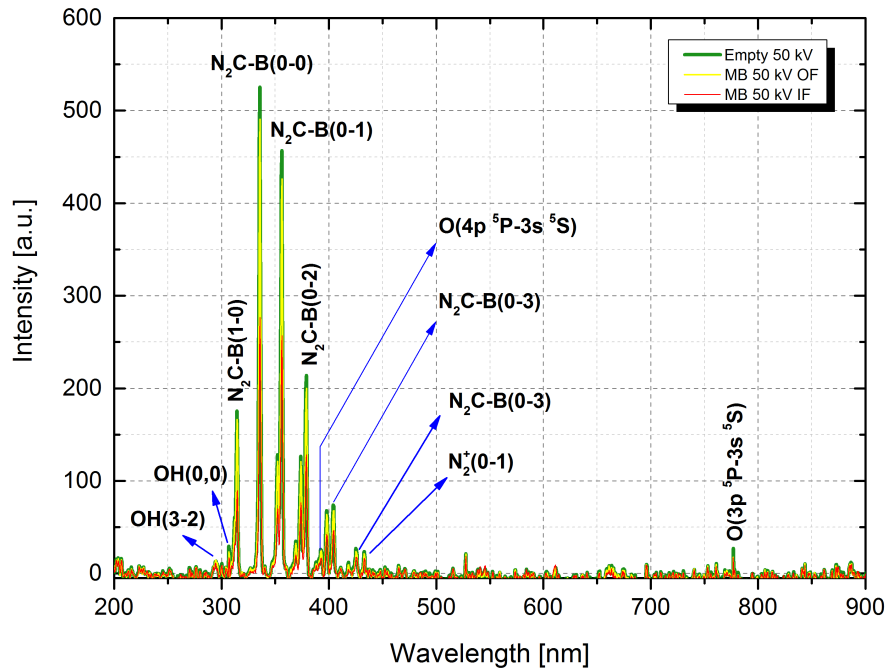


Figure 4.5: Typical Optical Emission Spectrum (OES) of the in-package non-thermal plasma discharge. Operating voltage- 50 kV (RMS).

tensities of peaks associated with oxygen can be explained based on the quenching of  $O(^3P)$  and  $O(^5P)$  in the air plasma [Walsh et al., 2010]. A low intensity OH peak around 300 nm was also observed. The decreasing order of intensity can be explained on the basis of decreased gas volume available when dye sample is present in the package compared to that in an empty package. The difference in intensity among directly and indirectly treated samples is likely due to the diffusion of the reactive species into the liquid as they form. This also explains the observed degradation patterns of the MB dye.

#### 4.4 Dye discolouration for diagnostics

A simple means to monitor the in-package plasma generated reactive species, particularly ozone, is desirable considering the wide applicability of the technology. In the following experiments, non-thermal plasma was generated inside the sealed package and sensitivity of MB to plasma species was evaluated as a marker reac-

tion.

#### 4.4.1 Absorbance spectra of dye

The visible spectra of the dyes exhibited a time and voltage dependent reduction in absorption intensity. A typical absorption spectrum for the dye as a function of treatment time is presented in Figure 4.6 for direct treatment at 30 kV. The

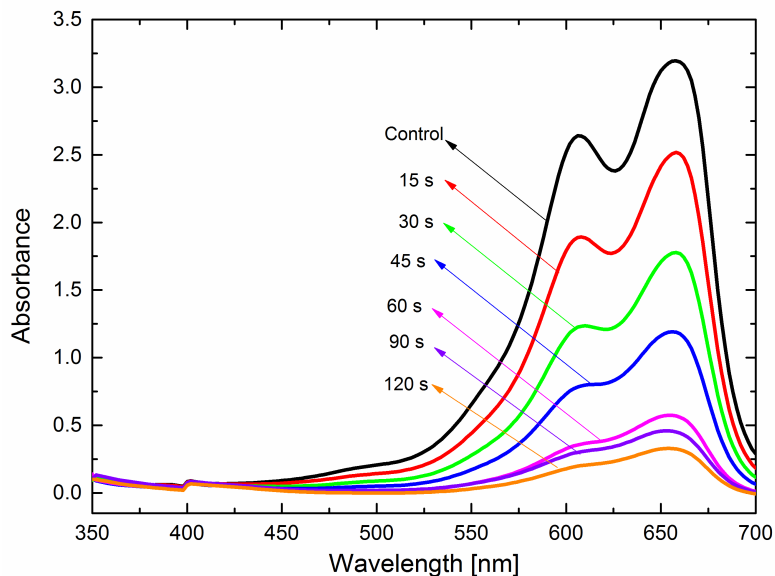
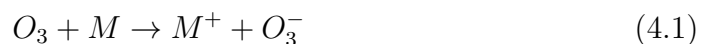
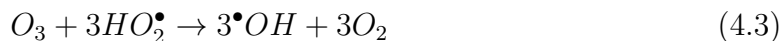


Figure 4.6: Absorption spectra of methylene blue dye treated directly at 30 kV across the electrodes, after 24 h storage.

absorption maxima of the dye samples as a function of treatment variables are presented in Figure 4.7. The recorded spectrophotometric readings were visually appreciable based on the colour of the methylene blue solution, which gradually faded as the degradation reaction proceeded in the presence of reactive species. This discolouration was irreversible and in turn indicated the degradation of the dye by ozone and other oxidative species. Ozone reacts with the dye either by direct oxidative reaction or indirectly by conversion into hydroxyl radicals in the aqueous phase, which in the next step oxidizes matter [Huang et al., 2010]-





The reaction with MB usually involves the oxidant attack on the sulfinic group [Grabowski et al., 2007]. The extent of discoloration was more pronounced for MB dye treated directly in the plasma field relative to those treated indirectly (out-of-field) as can be seen from Figure 4.7. This difference could be explained on the basis of difference in spatio-temporal parameters of diffusion and absence of short half-life metastable species during indirect exposure. When indirectly treated, the charged particles and short-lived transient state species do not affect the sample under treatment as they recombine before reaching it. This leaves mainly the long-lived radicals to directly interact with the sample [Laroussi, 2009].

#### 4.4.2 Kinetics of discoloration

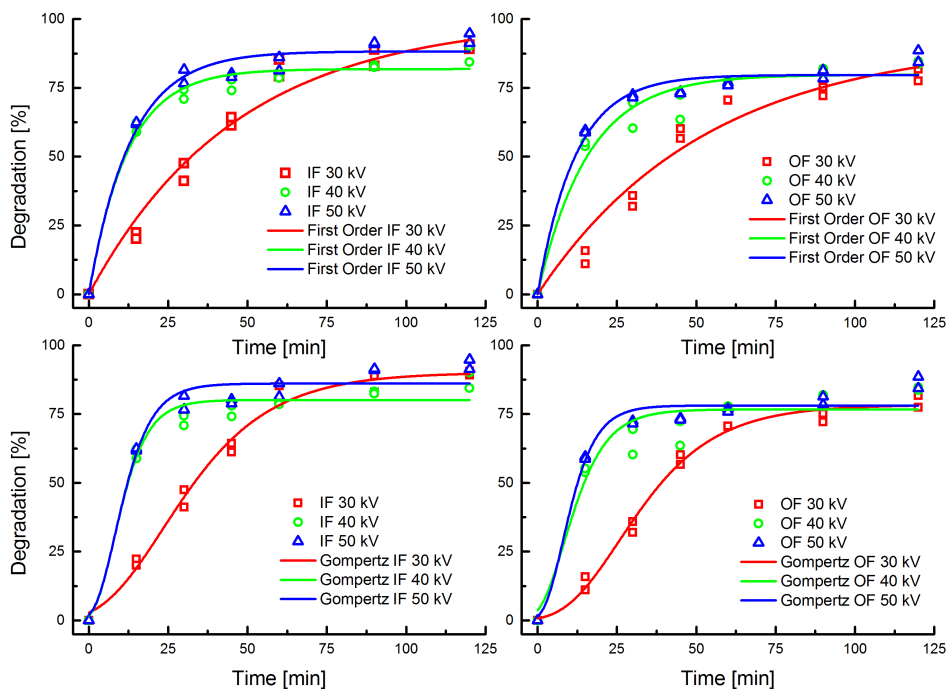


Figure 4.7: Experimental data and fitted lines for degradation kinetics of methylene blue treated in-field (IF) and Out-of-field (OF).

The model parameters obtained from the regression have been summarised in

Table 4.4.2. It is clear that both models are not completely suitable for describing the kinetics. The Gompertz model is efficient in describing the sigmoidal trend for treatments at 30 kV but not at the higher voltages. The peculiar nature (extended lagging) of the degradation at 30 kV relative to other voltages remains unknown at this point. This is more likely an outcome of the plasma chemistry, which is quite complex. Overall, the first-order model can be considered better compared to the Gompertz model based on the RMSE values. The suitability of a general quadratic model for describing the degradation of MB dye taking into account both treatment time and voltage simultaneously (interaction effect) was also evaluated in this study (data not shown). However, the quadratic model was found inadequate as a global model, which was explained by the simultaneous non-linear effects of both variables.

Table 4.1: Parameters of fitted model and goodness of fit in terms of coefficient of determination and root mean square error for degradation kinetics of methylene blue.

Voltage, Mode	Gompertz Model			First-Order Kinetics		
	Param	Value ( $\pm$ S.E.)	RMSE, $R_{adj}^2$	Param	Value $\pm$ S.E.	RMSE, $R_{adj}^2$
30kV, Direct	$A_{max}$	$90.09 \pm 2.09$	3.64, 0.98	$A_{max}$	$100.00 \pm 5.78$	5.55, 0.97
	$t_c$	$23.28 \pm 1.14$		$k$	$0.021 \pm 0.002$	
	K	$0.05 \pm 0.004$				
30 kV, Indirect	$A_{max}$	$78.33 \pm 1.55$	2.82, 0.99	$A_{max}$	$92.25 \pm 8.06$	6.45, 0.95
	$t_c$	$25.67 \pm 0.93$		$k$	$0.03 \pm 0.003$	
	K	$0.059 \pm 0.004$				
40 kV, Direct	$A_{max}$	$80.13 \pm 1.61$	4.86, 0.97	$A_{max}$	$81.84 \pm 1.39$	3.66, 0.98
	$t_c$	$7.91 \pm 1.53$		$k$	$0.082 \pm 0.007$	
	K	$0.17 \pm 0.03$				
40 kV, Indirect	$A_{max}$	$76.67 \pm 2.45$	7.08, 0.94	$A_{max}$	$79.76 \pm 2.16$	5.15, 0.97
	$t_c$	$8.34 \pm 1.82$		$k$	$0.06 \pm 0.007$	
	K	$0.13 \pm 0.03$				
50 kV, Direct	$A_{max}$	$86.09 \pm 1.80$	5.35, 0.97	$A_{max}$	$88.26 \pm 1.58$	4.04, 0.98
	$t_c$	$8.36 \pm 1.50$		$k$	$0.075 \pm 0.006$	
	K	$0.16 \pm 0.03$				
50 kV, Indirect	$A_{max}$	$78.09 \pm 1.60$	4.83, 0.97	$A_{max}$	$79.68 \pm 1.45$	3.84, 0.98
	$t_c$	$7.96 \pm 1.66$		$k$	$0.083 \pm 0.008$	
	K	$0.17 \pm 0.04$				

## 4.5 Change in pH

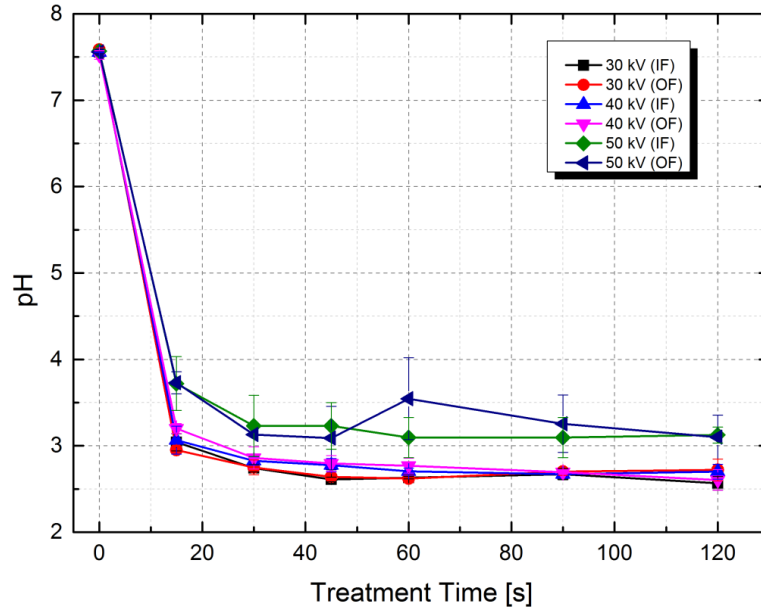


Figure 4.8: Time evolution of pH of MB dye following plasma treatments.

It was noticed during the experiments that the pH value decreases after the in-package plasma treatments (Figure 4.8). This decrease in pH was statistically significant ( $p \leq 0.05$ ) compared to that of untreated dyes. Such a decrease in pH of DBD treated methylene blue solution has also been reported by [Huang et al. \[2010\]](#). The process chemistry may be modulated by changing the pH value [[Grabowski et al., 2007](#)]. The pH shifts of growth media and suspensions subjected to non-thermal plasmas has been explained based on the formation of nitric acid ( $\text{HNO}_3$ ) and nitrous acid ( $\text{HNO}_2$ ) as well as hydrogen peroxide ( $\text{H}_2\text{O}_2$ ), in previous studies [[Oehmigen et al., 2010](#)]. Thus, the drastic drop in the pH is suspected to be the outcome from the formation of strong acids as a consequence of diffusion of active species into the solution and oxidation of the dyes.



## 4.6 Conclusions

The dielectric barrier discharge plasma source was electrically characterised and found to operate in the filamentary regime. The operation in a filamentary regime is acceptable in that the purpose of the discharge is only to generate active species which possess antimicrobial activity. Traditionally DBDs operate in a glow discharge regime to attain a homogeneous distribution of discharge filaments for uniform surface treatments.

The use of high voltages allow a stable discharge even at large gaps in the order of the centimetre scale. Under typical operating conditions, depending on the configuration, the power input to the gas can be as high as 150 W. Such low power requirements point to the fact that the technology is energy efficient and therefore could prove to be very sustainable.

The UV-Vis emission spectrum of the plasma revealed emission bands for excited nitrogen and oxygen species including strong emission lines for excited states of the atomic species. The ozone measurements revealed a voltage and time dependent rise in ozone concentrations, which was in the order of thousands of ppm. The sudden change of the air into a high ozone environment would permit rapid inactivation of micro-organisms. However, a limit over the concentrations should be established in light of the possible loss quality.

The dye samples exhibited a non-linear time and voltage dependent degradation with a typical sigmoidal shape with respect to time. Such observations are most likely an outcome of the complex plasma chemistry. Discolouration of dyes can be employed for assessing the effectiveness of plasma for short operation times in the order of 1 minute, i.e. only in within the exponential phase of kinetics. However, dye discolouration as a diagnostic is not an ideal approach for situations where the concentration of reactive species is very high.

## Chapter 5

# Effect of nonthermal plasma on quality of cherry tomatoes

This study was undertaken to investigate the effects of nonthermal plasma generated within a sealed package on the quality parameters and respiration rates of cherry tomatoes. Respiration rates and weight loss were monitored continuously, while other parameters were measured at the end of storage period. Differences among weight loss, pH and firmness of control and treated cherry tomatoes were insignificant towards the end of storage life. Changes in respiration rates and colour of tomatoes were recorded as a function of treatment, which were not drastic. The results implicate that cold plasma could be employed as a means for decontamination of cherry tomatoes while retaining product quality.

### 5.1 Apparent density & free volume

The apparent density of the tomatoes was estimated to be  $1.026 \pm 0.003$  based on water displacement measurements for 10 samples. This value is in agreement with that reported by [Stertz et al. \[2005\]](#) for organically grown Brazilian cherry tomato variety. Based on the density and weight of tomatoes, the free volume of air in the packages was determined as presented in [Table 5.1](#).

Table 5.1: Free volume of the package(s) and weight of cherry tomatoes taken for the respiration studies.

Package	Produce Weight (W, g)	Free Volume (V, mL)
Control (untreated)	118.90±4.14	3384.12±4.03
T1 (30s treated)	117.97±2.50	3385.02±2.44
T2 (60s treated)	119.82±4.73	3383.22±4.61
T3 (180s treated)	122.14±2.38	3380.96±2.32
T4 (300s treated)	121.83±4.18	3381.26±4.07

## 5.2 Respiration rate of cherry tomatoes

A regression function is often used to fit the data of gas concentration versus time, and the respiration rate at a given time is determined from the first derivative of the regression function [Bhande et al. \[2008\]](#); [Cameron et al. \[1989\]](#). A two parameter, non-exponential equation similar to the Peleg model was fitted to average O<sub>2</sub> and CO<sub>2</sub> concentrations of control and treated packages at different storage periods using nonlinear regression analysis. A similar model has been applied for respiration data of apples by [Mahajan and Goswami \[2001\]](#) and [Bhande et al. \[2008\]](#). The resultant regression equations for O<sub>2</sub> consumption and CO<sub>2</sub> evolution are shown in equations (3) and (4) to determine the values of the coefficients:

$$[O_2] = 0.209 - \left[ \frac{t}{K_1 t + K_2} \right] \quad (5.1)$$

$$[CO_2] = \frac{t}{K_1 t + K_2} \quad (5.2)$$

where  $K_1$  and  $K_2(h)$  are the regression coefficients,  $t$  is the time in hour,  $[O_2]$  is the oxygen concentration in decimal and  $[CO_2]$  is the carbon dioxide concentration in decimal. The regression coefficients  $K_1$  and  $K_2(h)$  of equations 5.1 and 5.2 and coefficients of determination of the best fit for control and plasma treated cherry tomatoes are shown in Table 5.2.

The rate of change of gas concentration was determined from the first derivative of the regression functions as outlined in equations 5.3 and 5.4

$$\frac{d[CO_2]}{dt} = -\frac{K_1 t}{(K_1 t + K_2)^2} + \frac{1}{(K_1 t + K_2)} \quad (5.3)$$

Table 5.2: Regression coefficients  $K_1$  and  $K_2$  (h) of equations 5.1 and 5.2 for  $O_2$  consumption and  $CO_2$  evolution respectively, for different process times.

Package	Respiration index	Parameter		$R_{adj}^2$
		$K_1$	$K_2$ (h)	
Control (untreated)	$CO_2$ evolution	$11.24 \pm 1.15$	$1228.72 \pm 194.38$	0.945
	$O_2$ consumption	$15.74 \pm 1.28$	$1000.42 \pm 185.57$	0.911
T1 (30s treated)	$CO_2$ evolution	$12.08 \pm 1.49$	$1628.47 \pm 265.85$	0.943
	$O_2$ consumption	$17.68 \pm 2.09$	$1242.02 \pm 312.68$	0.852
T2 (60s treated)	$CO_2$ evolution	$7.99 \pm 1.57$	$1822.51 \pm 310.31$	0.944
	$O_2$ consumption	$10.41 \pm 1.49$	$1726.67 \pm 278.11$	0.937
T3 (180s treated)	$CO_2$ evolution	$6.33 \pm 0.89$	$1718.64 \pm 181.66$	0.978
	$O_2$ consumption	$7.37 \pm 1.07$	$1902.23 \pm 299.95$	0.943
T4 (300s treated)	$CO_2$ evolution	$10.51 \pm 1.09$	$963.906 \pm 176.22$	0.924
	$O_2$ consumption	$12.99 \pm 1.08$	$867.325 \pm 158.43$	0.91

$$\frac{d[O_2]}{dt} = \frac{K_1 t}{(K_1 t + K_2)^2} - \frac{1}{(K_1 t + K_2)} \quad (5.4)$$

At each sampling time, the respiration rates in terms of  $CO_2$  evolution and  $O_2$  consumption were calculated with Equations 5.5 and 5.6 and are presented in Figure 5.1.

$$R_{CO_2} = \frac{d[CO_2]}{dt} \frac{V}{W} \quad (5.5)$$

$$R_{O_2} = -\frac{d[O_2]}{dt} \frac{V}{W} \quad (5.6)$$

The respiration rate was found to decrease with time for the control as well as treated tomatoes due to decreasing  $O_2$  concentration and increasing  $CO_2$  concentration in the gaseous environment. At the end of the storage period, the respiration rates appeared to converge to similar values for control and strawberries with plasma for 1 minute. Such observations have also been reported by Tappi et al. [2014], who hypothesise the alteration of the cellular respiratory pathway. In general, a drastic change in the respiration rate was not observable. The difference between the treatments, however, at this point remains unclear and requires further investigation. It may be noted that diffusion across the packaging film also occurs, which in our study has been ignored. This approximation is justifiable to some extent, considering the high barrier nature of the packaging material. However, the packaging requirements for this novel technology needs further studies to attain a

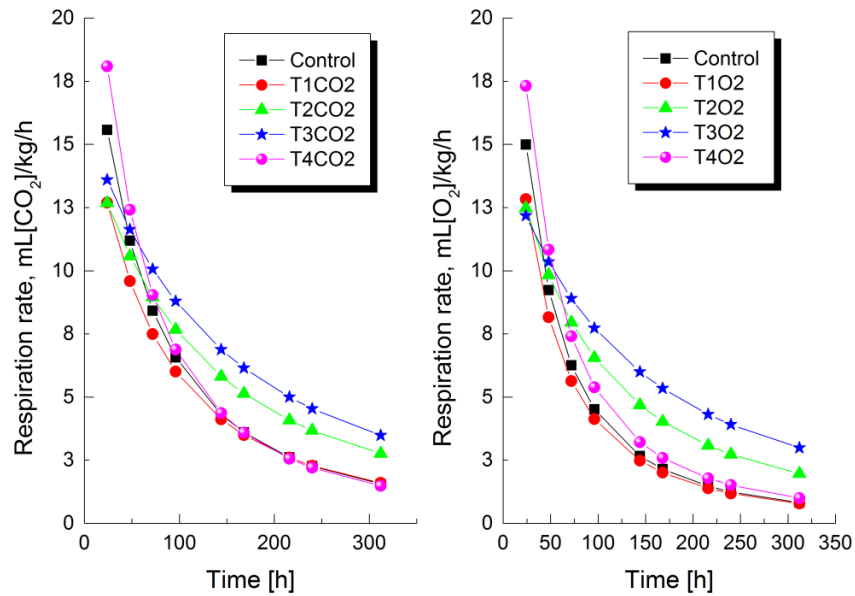


Figure 5.1: Respiration rates of control and plasma treated cherry tomatoes at 22°C.

balance between the plasma kinetics, respiratory dynamics, and diffusion across the film.

### 5.3 Weight loss and visual fungal

The relative loss in weights of cherry tomatoes at the end of thirteen days storage is presented in Figure 5.2. It can be seen that the total loss in weight did not exceed 2% for all the samples including controls. This is less than that reported by [Javanmardi and Kubota \[2006\]](#), who observed up to 5% weight loss after 7 days storage at room temperature (25-27 °C) for cluster tomatoes (cv. Clermon). This weight loss can be accounted for partly based on the CO<sub>2</sub> that escapes from the tissue and possibly, the higher rates of transpiration in the room temperature stored tomatoes [[Javanmardi and Kubota, 2006](#)]. [Venta et al. \[2010\]](#) have reported that ozonated cultivar tomatoes (25 and 45 mg/m<sup>3</sup> ozone for 2 h/day over a 16 day period) tended to have a smaller weight loss than the control tomatoes. However, in the present study such an effect was not observed, probably due to

the differences in treatment conditions and the tomato cultivar used. It is worth noting that the weight losses in the present study (up to a maximum of  $\sim 1.7\%$ ) are much less than that of [Venta et al. \[2010\]](#) (up to a maximum of  $5.7\%$ ). It has been shown that storage duration, storage temperature, and treatment have significant effects on weight loss [[Kumar et al., 1999](#)]. It is generally considered that fruits and vegetables are deprived of their characteristic freshness when they lose more than 3-5% of their weight [[Robertson, 2012](#)].

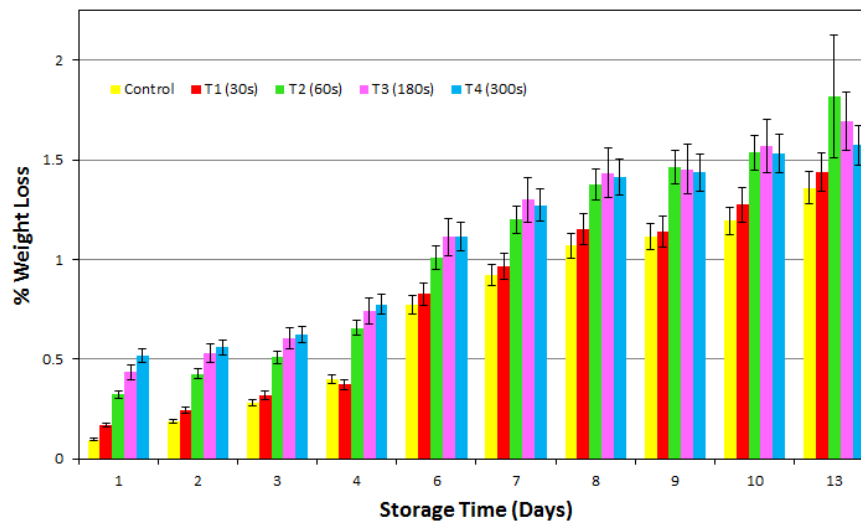


Figure 5.2: Weight loss (expressed as % of initial weight) of control and in-package treated cherry tomatoes over the storage period.

The control and treated cherry tomatoes were constantly monitored for any sign of fungal growth over the entire storage period. On day thirteen, fungal growth (tiny white mass of filamentous hyphae near the stem scar) was observed on one tomato in the control (untreated) package only (which means a 10% visual fungal), while no visual fungal was detected in any of the treated tomatoes. Following this, the packages were opened to measure the instrumental colour and firmness. It is worth mentioning that a recent study by [Ziuzina et al. \[2014\]](#) has revealed the inactivation of a range of bacteria on cherry tomatoes, following in-package cold plasma treatments.

Table 5.3: The CIE-L\*-a\*-b\* values of fresh, control and treated group of tomatoes. Values represent mean ( $\pm$ S.D.) of measurements of measurements made on three tomatoes in quadruplicates along four different sections. Values within a column followed by the same letter do not differ significantly ( $p>0.05$ )

Sample	L*	a*	b*	C*	h*	TI
Fresh	49.12 $\pm$ 1.19 <sup>a</sup>	31.57 $\pm$ 2.59 <sup>b</sup>	35.45 $\pm$ 1.77 <sup>c</sup>	47.98 $\pm$ 3.19 <sup>a</sup>	0.79 $\pm$ 0.03 <sup>a</sup>	1.00 $\pm$ 0.06 <sup>a</sup>
Control	48.15 $\pm$ 1.22 <sup>a</sup>	33.86 $\pm$ 2.61 <sup>b</sup>	33.98 $\pm$ 1.75 <sup>c</sup>	46.66 $\pm$ 2.27 <sup>b</sup>	0.86 $\pm$ 0.05 <sup>b</sup>	0.87 $\pm$ 0.08 <sup>a</sup>
T1 (30s)	48.27 $\pm$ 1.03 <sup>a</sup>	33.82 $\pm$ 1.95 <sup>b</sup>	33.99 $\pm$ 1.39 <sup>c</sup>	45.60 $\pm$ 1.38 <sup>b</sup>	0.087 $\pm$ 0.04 <sup>b</sup>	0.84 $\pm$ 0.07 <sup>b</sup>
T2 (60s)	48.04 $\pm$ 1.28 <sup>a</sup>	34.08 $\pm$ 2.11 <sup>b</sup>	33.88 $\pm$ 2.35 <sup>c</sup>	46.37 $\pm$ 1.62 <sup>b</sup>	0.89 $\pm$ 0.06 <sup>b</sup>	0.81 $\pm$ 0.10 <sup>b</sup>
T3 (180s)	48.11 $\pm$ 1.19 <sup>a</sup>	34.34 $\pm$ 2.06 <sup>b</sup>	33.96 $\pm$ 1.73 <sup>c</sup>	47.96 $\pm$ 1.56 <sup>c</sup>	0.81 $\pm$ 0.05 <sup>a</sup>	0.95 $\pm$ 0.09 <sup>c</sup>
T4 (300s)	48.87 $\pm$ 0.88 <sup>a</sup>	34.00 $\pm$ 2.22 <sup>b</sup>	35.23 $\pm$ 1.04 <sup>c</sup>	46.65 $\pm$ 1.10 <sup>b</sup>	0.89 $\pm$ 0.05 <sup>b</sup>	0.81 $\pm$ 0.08 <sup>b</sup>

## 5.4 Changes in Instrumental colour

Colour is probably the first quality factor judged by tomato product consumers. There was no significant difference ( $p\geq 0.05$ ) between the mean L\*, a\* and b\* values of fresh, control and treated groups of tomatoes at 95% confidence level (Table 5.3).

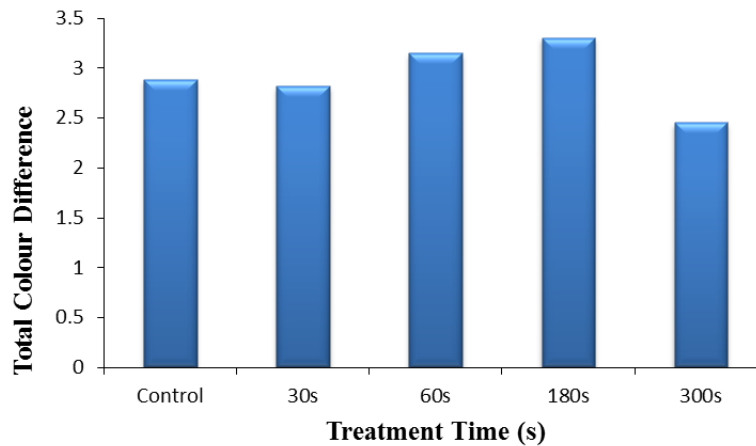


Figure 5.3: Total Colour Difference (TCD) of control and treated group of tomatoes relative to fresh tomatoes.

The overall change in hue and chroma value (indicating colour saturation) of the control and treated samples was also insignificant (except T3). The difference in C\* and h\* was however, significant between fresh and control samples, as would be expected. The TCD of control and plasma treated tomatoes relative to the fresh tomatoes is presented in Figure 5.3. Differences in perceivable colour can be

analytically classified as very distinct ( $TCD > 3$ ), distinct ( $1.5 < TCD < 3$ ) and small difference ( $TCD < 1.5$ ) [DrLange, 2000]. The control (2.88) and 30s plasma treated tomatoes had a distinct colour from that of fresh tomatoes. Tomatoes treated for extended durations had a very distinct colour than fresh tomatoes under the classification scale mentioned above. The relatively lower tomato colour index (TI), which was significant ( $p \leq 0.05$ ), indicated the possibility of degradation of carotenoid pigments. These changes were also attributed to the inherent variability in the colour of the produce, considering that the  $L^*$ ,  $a^*$  and  $b^*$  values were not significantly different from each other. However, it is worthwhile mentioning that despite the instrumental colour differences, the changes in colour of the tomatoes were unperceivable as observed by naked eye under normal lighting conditions (with fluorescent tube light). These results are in agreement with those of cold plasma treated strawberries, where changes in colour among control and treated groups were found to be insignificant [Misra et al., 2014]. Bermúdez-Aguirre et al. [2013] have also reported insignificant changes in the colour of tomatoes following cold plasma treatments using a plasma jet array with Argon gas.

## 5.5 Change in pH

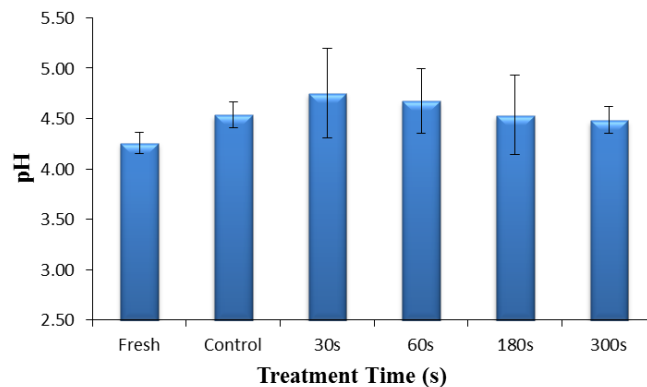


Figure 5.4: pH of control and treated tomatoes at the end of storage period. Values represent mean ( $\pm$ S.D.) of measurements made on three tomatoes in duplicate.

Among the parameters commonly analysed for the assessment of tomato quality, pH is very important because acidity influences the processing conditions



required for producing safe products. The pH of the cherry tomatoes was found to increase at the end of the storage period for the control as well as treated tomatoes (Figure 5.4). The relative increase in pH was slightly higher for plasma treated tomatoes, with this increment being inversely related to the treatment time. However, there was no significant difference ( $p>0.05$ ) between the pH of the control and treated tomatoes. The pH values are comparable to those reported in the literature [Rodriguez-Lafuente et al., 2010; Tzortzakis, 2007]. An increase in pH of cherry tomatoes in storage under natural conditions has also been reported by Rodriguez-Lafuente et al. [2010]. The change in pH could be attributed to the metabolic changes and water loss in the tomatoes [Casariego et al., 2014].

## 5.6 Fruit firmness

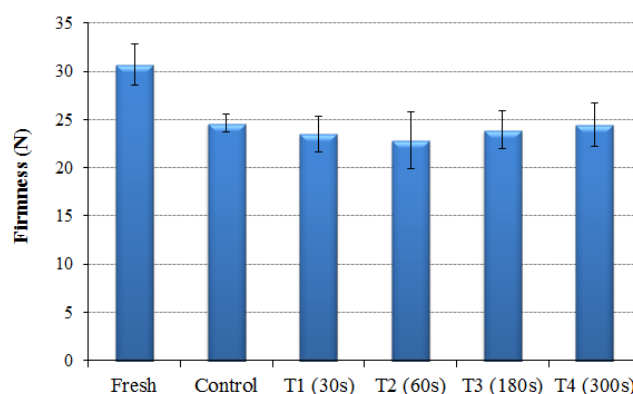


Figure 5.5: Firmness (force at break, N) of control and treated tomatoes. Values represent mean ( $\pm$ S.D.) of measurements made on three tomatoes from each package.

The mean values of peak force (N) required for puncturing the fruits is presented in Figure 5.5. The firmness of the control and treated group of the produce was less than that of fresh tomatoes and this difference was significant ( $p\leq 0.05$ ). An insignificant difference ( $p>0.05$ ) between the firmness values of the control and treated tomatoes was recorded at the end of storage period, meaning that the tissue structure of the produce remained intact. Tappi et al. [2014] recently reported that gas plasma treatments cause a loss of firmness in fresh-cut apples

with treatment times of the order of 10 to 30 min. This was most likely an outcome of the exposed tissues surface in their studies, which cause cell leakage during prolonged exposure, making the process more challenging. However, in the present study whole tomatoes with intact skin were treated which allowed retention of the firmness.

## 5.7 Conclusions

In this chapter, the out-of-field (indirect) plasma treatment of cherry tomatoes was carried out inside a sealed package at 30 kV RMS. Although the modified gas composition induced through complex plasma chemistry may persist for several hours (< 24 h) inside the package, a drastic change in respiration rate of strawberries was not observed. The plasma treatment of cherry tomatoes did not adversely affect critical quality parameters of colour, firmness, pH and weight loss. The retention of firmness was attributed to the thick cuticle of the cherry tomatoes. The weight loss was attributed to the metabolism of tomatoes, where water and CO<sub>2</sub> escape from the fruits.

The acceptable retention of quality and respiration rates were most likely due to two reasons. Firstly, when indirectly treated, the charged particles and short-lived transient-state species do not affect the sample under treatment, as they recombine before reaching it. Secondly, the large volume of the packages could be responsible for maintaining conducive environments for the tomatoes to respire.

It is to be noted that the optimisation of packaging conditions for meeting the requirements of high barrier nature for in-package plasma while relatively high permeability desired for respiring produce, needs to be addressed in future studies. In addition, the evaluation of the physical quality parameters offers only a good starting point, and changes in the produce chemistry need further investigation.

# Chapter 6

## Effect of nonthermal plasma on quality of strawberries

In this study, strawberries were treated with nonthermal plasma generated with a 60 kV dielectric barrier discharge (DBD) pulsed at 50 Hz, across a 40 mm electrode gap, generated inside a sealed package containing ambient air (42% relative humidity) or 65% O<sub>2</sub> + 16% N<sub>2</sub> + 19% CO<sub>2</sub> (G1) or 90% N<sub>2</sub> + 10% O<sub>2</sub> (G2). The current-voltage characteristics revealed that the plasma operated in the filamentary regime. The respiration rate of nonthermal plasma treated produce, measured by the closed system approach, showed an initial increase. Nonthermal plasma was found to alter strawberry colour and firmness; however, these were not drastic.

### 6.1 Electrical characterisation

The I-V waveforms and the Q-V characteristics for the discharge with and without strawberries are shown in Figure 6.1 (a, b), respectively. See Figure 3.2 in 45 for details on interpretation. The I-V waveforms indicate the presence of a filamentary-type discharge without noticeable differences between the empty package and the package with produce. Similar results were obtained for discharges in MAP gases.

The discharge performance in air is not significantly affected by the presence

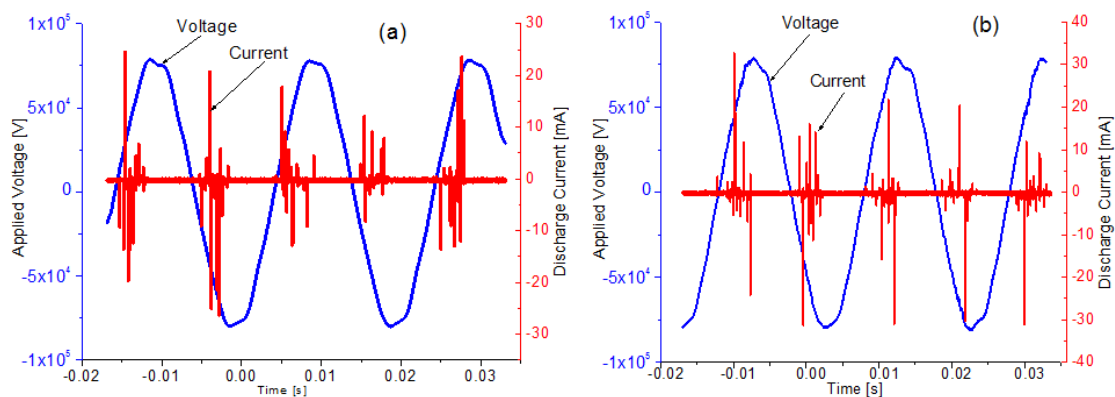


Figure 6.1: (a) The I-V characteristics of discharge in an empty package and (b) package containing strawberries in ambient air.

of fresh produce as electrical parameters for the box with and without produce have close values, within the range of estimation errors (Table 6.1). Since there are no differences in discharge behaviour for dry air and room air, it is expected that the discharge in air will not be affected by the presence of the produce as long as the produce is placed outside the electrode area (outside field).

Table 6.1: Discharge electrical parameters derived from Q-V measurements.

Gas	Package	$C_d$ [pF]	R.E.** [%]	$C_{gap}$ [pF]	P [W]	$\Delta Q$ [nC]	$\Delta t$ [ms]
Air	Empty*	89	6.00	1.62	17.43	8098	3.6
	Strawberry*	83	2.10	1.58	17.03	7924	3.7
	Change [%]	7.2		2.4	2.3	2.1	2.8
65% O <sub>2</sub> + 16% N <sub>2</sub> + 19% CO <sub>2</sub> (G1)	Empty*	72.41	2.9	1.35	12.2	6551	3.3
	Strawberry*	82.91	5.28	1.54	17.16	7206	3.85
	Change [%]	9		8.7	20.4	6.4	5
90% N <sub>2</sub> + 10% O <sub>2</sub> (G2)	Empty*	80.36	1.52	1.46	13.99	7077	3.39
	Strawberry*	95.92	2.06	1.66	17.72	8743	3.78
	Change [%]	11.5		8.5	14.9	13.5	7.3

\* refers to the empty and strawberry filled packages; \*\*R.E. refers to the relative error estimating  $C_{diel}$ ; 'Change' is the relative increase in each quantity.

In modified environments, the obtained values of  $C_d$  increase for the packages with strawberries by 11% and 9%, while errors due to incertitude in the C-V estimations of  $C_d$  are below 5% (Table 6.1). Increases in transferred power (17%

and 20%) and charge (13% and 5%) and discharge on-time (7% and 5%) are also observed (for the G2 and G1 respectively). The packages with strawberries have larger transferred power, charge and discharge on-time for both gas mixtures (Table 6.1), the increase being larger for the G2 mixture (except for the transferred power). An interesting particularity is that the packages with produce have a lower breakdown voltage,  $V_{min}$  and an increase in transferred power for both gases, which can be ascribed to an increased conductivity of the gas.

The differences between  $C_{gap}$ , power and charge transfer which can be ascribed to different properties of the filling gas can be observed by comparing the values for the empty package. While the estimation errors for  $C_{gap}$  are below 1% for both gases, there is a 5% difference in  $C_{gap}$  between the two gases (for both the empty and strawberry containing package). For the empty packages, the DBD on G2 gas has larger  $C_{gap}$ , transmitted power and charge and on-time than for G1 (by 5.7%, 10%, 5.7% and 2% respectively). For the package with strawberries, the transferred power is the same for both gases while the transmitted charge is 15% larger for the G2 gas. Such differences are clearly due to different electrical properties of each gas and may affect the final gas chemistry and composition influencing produce physiology.

## 6.2 Ozone concentrations

The  $O_2$  molecules in a DBD undergo bombardment with the electrons in the discharge resulting in oxygen atoms, which subsequently combine with oxygen molecules to form ozone. This process can be summarised as follows [Fang et al., 2008]-



where,  $M$  is  $O$ ,  $O_2$  or  $O_3$ . However, it is also worth mentioning that the ozone generation and its destruction occur simultaneously. In our studies, ozone concentrations inside the package containing strawberries were measured to be  $(2800 \pm 200)$  and  $(600 \pm 100)$  ppm for 65%  $O_2$  + 16%  $N_2$  + 19%  $CO_2$  and 90%

$\text{N}_2 + 10\% \text{O}_2$  gas mixtures respectively, immediately post-treatment. We have observed that ozone concentrations, generated in similar conditions but without strawberries, can be as high as  $(4200 \pm 100)$  and  $(1000 \pm 200)$  ppm after 5 min in  $65\% \text{O}_2 + 16\% \text{N}_2 + 19\% \text{CO}_2$  and  $90\% \text{N}_2 + 10\% \text{O}_2$  compositions respectively, within the errors. The relatively low ozone level in packages with product is probably due to the lesser volume of available gas, and therefore oxygen too. This assumption is also justifiable based on our previous observations for discharges in air (21% oxygen) where we noted ozone levels in the range of  $1000 \pm 100$  ppm in packages containing strawberries. In addition, the ozone generated is very likely to undergo decomposition by reacting with the water at the produce surface. Using ultraviolet absorption spectroscopy we have confirmed the presence of ozone in packages for up to 4-6 h even after the discharge is turned off.

### 6.3 Respiration Rate

It is well-known that the fundamental processes of respiration, transpiration and biochemical changes proceed in fruits and vegetables even after harvest. If the produce undergoes physiological stress, often due to damage or processing, the respiration rate of the produce increases [Laties, 1978; Rico et al., 2007]. Practical experience reveals that tissues with high respiratory rates and/or low energy reserves have shorter postharvest lives [Eskin, 1990]. Therefore, it is important to examine the respiration rate of the plasma treated produce. Table 6.2 summarises the model parameters and fit statistics for the respiration data. The models exhibit a good fit to the experimental data as evident from the high  $R_{adj}^2$  and low RMSE values. The respiration rate was calculated from the first derivative of the functions fitted to the data. In this study, the respiration rate was observed to decrease with time for control as well as treated strawberries (Figure 6.2). This decline is due to the decreasing  $\text{O}_2$  concentration and increasing  $\text{CO}_2$  concentration in the gaseous environment. The respiration rate of the treated produce was found to be lower than that of the control following a period of delay, which is most likely due to the decreased microbial count. Based on these observations it can be said that ACP does not induce significant stress in strawberries treated within the set of conditions employed. Elevated  $\text{O}_2$  atmospheres have been used as an alternative

Table 6.2: Regression coefficients  $K_1$  and  $K_2(h)$  of the two parameter equations fitted to experimental data for  $O_2$  consumption and  $CO_2$  evolution for strawberries.

Gas	Model	Package	Principle for respiration rate	Regression coefficients		$R^2$ (adj.)	RMSE
				$K_1$	$K_2$ (h)		
65% $O_2$ + 16% $N_2$ + 19% $CO_2$ (G1)	$[O_2] = 0.65 - \frac{t}{k_1 \cdot t + k_2}$	Control	$CO_2$ evolution	$0.744 \pm 0.26$	$917.56 \pm 67.69$	0.97	0.015
			$O_2$ consumption	$0.765 \pm 0.09$	$503.12 \pm 23.25$	0.98	0.015
90% $N_2$ + 10% $O_2$ (G2)	$[CO_2] = 0.19 + \frac{t}{k_1 \cdot t + k_2}$	5 min treated	$CO_2$ evolution	$2.664 \pm 0.17$	$512.34 \pm 37.37$	0.96	0.015
			$O_2$ consumption	$1.247 \pm 0.06$	$338.81 \pm 14.51$	0.98	0.017
21% $O_2$ + 78% $N_2$ (Air)	$[O_2] = 0.11 - \frac{t}{k_1 \cdot t + k_2}$	Control	$CO_2$ evolution	$4.154 \pm 0.61$	$518.77 \pm 51.24$	0.98	0.006
			$O_2$ consumption	$3.86 \pm 3.66$	$1480.6 \pm 365.09$	0.87	0.007
	$[CO_2] = \frac{t}{k_1 \cdot t + k_2}$	5 min treated	$CO_2$ evolution	$4.674 \pm 0.35$	$457.37 \pm 6.45$	0.98	0.007
			$O_2$ consumption	$9.349 \pm 1.79$	$997.2 \pm 191.54$	0.89	0.008
	$[O_2] = 0.21 - \frac{t}{k_1 \cdot t + k_2}$	Control	$CO_2$ evolution	$4.078 \pm 0.10$	$300.67 \pm 7.19$	0.99	0.002
			$O_2$ consumption	$4.497 \pm 0.12$	$306.96 \pm 7.87$	0.99	0.002
	$[CO_2] = \frac{t}{k_1 \cdot t + k_2}$	5 min treated	$CO_2$ evolution	$5.064 \pm 0.59$	$272.27 \pm 20.24$	0.98	0.005
			$O_2$ consumption	$2.962 \pm 0.91$	$476.76 \pm 40.64$	0.99	0.004

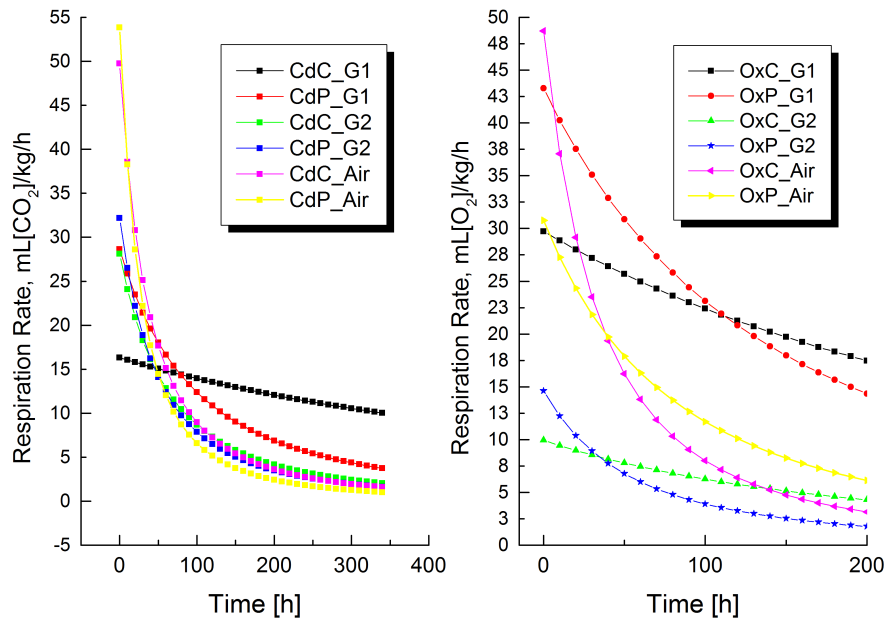


Figure 6.2: Respiration rate of control and plasma treated strawberries in terms of carbon dioxide released and oxygen consumed. Ox and Cd refer to oxygen and carbon dioxide gases respectively; C and P refer to control and plasma treated respectively; G1, G2 same as in Table 6.2.

to traditional low  $O_2$  and high  $CO_2$  atmospheres to maintain the quality and safety of fresh-cut products [Day, 1996]. The lower respiration rate of strawberries even at elevated oxygen levels (superatmospheric condition) has already been reported in literature [Wszelaki and Mitcham, 2000]. Therefore, the results are most likely an outcome of a similar effect. A lower respiration rate of ozonated water washed strawberries compared to control has also been reported in a recent study [Aday et al., 2014]. As a caveat against drawing any conclusions regarding the response of strawberries to superatmospheric (G1) or subatmospheric (G2) environments, it may be noted that such conditions may stimulate, have no effect, or reduce rates of respiration depending on the commodity, maturity, ripeness stage, storage time and temperature, and concentrations of gases present in the atmosphere [Kader and Ben-Yehoshua, 2000].



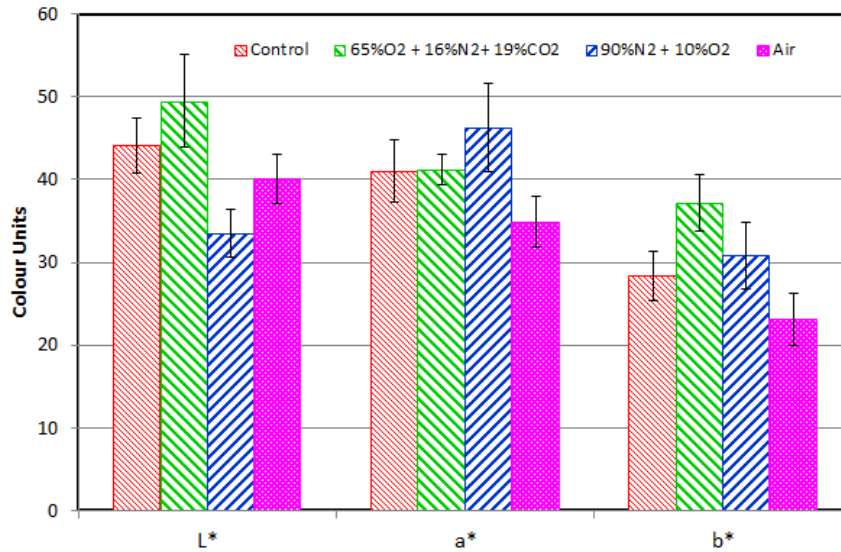


Figure 6.3:  $L^*$ - $a^*$ - $b^*$  colour parameters of untreated control and ACP treated strawberries, both after 24 h storage.

## 6.4 Strawberry Colour

Colour is the most obvious parameter for consumers [Del-Valle et al., 2005] and plays a key role in food choice, food preference and acceptability, and may influence taste thresholds, sweetness perception and pleasantness [Clydesdale, 1993]. A change in the  $L^*$ - $a^*$ - $b^*$  colour parameters of air plasma treated strawberries was observed (Figure 6.3). However, the changes in individual colour parameters viz. lightness, redness or greenness were statistically insignificant ( $p > 0.05$ ) in comparison to the untreated control stored under the same conditions, for strawberries treated in air. The lightness parameter ( $L^*$ ) of treated and untreated strawberries was found to be significantly different ( $p \leq 0.05$ ) for strawberries treated in gases G1 and G2. The strawberries treated in a high oxygen environment (G1) turned brighter, while those treated with high nitrogen environment (G2) exhibited a decline in  $L^*$  parameter. The former effect is probably due to a superficial bleaching effect brought by the high ozone levels. The redness values ( $a^*$ ) of the treated strawberries were significantly different ( $p \leq 0.05$ ) from that of control. However, there was no significant difference in  $a^*$  among the strawberries treated with G1 or G2 ( $p > 0.05$ ). Visually judging, the strawberries treated with high oxygen en-

vironment (G1) were relatively appealing.

## 6.5 Firmness

The firmness of control, untreated strawberries stored at 10 °C for 24 h, air plasma, plasma in G1 and G2 treated strawberries were found to be  $3.55 \pm 0.16$ ,  $3.26 \pm 0.10$ ,  $3.19 \pm 0.22$ ,  $3.62 \pm 0.14$ , and  $2.97 \pm 0.19$  N respectively. A significant ( $p \leq 0.05$ ) decrease in firmness of all strawberry samples was recorded within 24h, except for G1 (high  $O_2$ ). The difference in firmness among untreated control and plasma treated group was found to be statistically insignificant ( $p > 0.05$ ), for air plasma and G2 treatments. Recently, [Aday et al. \[2014\]](#) also reported the loss of firmness in strawberries following ozone treatments in water. Ozone is one of the main reactive species in plasma and especially of importance when treating samples in indirect mode. Overall, treatment in G1 resulted in the best retention of firmness. Strawberry is a soft fruit that suffers a rapid loss of firmness during storage, which contributes greatly to its short postharvest life and susceptibility to fungal contamination [[Hernández-Muñoz et al., 2006](#)]. Furthermore, the ability of ozone to retain the texture of strawberries has already been reported in the literature [[Zhang et al., 2011](#)]. Retention of strawberry firmness under elevated oxygen atmospheres has also been reported earlier [[Wszelaki and Mitcham, 2000](#)]. Besides instrumental colour and firmness, no obvious change in the flavour or edible quality of the strawberries, relative to control, was noticed.

## 6.6 Conclusion

The dielectric barrier discharge based plasma source was electrically characterised using I-V and Q-V methods, both in presence and in the absence of strawberries inside package. The results indicated that the presence of the produce did not significantly affect the discharge characteristics. In fact, the discharge in air was found to be slightly more effective in presence of strawberries. This is suspected to be an outcome of the humidity introduced by the produce.

The use of plasma induced in air and MAP gases (G1 and G2) for fresh

strawberries in a closed package environment was also investigated to observe the evolution of changes in quality parameters over a 24 h period post-plasma exposure. Although the modified gas composition induced through complex plasma chemistry may persist for several hours (<24 h) inside the package, a drastic change in respiration rate of strawberries does not occur. Even the minor differences in respiration rates is likely to diminish when a moderately permeable polymeric film is employed for the packaging and plasma treatment of strawberries. Comparing the modified gas environments, a high oxygen environment can be considered beneficial in light of the microbial reductions with good retention of quality attributes. However, some loss of colour is expected due to the generation of high amounts of ozone. A high nitrogen and low oxygen environment (G2), although effective in background flora reduction, causes significant decreases in firmness and leads to unpleasant dark colour. The dark colour could be an outcome of the effect of nitrogen oxides and nitrogen peroxides formed on the surface of strawberries by the reaction of water with excited nitrogen species in the gas phase. It is worth mentioning that, these results were specific for strawberries and other produce could behave differently.

The results demonstrate the ability of in-package NTP to decontaminate without inducing significant physiological (respiratory) stress or extremely affecting the colour and firmness. The plasma source achieved these desired effects with a power input of only 15-20 W, without increasing the temperature of the samples significantly.

# Chapter 7

## Enzyme Inactivation Studies

The objectives of this study were (i) to evaluate the effects of atmospheric pressure dielectric barrier discharge based nonthermal plasma process variables upon the activity of peroxidase and (ii) model the kinetics of enzyme activity. POD being one of the most heat stable enzymes is conventionally used as a marker to monitor and evaluate the efficiency of thermal treatments. The enzyme activity was found to decrease with both treatment time and voltage, the former variable exhibiting a more pronounced effect. Kinetic models viz. first-order, Weibull and logistic models were fitted to the experimentally observed data to numerate the model parameters. The enzyme inactivation kinetics was found to be best described by the sigmoidal logistic function.

### 7.1 Effect of voltage and treatment time

Dielectric barrier discharge (DBD) plasma treatments were significantly ( $p < 0.05$ ) effective in reducing the peroxidase activity. Since temperatures that could have caused thermal inactivation of the enzyme were never reached, the inactivation that was observed was attributed to DBD plasma treatment alone. This was confirmed by recording the temperature rise using a hand-held infrared thermometer (Maplin Electronics, UK), which recorded a maximum temperature rise of only 5 °C for all experiments. Treatment times and voltage both were found to have a significant effect ( $p \leq 0.05$ ) on residual activity of peroxidase. There was a signif-

icant difference in residual activity for all three applied voltages at 95% level of confidence. The interaction between voltage and time was also found to be significant ( $p \leq 0.05$ ). The maximum inactivation was higher in crude enzyme extracts of tomato compared to that of whole strawberries. This is more likely because of faster diffusion of gases in liquids compared to that of solids.

## 7.2 First-order kinetic model

The inactivation rate constants ( $K_p$ ) were calculated from the slope of the lines and are summarised in Table 7.1 along with the regression coefficients for the first-order kinetic model at the different voltage levels. It can be observed that although the  $R_{adj}^2$  values are high ( $\geq 0.85$ ), the RMSE values are not satisfactory. Therefore, a first-order model was considered inefficient in describing the POD residual activity. Moreover, in view of the complexity of the structure of an enzyme and the possible variety of different phenomena involved in the inactivation, the assumption that the disruption of a single structural element of the protein is sufficient to inactivate the enzyme, as proposed in first-order kinetics seems to be exceedingly simple [Adams, 1991]. The inactivation seems to occur due to a two phase (or higher) structural change in the enzyme.

## 7.3 Model based on Weibull distribution

The scale parameter ( $\alpha$ ) and shape parameter ( $\gamma$ ) of the Weibull model were obtained by fitting experimental data to the model. The estimates of  $\alpha$  and  $\gamma$  along with  $R_{adj}^2$  values are listed in Table 7.1. The Weibull model exhibited a strong fit to predict residual POD activity after DBD plasma treatments as indicated by the high coefficients obtained ( $R_{adj}^2 \geq 0.98$ ) for all voltage levels studied in this experiment. The scale parameter ranged from 1.09 to 1.64 for tomato extract 2.49 to 2.99 for strawberries respectively, and exhibited an inverse dependency on voltage levels i.e. the higher the applied voltage level, the lower will be the scale parameter obtained. The shape parameter ranged from 1.48 to 2.00 for tomato extract and 1.81 to 2.14 for strawberries, respectively. Figure 7.1 shows

Table 7.1: Results on the parameters of the models fitted to inactivation kinetics of POD enzyme.

Model	Parameter	Estimated Value		
		30kV	40kV	50kV
Cherry Tomato				
First Order	$K_p(min^{-1})^a$	$0.63 \pm 0.06$	$0.71 \pm 0.07$	$0.99 \pm 0.05$
	$R^2(adj.)$	0.94	0.95	0.99
	RMSE	9.14	9	3.63
Weibull	$\alpha(min)^a$	$1.64 \pm 0.05$	$1.52 \pm 0.03$	$1.09 \pm 0.02$
	$\gamma^a$	$2.00 \pm 0.16$	$2.00 \pm 0.08$	$1.48 \pm 0.07$
	$R^2$	0.99	0.99	0.99
	RMSE	3.53	1.79	1.44
Logistic	$A_{min}^a$	$2.20 \pm 0.56$	$0.00 \pm 0.89$	$0.00 \pm 0.99$
	$t_{50}^a$	$1.29 \pm 0.012$	$1.23 \pm 0.02$	$0.89 \pm 0.02$
	$P^a$	$3.42 \pm 0.09$	$3.29 \pm 0.15$	$2.94 \pm 0.28$
	$R^2$	0.99	0.99	0.99
	RMSE	0.93	1.46	1.54
Strawberry				
First Order	$K_p(min^{-1})^a$	$0.32 \pm 0.04$	$0.36 \pm 0.03$	$0.41 \pm 0.04$
	$R^2(adj.)$	0.87	0.91	0.93
	RMSE	13.58	10.95	9.82
Weibull	$\alpha(min)^a$	$2.99 \pm 0.09$	$2.78 \pm 0.07$	$2.49 \pm 0.05$
	$\gamma^a$	$2.14 \pm 0.21$	$1.89 \pm 0.14$	$1.81 \pm 0.09$
	$R^2$	0.98	0.98	0.99
	RMSE	5.48	4.19	3.03
Logistic	$A_{min}^a$	$9.79 \pm 1.90$	$0.00 \pm 6.32$	$0.00 \pm 0.6.57$
	$t_{50}^a$	$2.27 \pm 0.04$	$2.23 \pm 0.14$	$2.02 \pm 0.15$
	$P^a$	$4.40 \pm 0.33$	$2.86 \pm 0.42$	$2.58 \pm 0.38$
	$R^2$	0.99	0.98	0.99
	RMSE	2.04	4.08	3.47
$R^2$ =regression coefficient; $^a$ =Value $\pm$ Standard Error				

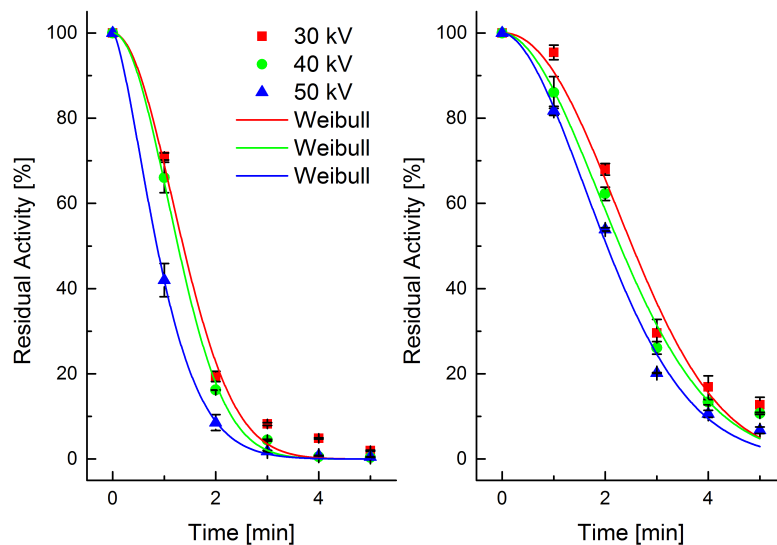


Figure 7.1: Weibull model curve fitting at different voltage levels for POD residual activity in (left) cherry tomato extract, and (right) whole strawberries.

the fitted curves of the Weibull model at different voltage levels. It can be clearly observed that the Weibull fit could not account for the tailing observed at 30kV treatment voltage, which is also obvious from the corresponding higher *RMSE* value. Therefore, a logistic model was proposed for further explanation.

## 7.4 Logistic model

The characteristic parameters of the Logistic model for POD inactivation were obtained from the experimental data fitted to equation 3.15 and shown in Figure 7.2. Estimates of parameters were significant at  $p \leq 0.05$  and  $R_{adj}^2$  values indicated that this model explained 99% of the variability in RA. The  $A_{min}$  value of  $2.20 \pm 0.56$  for tomato extract and  $9.79 \pm 1.90$  for strawberries at 30 kV treatment explained the observed tailing effect. The  $t_{50}$  value of 0.89 min for tomato extract and 2.02 min for strawberry accounted for the rapid POD inactivation at 50 kV compared to 30 and 40 kV treatments. Thus, it was concluded that the POD inactivation followed a sigmoidal inactivation, which can be explained by the logistic model.

We observed a general lack of published work on effects of DBD plasma on enzyme systems from fruit and vegetable sources. Therefore, the proposed mech-

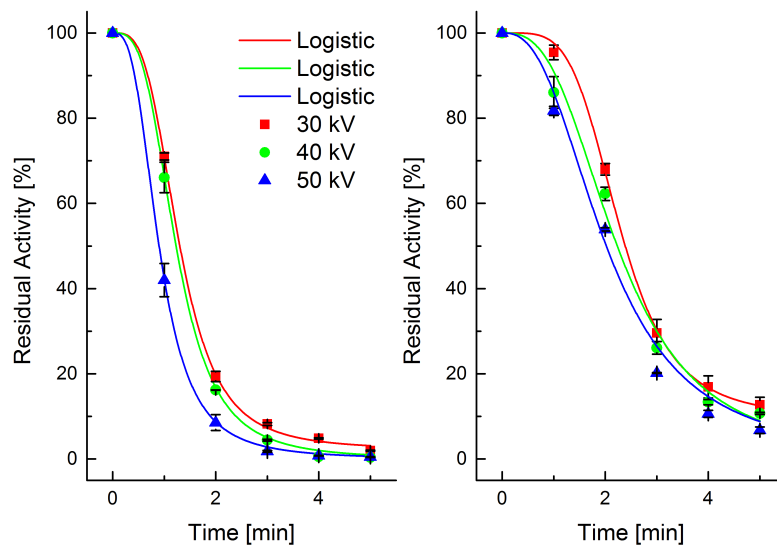


Figure 7.2: Logistic model curve fitting at different voltage levels for POD residual activity in (left) cherry tomato extract, and (right) whole strawberries.

anisms of inactivation were based on the works done on egg white lysozyme using a low frequency helium plasma jet system by Takai et al. [2012], and nitrogen-oxygen plasma by Bernard et al. [2006]. Takai et al. [2012] and Bernard et al. [2006] attributed the decrease in the enzyme activity to a change in the secondary protein structure and modification of some amino acids side chains of the enzyme. In a former study on exposure of lipase derived from *Candida rugosa* (Type VII, L-1754) to radio-frequency, atmospheric-pressure glow discharge Helium plasma jet an increase in the lipase activity was reported [Li et al., 2011]. Irrespective of the positive or negative effects on enzyme activity, this was also assigned to the changes in secondary and tertiary structure of protein by the reactive species of the plasma discharge. The study of effect of atmospheric pressure glow discharge plasma on bovine serum albumin has also confirmed the degradation of protein integrity [Deng et al., 2007] upon plasma treatment. One possible mechanism of reaction between plasma generated reactive species and protein suggested by Takai et al. [2012] is that hydroxyl radicals ( $\text{OH}^\bullet$ ), superoxide anion radicals ( $\text{O}_2^{\bullet-}$ ), hydroperoxy radicals ( $\text{HOO}^\bullet$ ) and nitric oxide ( $\text{NO}^\bullet$ ) leads to the chemical modifications of chemically reactive side-chain of the amino acids, such as cysteine, aromatic rings of phenylalanine, tyrosine, and tryptophan causing loss of enzyme



activity. Similar mechanism for decomposition of C-H, C-N and N-H bonds of protein is also described by [Hayashi et al. \[2013\]](#). The DBD employed in the present study also generates reactive nitrogen species and primarily ozone when humid air is used as an operating gas. By analogy, it is intuitive to suggest that DBD plasma operating in atmospheric air causes changes in POD in enzyme extract through similar action of the species formed in the liquid media by diffusion from the gas phase plasma. Very recently, [Surowsky et al. \[2013\]](#) have shown that a simultaneous reduction of  $\alpha$ -helix structure and increase of  $\beta$ -sheet content leads to the inactivation of POD and polyphenol oxidase in a model food system, subjected to cold plasma treatment.

## 7.5 Conclusion

The effect of atmospheric cold plasma generated inside a sealed package on enzyme activity as a function of voltage and treatment time is reported. Treatment voltage and time were both found to have a significant effect on POD inactivation. The inactivation curve followed a sigmoidal curve. The kinetics of inactivation were modelled using first-order, Weibull, and Logistic models. Treatment conditions were found to influence the inactivation rates and the shape of the inactivation curve, with tailing evident at the lowest voltage employed. The inactivation is very rapid and the treatment time has a significant impact compared to the treatment voltage.

Considering the complexity of the plasma chemistry, there could be a myriad of reactions ultimately leading to protein structural changes; however, the well documented species include ROS and UV photons. The significant amount of ozone generation with the current system configuration of DBD plasma and the post-treatment storage of in-pack treated tomato enzyme extracts and whole strawberries also makes ozone a likely species contributing to the enzyme inactivation. The sigmoidal inactivation curve indicates that the structural changes in the enzyme occur at multiple sites and their rates are different. These speculations should further be confirmed by purification of enzymes from the extract followed by CD spectroscopy of the extracts.

The results from this study indicate that cold plasma can inactivate enzymes,

in addition to the reported studies on microbial inactivation. The inactivation of peroxidase enzyme is important as this will allow to retain the quality and sensorial properties during the storage of the produce. In addition, the fact that enzymes are inactivated by NTP also points to the fact that changes to biochemical pathways and flavour biosynthesis would follow.

## Chapter 8

# Infrared spectroscopy of plasma treated strawberries

Infrared spectroscopy is a rapid analytical method which is capable of providing information regarding major chemical changes in food matrices. In combination with multivariate data analysis, the spectroscopic methods possess the speed, simplicity, and low cost per analysis required for screening techniques [Zhu et al., 2010]. Principal Component Analysis (PCA) is a powerful technique for feature extraction. Grouping of spectral data can be achieved by unsupervised methods which rely on identification of the natural clustering pattern and group data on the basis of similarities or dissimilarities among the samples. The most common method of unsupervised pattern recognition is cluster analysis (CA), widely recognised as a very powerful tool for obtaining better information about relations within datasets [De Luca et al., 2011; Forina et al., 2008]. In the past, Kim et al. [2009] employed Fourier transform infrared (FTIR) spectroscopy with multivariate analysis for the rapid discrimination of commercial strawberry cultivars.

The objectives of this study were to identify if in-package plasma treatment causes changes to the chemical composition of strawberries as observed through mid-infrared spectroscopy. In order to identify the changes the FTIR spectroscopic data was analysed using multivariate chemometric techniques, viz. PCA and cluster analysis.

## 8.1 Data pre-processing

The spectral features of the freeze-dried strawberry samples were conserved, while background offsets and slopes were largely removed after the MSC. The MSC, thus facilitated the removal of physical effects like particle size and surface blaze from the spectra, which do not carry any chemical or physical information [Maleki et al., 2007].

## 8.2 Spectral observations and group assignment

The importance of IR spectroscopy in the identification of molecular structures originates from the rich information content obtained and the possibility to assign certain absorption bands related to its functional groups [Rohman and Man, 2010]. The resulting IR spectral feature overlaps significantly due to compositional complexity from hundreds of extracted metabolites without separation. The infrared spectrum in the region 400-4000  $\text{cm}^{-1}$  frequency is presented in Figure 8.1 (a). The wide band extending across the wavelengths between 2700 and 3600  $\text{cm}^{-1}$  originates from the OH and alkyl C-H bond stretching and does not provide useful information regarding any potential changes. The N-H stretch vibrations in the 3300-3400  $\text{cm}^{-1}$  region originating from amido group of proteins also overlap in this frequency range. Therefore the fingerprint region of 400 to 1800  $\text{cm}^{-1}$  [8.1 (b)] remained in focus for our study and for all further analysis. Moreover, the effect of noise, baseline drift, and peak overlap on estimations can be reduced by removing non-essential spectral regions.

The major constituents in dried strawberry include sugars, mainly fructose and glucose, besides fibre and protein [Giampieri et al., 2012]. The FTIR spectrum of fresh strawberry samples were compared with that of anhydrous glucose and fructose available from NIST database and found several spectral similarities of the signals in the 400-1000  $\text{cm}^{-1}$  region (see Figure 8.2). The signals in 620 and 655  $\text{cm}^{-1}$  region originate from C-CH<sub>3</sub> vibrations, while those of 1410-1480  $\text{cm}^{-1}$  originate from C-H bend in sugars. The spectra exhibit evidence of the presence of pectin by the appearance of the CO stretching vibration band at approximately 1725  $\text{cm}^{-1}$  [Suutarinen et al., 1998]. Nevertheless, the overlap from CO stretch-

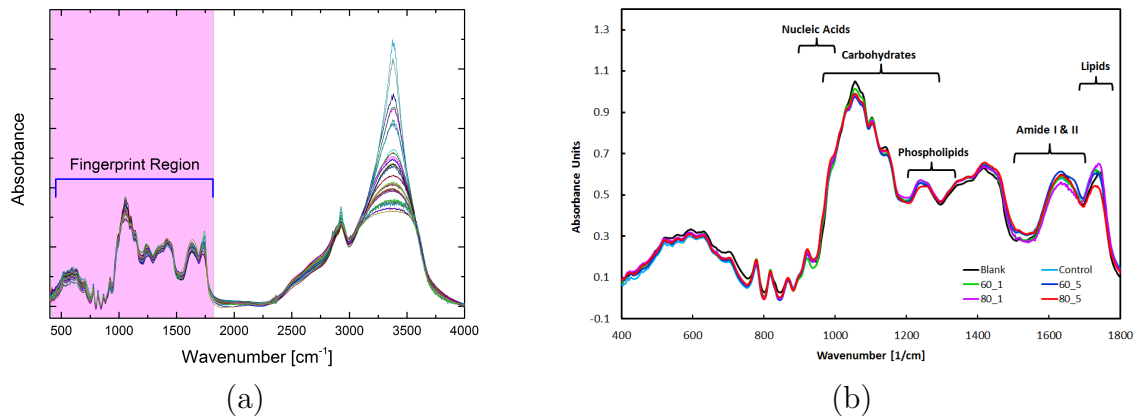


Figure 8.1: (a) Overlaid raw FTIR spectra of strawberry samples. (b) Average spectra of the strawberry samples in the fingerprint region ( $400\text{-}1800\text{ cm}^{-1}$ ). Blank refers to untreated samples on Day 0, while control refers to untreated samples after 24 h storage. The major chemical components responsible for vibrational signals in the respective regions are indicated.

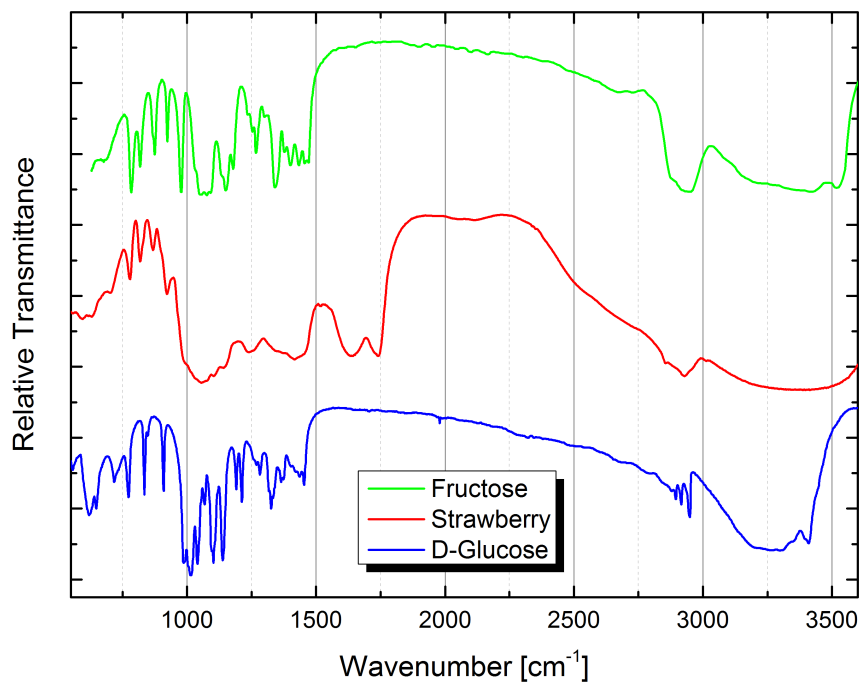


Figure 8.2: Comparison of FTIR spectra of strawberry with glucose and fructose obtained from NIST database.

ing vibration of the esters in this region cannot be ruled out. The wide band in the range  $1350\text{-}1450\text{ cm}^{-1}$  was assigned to O-H deformation from structural carbohydrates. The band in the region of  $1150\text{ to }1170\text{ cm}^{-1}$  originates from C-O vibrations in carbohydrates. The bands between  $1730\text{-}1755\text{ cm}^{-1}$  and  $1205\text{-}1265\text{ cm}^{-1}$  originated from C=O stretch and C-O-C stretch respectively and were most likely an outcome of the fatty substances. The carbonyl vibrations of the protein backbone were also noticeable between  $1700\text{ cm}^{-1}$  and  $1600\text{ cm}^{-1}$  (amide I region) in a second derivative spectrum (not shown).

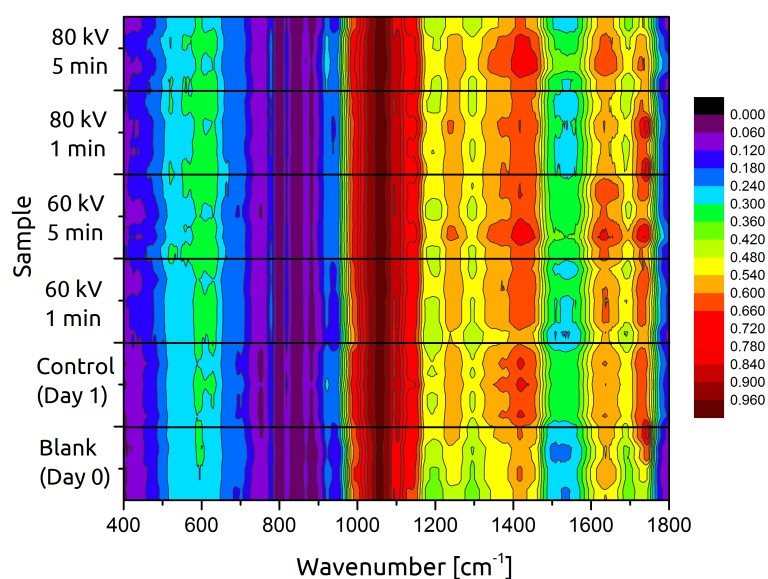


Figure 8.3: Contour plot of raw spectra for control and treated samples.

Figure 8.3 presents the raw spectrum of the blank, control, and treated samples as 2D contour plot in the fingerprint region. This plot helps to assess the major changes quickly, which are mainly confined to the  $500\text{-}700\text{ cm}^{-1}$  frequency. A minor loss of spectral peaks and/or peak narrowing can be observed in  $500\text{-}700\text{ cm}^{-1}$ . This region being mainly confined to peaks from sugars is difficult to be attributed as an effect of the plasma species. However, it is also worthwhile noting that the total soluble solids levels have been reported to steadily increase in ozonized fruit, reaching significantly higher levels than in controls during one week of storage [Kute et al., 1995]. The increase in the peak intensities and peak shifts in  $1500\text{-}1750\text{ cm}^{-1}$  region observed in treated samples can be ascribed to

possible changes in proteins.

### 8.3 Correlation heatmap analysis

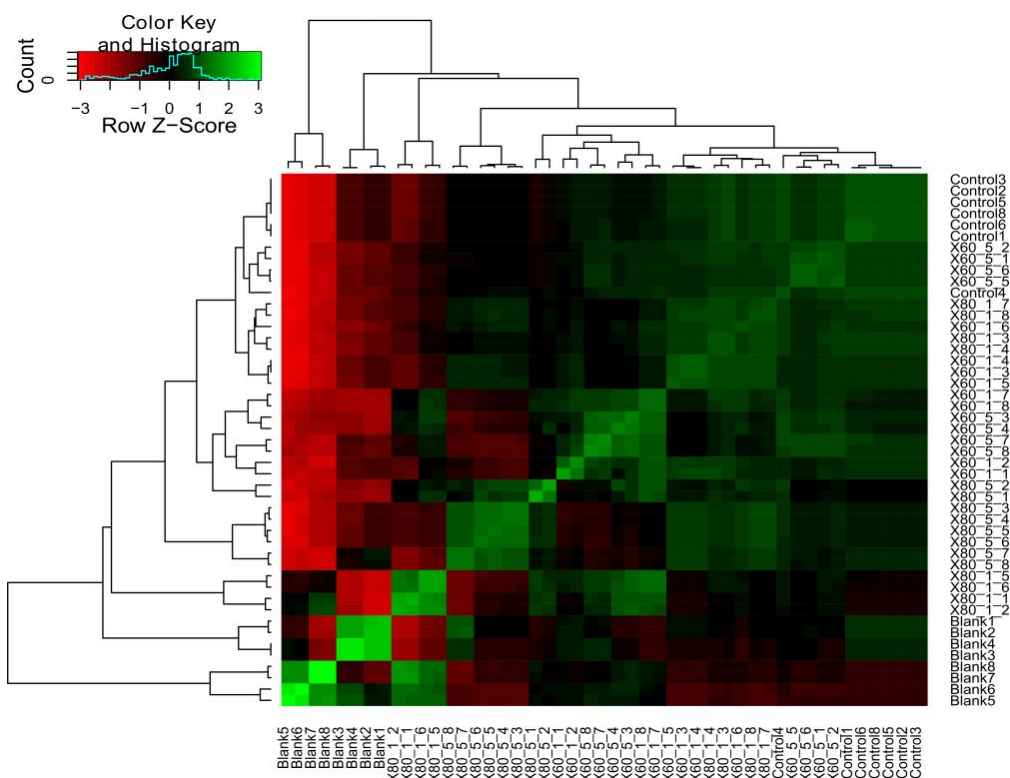


Figure 8.4: Correlation heat map and dendrogram of the second-derivative spectra. The last numeral represents sample replicate.

Data smoothing and taking derivatives while decreasing the information content of a spectrum can, however, increase the ability to distinguish between different spectra, especially when exploring correlation analysis [Li Yoon et al., 1999]. This is because the correlation coefficients between absorbance spectra are often very high and not suitable for identification purposes. Correlation heat maps allow evaluation of the qualitative changes in the spectra. Figure 8.4 presents the correlation heat map and the dendrogram of the classification based on the correlation coefficients (scaled on row data). From Figure 8.4 it becomes clear that the control samples (Day 1) were distinct from that of the blank (Day 0 samples)

observed from the red zone on the left. This is in agreement with our previous studies for changes in physico-chemical parameters [Misra et al., 2014]. Moving further down the branches, we also note that the treated samples are all distinct from the control and blank (with the exception of some outliers, possibly due to natural variability). The absence of a trend in the growth of the branches within the region of treated samples suggests that the effects of nonthermal plasma could be non-linear in nature. In order to reduce the effect of the correlated variables, and dig further the information contained in the dataset, PCA was performed.

## 8.4 Principal Component Analysis

PCA involves a mathematical procedure that transforms a number of possibly correlated variables into a smaller number of uncorrelated variables called principal components. It uses projections to extract from a large number of variables, a much smaller number of new variables, which account for most of the variability between samples. The unique feature of these principal components is that the first accounts for the most variability in the data, the second component accounts for the most of the remaining variability in the data, and each succeeding component takes accounts for less variability in the data [Innawong et al., 2004]. We conducted PCA on the second derivative spectral data to reveal any grouping between the samples.

The first two principal components (PCs) account for  $> 85\%$  of the total variance and thus contain most of the information of the original data, which is associated with the chemical groups of samples. The within sample variability, due to technical repetitions, is small compared to the between treatments variability as observed from the minimal separation between duplicate measurement points. There is no overall clear separation between the sample sets with the exception of closely distributed control samples (Figure 8.5). The blank samples were entirely distinct from that of control and corroborate the observation made from heatmap analysis. The large separation between blank replicates was suspected to be the result of natural variability in the composition of the strawberries.

Furthermore, samples treated at 80 kV for 5 minute are distinct from that of control (Figure 8.5, top and bottom). About 50 % of the samples treated at



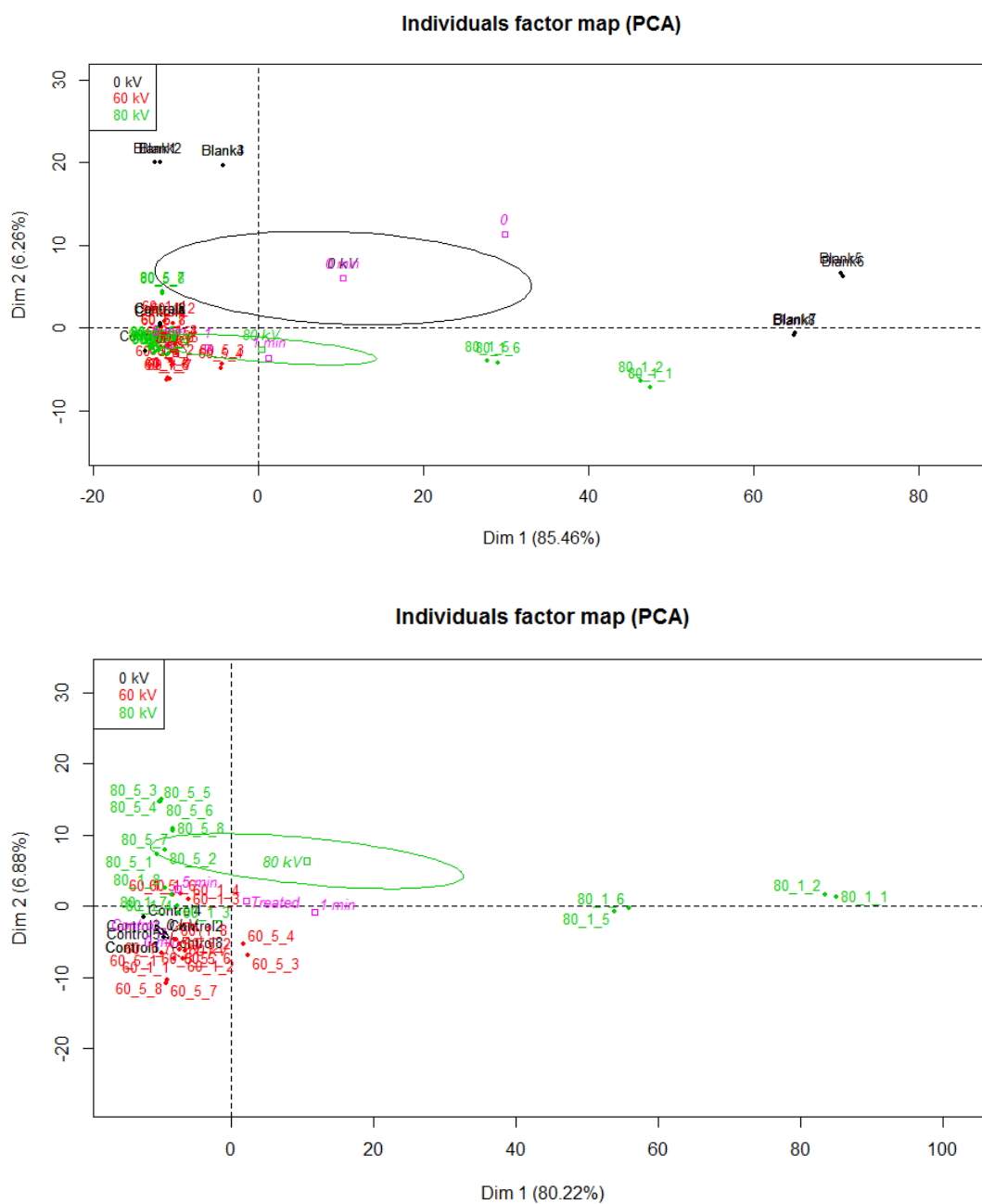


Figure 8.5: PCA of second derivative spectra. Top: Analysis on entire sample set. Bottom: Analysis on sample set excluding blank samples.

80 kV for 1 minute were distinct from that of control. This raises a key question of whether this is due to the carry over of natural variability or is an outcome of the process variations. The process variability could arise from different relative humidities inside the package, which in turn leads to variable concentrations of the species; or due to the inherent stochastic nature of the discharge and the electrical parameters. In fact, it motivates for further research to evaluate the statistical process efficiency of the NTP treatments. An absence of distinct grouping for samples treated at 60 kV could be interpreted as either the absence of major degradation reactions or the insensitivity of FTIR spectroscopy to capture the chemical transformations that occur.

## 8.5 Hierarchical Clustering on Principal Components (HC-PC)

Hierarchical clustering of the spectral data in the principal co-ordinates space was performed to observe any inherent clustering patterns in the datasets. In order to impose homogeneity, we performed clustering of the spectral with (Case I) and without blank (Case II). The dendrograms generated by cluster analysis were cut at the branches as recommended by the FactoMineR algorithm which is based on branching level where inertia gain is significant. The cluster analysis algorithm divided the sample sets in Case I into three clusters (see Figure 8.6) with the blank samples (coloured black being a separate cluster. The second cluster (coloured black) contains the control as well as the treated samples. This cluster was centred on control samples (specifically replicate 5 of control was the centre). The third cluster was centred about samples treated at 80 kV for 1 minute (replicate 4 was the centre). Similarly, for Case II, clustering revealed a maximum difference between the control and samples treated at 80 kV for 1 minute, with additional clusters centred around samples treated at 60 kV for 5 min and 1 min. In this case, samples treated at 80 kV for 5 min were more scattered. Detection of such natural clustering strongly suggested that there are changes in the chemical profile of strawberries following nonthermal plasma treatments at 80 kV irrespective of treatment time.

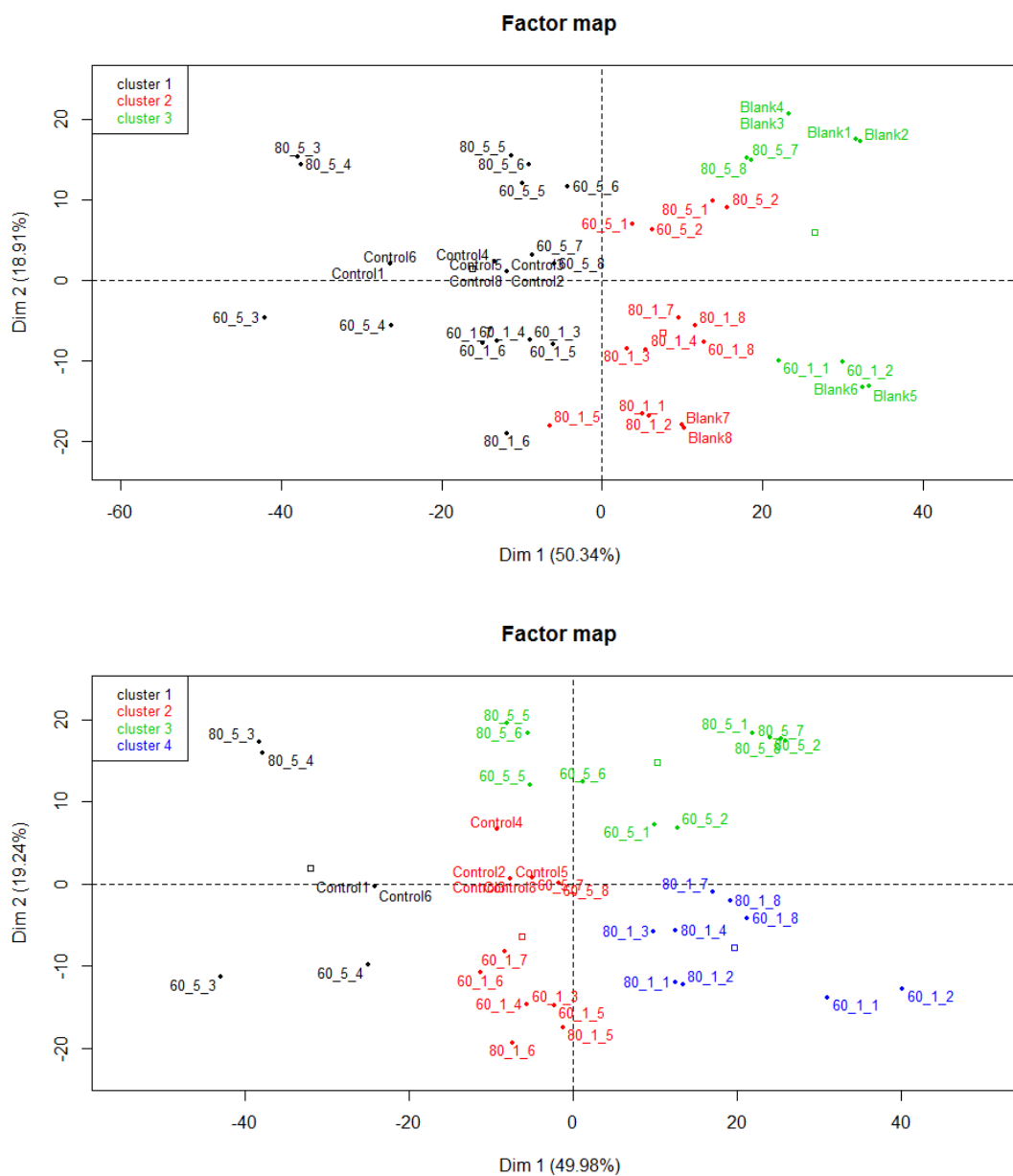


Figure 8.6: HC-PC of the raw data. Top: Cluster analysis on entire sample set. Bottom: Cluster analysis on sample set excluding blank samples.

## 8.6 Conclusion

The first objective of this chapter was to find out whether FTIR spectroscopy and chemometrics can be used for finding out if there are differences among control and plasma treated strawberries. The FTIR spectra were analysed for the origin of the peaks and vibrations from several groups were assigned to each peak. Taken together all the remarks from the FTIR spectra indicated that the NTP treatments induce changes in the chemical constituents of strawberries. The extent of change is also influenced by the process conditions, which followed a non-linear trend. The results from chemometric analysis indicated that the extent of changes in plasma treated strawberries stored for 24 h are in between that of fresh and control samples. Thus, the changes are not very drastic. The analysis of the spectra indicated that most of the changes are confined to the vibrations originating from amide I region.

The relative insensitivity of FTIR to identify the markers of change warranted the need for use of advanced analytical approaches such as liquid or gas chromatographic methods for separation and mass-spectrometric methods for identification of the changes in both major and minor chemical constituents. The insensitivity of the FTIR spectroscopy is due to the large number of overlapping (convoluted) peaks from the vibration of several functional groups of the complex chemical composition of strawberries. The exact identification and quantification of change will enable to conclude whether or not such effects of NTP are avoidable and if the process could be optimised, respectively.

# Chapter 9

## Effect on bioactives and volatiles

Strawberries are rich in bioactives such as phenolic compounds, including their abundant anthocyanins, which impart the bright red colour to the fruits [Hanum, 2004]. Strawberries are also rich in ascorbic acid [Cruz-Rus et al., 2011]. Strawberries undergo changes in sensory attributes such as texture and colour, as well as changes in the profile of bioactive and volatile compounds. The former aspects of effect of nonthermal plasma on colour and texture were described earlier. To obtain a complete insight into the changes induced by NTP treatment of strawberries, the changes in anthocyanin content, ascorbic acid, and flavour profile need to be assessed. In this chapter the ascorbic acid and anthocyanin content, and flavour profile of the control and plasma treated strawberries following 24 h storage in pack is presented.

### 9.1 Ascorbic acid content

The nutritional value of strawberries is mainly due to the content of ascorbic acid. The ascorbic acid content profile of control and plasma treated strawberries are shown in Figure 9.1. Both applied voltage for plasma induction and treatment time were found to have a significant effect ( $p < 0.05$ ) on the ascorbic acid content of strawberries. There was a statistically significant difference ( $p < 0.05$ ) between samples treated at 60 kV than those at 80 kV. This difference could be attributed to the changes in plasma chemistry. The reaction of ozone and other oxidising

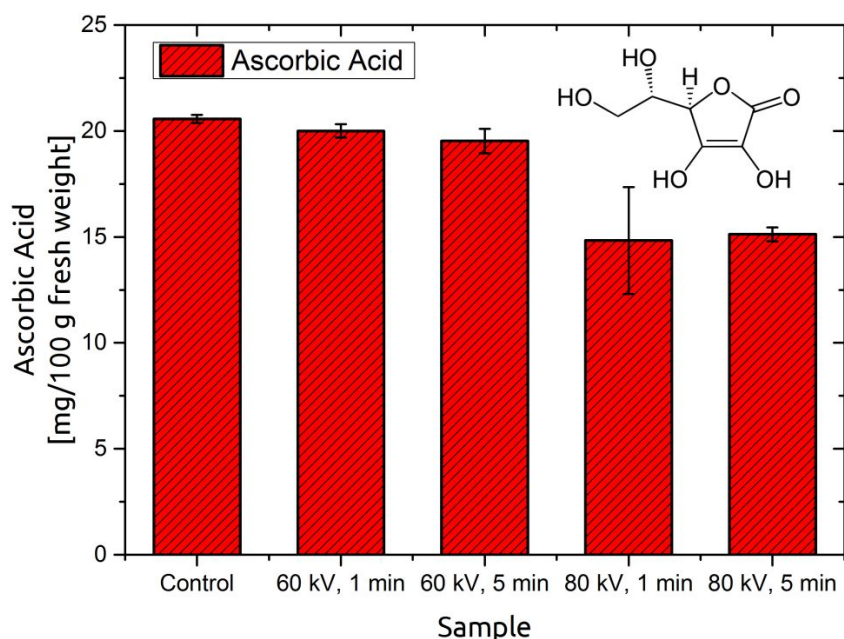


Figure 9.1: Changes in ascorbic acid content of control and NTP treated strawberries (24 h post-treatment).

species of NTP with ascorbic acid is proposed to be the major mode of action for the observed loss during processing. Furthermore, it is suspected that ascorbic acid degrades either by direct attack of ozone, described by Criegee mechanism or indirect reaction because of secondary oxidants. In an earlier study, [Tiwari et al. \[2009a\]](#) reported an exponential decay of ascorbic acid during ozonation of strawberry juice with more than 50% loss in 5 min at 7.8% (w/w) ozone concentration. However, the order of difference is relatively very low in this study. Contrary to our observations on day 1 with NTP, [Pérez et al. \[1999\]](#) reported an increase in the ascorbic acid content of continuous ozone treated strawberries after 3 days of storage.

## 9.2 Anthocyanin content

The group of phenolic compounds in strawberry which historically has received most attention, is the anthocyanin, responsible for the bright red colour of the

strawberries [Aaby et al., 2012]. Anthocyanins are also well known to contribute towards great health promoting effects. Different in vitro oxidation studies have shown that the antioxidant activity in fruit is directly correlated with the anthocyanins content [Cerezo et al., 2010]. Of all the polyphenols, pelargonidin-3-glucoside (P3G) has been reported to be the most abundant anthocyanin in strawberries (60-95%). The concentration of anthocyanin following cold plasma is therefore important for evaluating the sensory quality of berries, in addition to evaluation of the retention of their health beneficial properties. Therefore, in this study the evaluation of the anthocyanin stability following NTP treatments of strawberries was aimed.

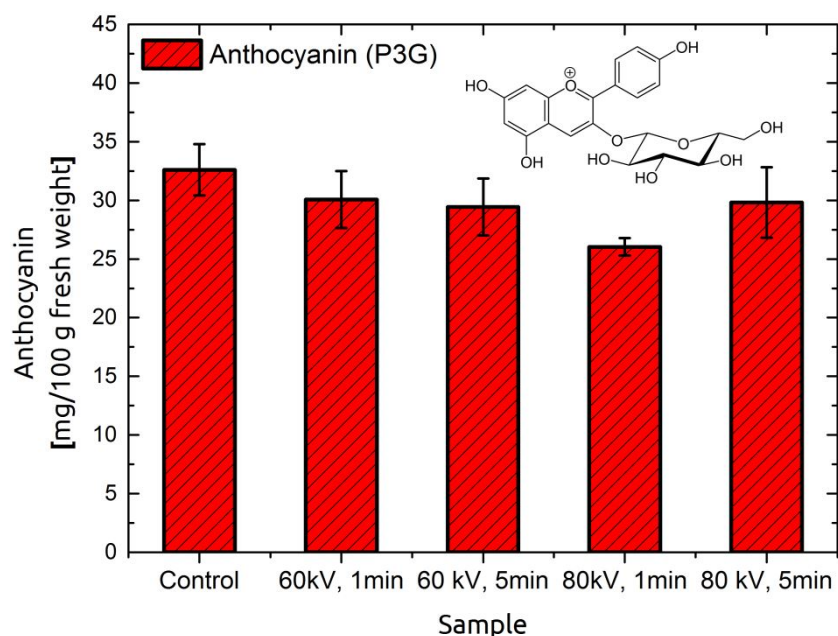


Figure 9.2: Anthocyanin content of control and plasma treated strawberries (24 h post-treatment).

The initial anthocyanin content of the control strawberries was found to be  $32.60 \pm 2.18$  mg/100 g fresh weight. The anthocyanin content of strawberry strongly depends upon the cultivar as well as on agronomic practices such as harvesting stage [Capocasa et al., 2008]. Aaby et al. [2012] studied the phenolic content of 27 cultivars of strawberries and reported that the P3G content could

vary between 6.9 to 47.7 mg/100 g fresh weight depending on cultivar. In the present study, the anthocyanin concentration appeared to be relatively unaffected by the plasma treatments (Figure 9.2). Results of statistical analysis confirmed that neither the applied voltage nor the treatment time had a significant effect on the overall anthocyanin content (expressed as P3G concentration,  $p > 0.05$ ). Ozone treatment is generally expected to cause the loss of antioxidant constituents, because of its strong oxidizing activity. Tiwari et al. [2009a] reported that ozonation of strawberry juice caused a decrease in anthocyanin content from 41.4 to 0.76 mg/L. However, ozone treatments (continuous exposure at 0.35 ppm) were previously reported to have minor effects on the total anthocyanin contents of whole strawberries, although changes were evident after 3 days [Pérez et al., 1999]. This difference could be attributed to the high mass transfer to liquid foods processed by direct injection of ozone into bubble columns, whereas relatively low diffusion of gas phase ozone (and other reactive species of plasma) into the interiors of fruit tissue. Earlier studies have also revealed the inactivation of polyphenol oxidase (PPO) in whole strawberry fruits following cold plasma treatments (Chapter 7). Therefore, it is envisaged that the anthocyanins are likely to be more stable even during storage. The colour of the strawberries can be directly related to the pigments, especially anthocyanin. A significant change in the colour of plasma treated strawberries was not observed in earlier works [Misra et al., 2014] and the insignificant change in anthocyanin content also supports this observation.

### 9.3 GC-MS Volatile Fingerprinting

Solid-phase microextraction (SPME), is a solvent-free sample-pretreatment technique that integrates sampling, isolation and enrichment of analytes into one step. The exposure of the fused-silica fiber coated with polymer to the headspace (HS) above the sample allowed enrichment and concentration of volatiles, which was then transferred to the GC port for thermal desorption and identification by MS.

Strawberries are known for their flavour. Strawberry aroma has one of the most complex fruit aromas made up of approximately 350 volatile compounds. Therefore, the GC-MS chromatogram of strawberries is very complex with many peaks eluting simultaneously as can be observed in the overlaid chromatograms



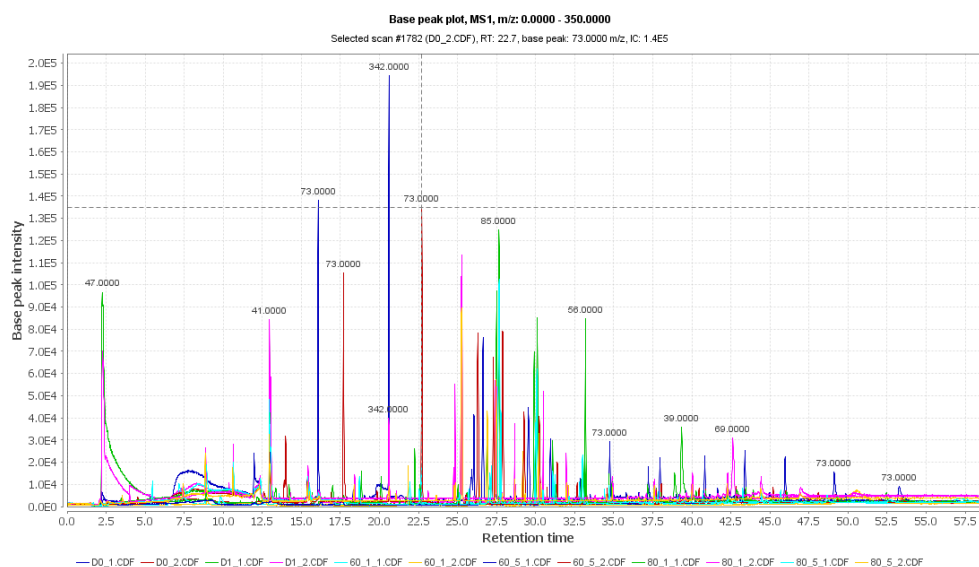
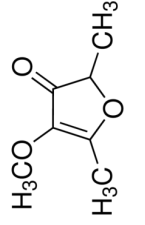
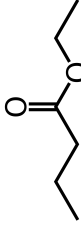

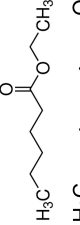
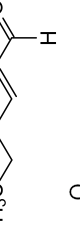




Figure 9.3: Overlaid raw GC-MS chromatograms of the control and plasma treated strawberries.




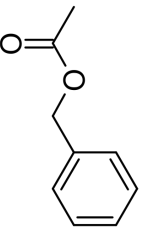
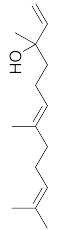
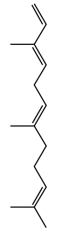


of the control and plasma treated strawberries, provided in Figure 9.3. Therefore, Automated Mass Spectral Deconvolution and Identification System (AMDIS, available from NIST) was used for deconvolution of the spectra. AMDIS de-skews and deconvolutes the ions of the TIC (Total Ion Chromatogram) from a raw GCMS data file, extracts a series of "cleaned" mass spectra ("components"), as well as their corresponding retention times, and identifies the compounds present in the sample (targets) by matching the mass spectra of the "components", and optionally also their retention times, against a reference library, either commercial such as the NIST<sup>TM</sup> libraries or self-built by the operator [Cerdán-Calero et al., 2012]. In spite of deconvolution, it is very difficult to identify all the volatile compounds with certainty considering the number of breakdown products, unavailability or high cost of the standard compounds. All the volatile compounds reported in Table 9.1 were identified with high probabilities when compared with standards from the NIST database (similarity coefficient or reverse similarity coefficient of *at least 80 % and higher*). Additional information regarding the odour characteristic of the compounds detected was obtained using flavour and human odour space databases [Acree and Arn, 2014; GARA, 2014; Jewison et al., 2012; SenseLab, 2014].

Table 9.1: HS-SPME-GC-MS analysis of volatile compounds in control and plasma treated strawberries.

#	Volatile Compound	Structure	Description	Control	60 kV- 1 min	60 kV- 5 min	80 kV- 1 min	80 kV- 5 min	Match %
1	2,5-Dimethyl-4-methoxy-3(2H)-furanone [OR mesifuran]		Caramel; Grape; Maple; Mushroom; Potato; Coffee; Nutty; Meaty	✓	✓	N.D.	N.D.	N.D.	86
2	ethyl butanoate		Banana, Pineapple, Berry, Cognac	N.D.	✓	N.D.	N.D.	N.D.	92
3	methyl hexanoate		Fruit; Fresh; Sweet	✓	✓	✓	✓	✓	88
4	ethyl hexanoate		Apple peel; fruit	✓	✓	✓	✓	✓	81
5	2-hexenal		Apple; Cherries; Green note	✓	N.D.	✓	N.D.	N.D.	88
6	1-hexyl acetate		Sweet ester odor; Fruity odor	✓	N.D.	N.D.	N.D.	N.D.	80
7	nonanal		Fat; Citrus; Green.	✓	✓	✓	✓	✓	89

N.D. = Not Detected; Match refers to minimum reverse match.

Contd... HS-SPME-GC-MS analysis of volatile compounds in control and plasma treated strawberries.

#	Volatile Compound	Structure	Description	Control	60 kV- 1 min	60 kV- 5 min	80 kV- 1 min	80 kV- 5 min	Match %
8	1-decanol		Fat	✓	✓	✓	✓	✓	81
9	octyl hexanoate		Fruity odor	✓	✓	✓	✓	✓	83
10	5-hexyldihydro- 2(3H)-furanone [OR $\gamma$ -decalactone]		Peach, Creamy, Fatty, Fruity	✓	✓	✓	✓	✓	84
11	acetic acid, phenylmethyl ester [OR benzyl acetate]		Sweet, Fruity, Floral, Pear. Fresh, Boiled vegetable	✓	✓	✓	✓	✓	89
12	3,7,11-trimethyl- 1,6,10-dodecatrien-3-ol [OR nerolidol]		Wood, Flower, Wax	✓	✓	✓	✓	✓	91
13	3,7,11-trimethyl-1,3, 6,10-dodecatetraene [OR $\alpha$ -farnesene]		Wood; Sweet	✓	✓	✓	✓	✓	81
14	5-octyldihydro- 2(3H)-furanone [OR $\gamma$ -dodecalactone]		Flower, Fruity, Sweet	✓	✓	✓	✓	✓	86
15	linalool		Flower, Lavender	✓	✓	✓	✓	✓	84

The analysis of the mass-spectral data allowed to identify 15 major volatiles in the strawberry samples. These mainly included esters, furanone, and alcohol containing compounds. Volatiles belonging to ester class are the most important compounds contributing to the fruity flavour in most horticultural plants. Fruity, green grass and other flavour notes of strawberries are emanated by a complex mixture of esters [Perez et al., 1993]. Several important esters including methyl hexanoate, ethyl hexanoate, ethyl butanoate, hexyl acetate and octyl hexanoate were identified in the control and treated group of strawberries, at varying levels. The changes in levels of ethyl and methyl- hexanoate were not statistically significant ( $p > 0.05$ ) among the samples. However, the general trend indicated a rise in treated strawberries. Among the esters, hexyl acetate was absent in plasma treated strawberries, indicating destruction of the ester volatiles. Similarly, the aldehyde, 2-hexenal, partially responsible for a green note was also found to absent in treated samples. Mesifuran (2,5-dimethyl-4-hydroxy-2H-furan-3-one) was not detected in the strawberries treated at 60 kV for 5 min or 80 kV at either treatment times, indicating that the NTP treatments adversely affected the mesifuran. This is highly undesirable and is an issue of concern, as 2,5-dimethyl-4-hydroxy-2H-furan-3-one is one of the most important volatile compound contributing to strawberry flavour [Zabetakis and Holden, 1997]. In addition, it is also believed to be associated with potential anti-infective activities in human microbial infections [Sung et al., 2007]. In general, a decrease in levels of 5-hexyl-dihydro-3H-furan-2-one ( $\gamma$ -decanolactone) was also observed. The ability of plasma to destroy volatile compounds was recently reported by Chen et al. [2010], who observed up to 80% decrease in the levels of dimethylamine in 5 min following treatments with a corona system at 40 kV. Therefore, it is proposed that the reactive species of the NTP, viz. ozone, nitric oxides and hydroxyl radicals generated by reaction of ozone with water, react with the volatiles during the storage period of 24 h. An electrophilic addition mechanism for  $\text{NO}_3$  reactions with ketones

The treated strawberries were found to have significantly higher levels of linalool than the control samples. Floral essences can be attributed to linalool (1,6-Octadien-3-ol, 3,7-dimethyl-), a terpene considered to be an important contributor to the fresh aroma of strawberry [Aguiló-Aguayo et al., 2009]. Aguiló-Aguayo et al. [2009] attributed the higher levels of linalool in pulsed electric field

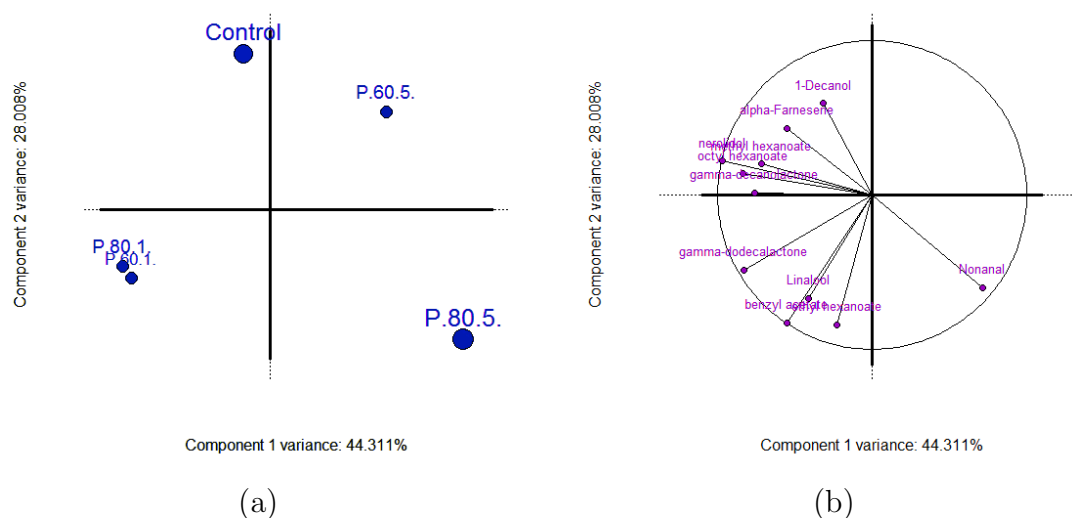


Figure 9.4: PCA of the volatile compounds identified by HS-SPME/GC-MS. (a) Score plot (b) Loadings plot.

treated strawberries to a higher retention of the higher retention of  $\beta$ -glucosidase activity, which releases linalool from its glycosidic precursor by enzymatic hydrolysis. In order to confirm that this is the mechanism in NTP treated strawberries, the kinetics of  $\beta$ -glucosidase activity should be evaluated. The ability of NTP treatments to modulate the enzyme activity has been reported earlier by several authors [Li et al., 2011; Pankaj et al., 2013; Surowsky et al., 2013]. It is however, suspected that the mechanism is likely to be more complex, considering that the mesifuran levels decrease, which should have released by hydrolysis, if it were  $\beta$ -glucosidase mediated. It is worth noting that if different pathways have common precursors, the activity of the enzymes involved in each pathway will be decisive in which synthesis will be favoured.

In order to correlate the change in the volatile compounds with respect to the sample classes, we undertook a multivariate approach by conducting PCA (taking into consideration only volatiles which were present in both control and treated samples). The results of PCA are presented in figure 9.4. By comparing the scores and the loadings plot it becomes clear that NTP treatment changes the volatile composition of strawberries. The aldehyde nonanal correlated well with the strongest treatment (80 kV, 5 min), indicating it to be a specific marker. The control samples were primarily dominated by presence of the alcohol, 1-decanol

and  $\alpha$ -farnesene (3,7,11-trimethyldodeca-1,3,6,10-tetraene), the content of which decreased following NTP treatments. Most of the fruity esters were retained in the samples treated by NTP for 1 min.

## 9.4 Conclusions

Following NTP treatments and 24 h storage inside the package, a loss of ascorbic acid was noticeable at a voltage level of 80 kV, irrespective of the treatment time. This could lead to a loss of antioxidant capacity of the strawberries. The loss of ascorbic acid was attributed to the direct attack by the ozone molecules. The anthocyanin content of the strawberries, expressed as pelargonidin-3-glucoside (P3G) was found to remain stable.

The changes in the volatile profiles of strawberries in following treatments with other nonthermal technologies have often been proposed to be an outcome of changes to the enzymatic pathways or enzyme activity. Such changes due to NTP treatments cannot be over-ruled. In fact, results of previous studies, as described in Chapter 7 have also shown the inactivation of peroxidase. However, the relative differences among the compounds belonging to the same class warrant the possibility of a complex mechanism, which needs further investigation.

A real-time analysis of the volatile compounds during the 24 h storage period should be carried out using relatively novel approaches such as proton-transfer reaction mass spectrometry (PTR-MS) to understand the dynamics of volatile evolution and link it with the degradation of ozone and nitrogen oxide species in gas phase.

The differential modulation of some volatiles relative to others strongly suggests that the active species of plasma act on a number of enzymes involved in the bio-formation of different aroma compounds. An attempt to unravel the dynamics of metabolites in strawberry (in a global sense) should remain in focus in future studies. This will enable linking the observed changes with that of the major biochemical pathways, thus allowing to identify the mechanisms by which NTP affects the metabolism of the fresh produce.

Overall, the effects of nonthermal plasma on the nutritional properties of strawberries or fruits in general, should be considered by fresh produce processors

prior to its adoption as a decontamination intervention.

# Chapter 10

## Degradation of Pesticides

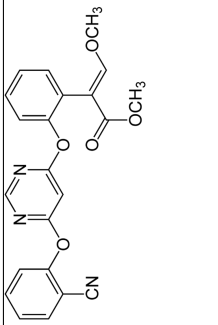
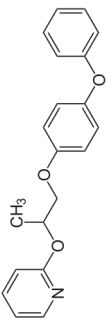
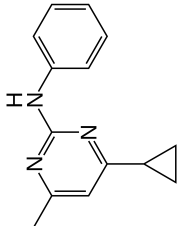
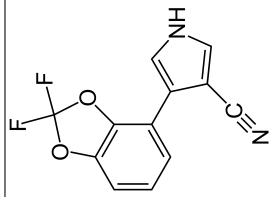
Besides microbiological concerns, pesticides residues in strawberries could also pose health risks above their maximum permitted levels, as they are often consumed without washing or are minimally processed. This work investigates the potential of in-package NTP for the degradation of pesticide residues on strawberries. The aims of the present study were to find out if in-package NTP can degrade pesticide residues on strawberries. More specifically, the study involves quantifying the degradation of fungicides, namely azoxystrobin, cyprodinil, fludioxonil, and pyriproxyfen on strawberry surface by gas chromatography- mass spectrometry (GC-MS/MS) analysis, under the influence of NTP treatment. A brief summary of these pesticides, including chemical structure, toxicity is provided in Table 10.1. With an aim to explain the observed effects, the electrical and optical characterisation of the plasma source has also been carried out.

### 10.1 Ozone Concentration

The ozone concentrations measured after 300 s of plasma treatment were found to be 900, 3100 and 3800 ppm (within  $\pm 10\%$  error) for applied bias voltages of 60, 70, and 80 kV (RMS) respectively.



Table 10.1: Summary of the pesticides studied in this work.

Pesticide	Class	Chemical structure	Mode of action	MRL <sup>†</sup>
Azoxystrobin, Methyl (2E)-2-(2-[[6-(2-cyanophenoxy)pyrimidin-4-yl]oxy]phenyl)-3-methoxyacrylate	Fungicide		Binds with the Q0 site of Complex III of the mitochondrial electron transport chain, thereby ultimately preventing the generation of ATP in fungi (Singh and Singh, 2010)	10 ppm (EU, USA)
Pyriproxyfen, 4-phenoxyphenyl (RS)-2-(2-pyridyloxy)propyl ether	Insecticide		A juvenile hormone analog; overloads the hormonal system of the target insect, ultimately affecting egg production, brood care and other social interactions, and inhibiting growth (Masner et al., 1994)	EU: 0.05 ppm; USA: 0.3 ppm
Cyprodinil, 4-cyclopropyl-6-methyl-N-phenylpyrimidin-2-amine	Fungicide		Broad spectrum; Synthetic; Inhibits methionine bio-synthesis (Masner et al., 1994)	5 ppm (EU, USA)
Fludioxonil, 4-(2,2-difluoro-1,3-benzodioxol-4-yl)-1H-pyrrole-3-carbonitrile	Fungicide		Non-systemic; Inhibits the osmosensing signalling pathway. This, in effect, inhibits spore germination and stops mycelial growth (Cabras et al., 1997)	3 ppm (EU, USA)

<sup>†</sup>Ref: [www.mrldatabase.com](http://www.mrldatabase.com)

## 10.2 Quantification of pesticide residues and degradation kinetics

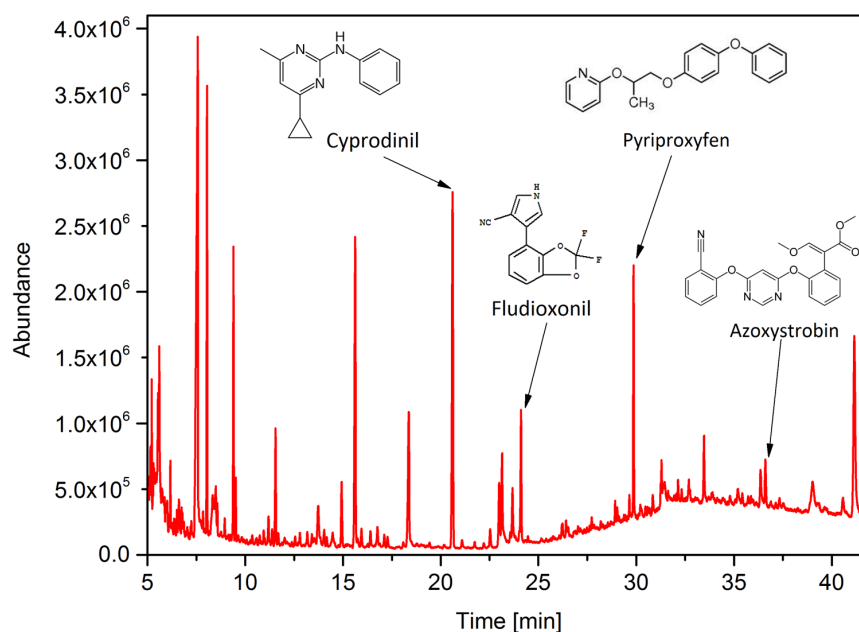


Figure 10.1: A representative chromatogram showing retention times of the four pesticides.

The four pesticides, namely azoxystrobin, cyprodinil, fludioxonil and pyriproxyfen were identified at retention times of 36.6, 20.6, 24.1 and 29.8 minute respectively (see Figure 10.1). The concentrations of the pesticides in the control samples were found to be  $1709.8 \pm 212.4$  ppb,  $2721.2 \pm 213.0$  ppb,  $2540.2 \pm 44.7$  ppb, and  $1569.7 \pm 186.7$  ppb for azoxystrobin, cyprodinil, fludioxonil and pyriproxyfen respectively. These values suggested the appropriateness of dipping method for introducing pesticide residues onto strawberries. Following nonthermal plasma treatments and 24 h post-storage, a time and voltage dependent degradation of all the four pesticides was observed (see Figure 10.2). The decrease in the concentrations of the pesticide residues relative to the control were significant ( $p \leq 0.05$ ) for all the samples. Both applied voltage and treatment time were significant ( $p \leq 0.05$ ) as process parameters governing the degradation. A maximum decrease of 69%, 45%, 71% and 46% was observed for azoxystrobin, cyprodinil, fludioxonil,

and pyriproxyfen respectively after 300 s of treatment at an applied voltage of 80 kV. Except pyriproxyfen, the final concentration of all other pesticides following plasma treatment was found to be below the permitted maximum residual limit (MRL) (see Table 10.1).

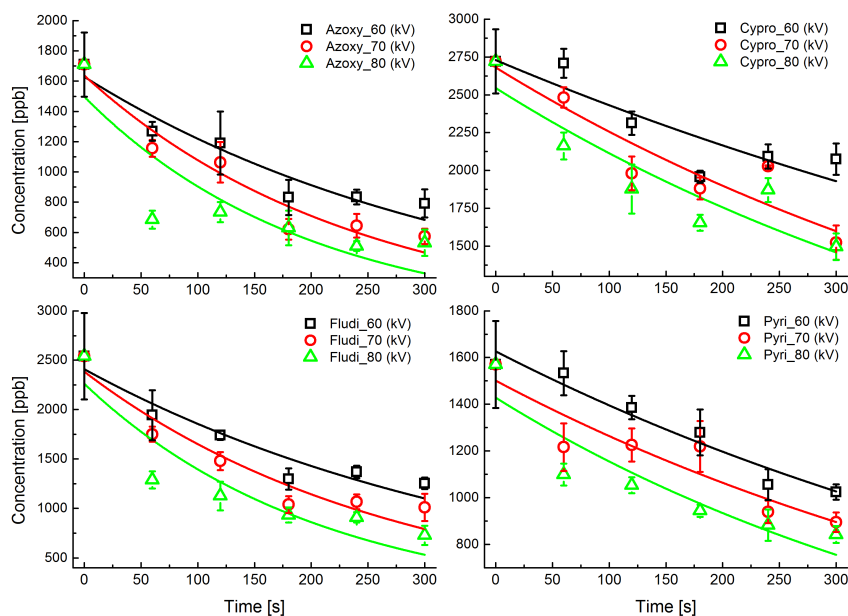


Figure 10.2: Residual pesticide concentrations in strawberries before and after plasma treatment.

Table 10.2 presents the first-order rate constant for the pesticide degradation under different voltages. Clearly, the rate constant ( $k$ ) increases with increase in voltage. It should be noted that the first-order rate kinetics is based on our assumption that ozone reacts with the pesticide to form the degraded product, c.f. Walse and Karaca [2011]. The deviations from typical first-order kinetics of the degradation could be attributed to the geometric complexity of strawberries and the possible diffusion of the pesticides into the fruit interiors.

### 10.3 Mechanism of Degradation

Degradation of pesticide residues on fruits by aqueous ozonation is already well established [Hwang et al., 2001; Ong et al., 1996; Reynolds et al., 1989]. Re-

Table 10.2: Model parameters for pesticide degradation based on first-order kinetics.

Pesticide	Voltage	Rate Constant, $k(s^{-1})$	$R^2(\text{adj.})$
Azoxystrobin	60 kV	$0.0029 \pm 4.9 \times 10^{-4}$	0.76
	70 kV	$0.0042 \pm 5.59 \times 10^{-4}$	0.85
	80 kV	$0.0051 \pm 1.00 \times 10^{-4}$	0.65
Cyprodinil	60 kV	$0.0012 \pm 2.45 \times 10^{-4}$	0.66
	70 kV	$0.0017 \pm 2.77 \times 10^{-4}$	0.78
	80 kV	$0.0019 \pm 3.33 \times 10^{-4}$	0.73
Fludioxonil	60 kV	$0.0026 \pm 4.86 \times 10^{-4}$	0.72
	70 kV	$0.0037 \pm 5.84 \times 10^{-4}$	0.79
	80 kV	$0.0048 \pm 9.14 \times 10^{-4}$	0.74
Pyriproxyfen	60 kV	$0.0015 \pm 2.68 \times 10^{-4}$	0.75
	70 kV	$0.0017 \pm 3.58 \times 10^{-4}$	0.68
	80 kV	$0.0021 \pm 3.92 \times 10^{-4}$	0.72

cently, [Karaca et al. \[2012\]](#) demonstrated a decline of fenhexamid, cyprodinil, and pyrimethanil on table grapes, when stored in atmospheres of  $0.3 \mu\text{L/L}$  ozone enriched air. Notably, very high ozone concentrations were detected immediately after plasma treatment in our experiments. By analogy, ozone can be considered as one of the active species responsible for the degradation of the pesticides, in addition to the other myriad of species generated by plasma. Ozone can also undergo reaction with water to yield peroxide and hydroxyl radicals. The degradation of cyprodinil is probably an outcome of the attack at the nitrogen bridge between the two rings or the phenyl ring and/or the pyrimidyl ring by hydroxyl radicals formed from ozone [[Anfossi et al., 2006](#)] as typified in [Figure 10.3](#) and further oxidation by Criegee mechanism.

As a general observation, the degradation kinetics indicates that the rate of degradation (slope) decreases with increase in treatment time. This can be linked with the kinetics of air plasma chemistry where excited nitrogen species are favoured over oxygen species for extended time scales [[Kossyi et al., 1992](#)]. This type of exclusive competitive reaction mode has also been suggested for photo-induced degradation of diuron (herbicide) in aqueous solution by nitrites and nitrates with photolysis of water (which yields OH radicals) [[Shankar et al., 2007](#)]. It may be noted that treatments for 240 and 300 s did not have a significant ef-

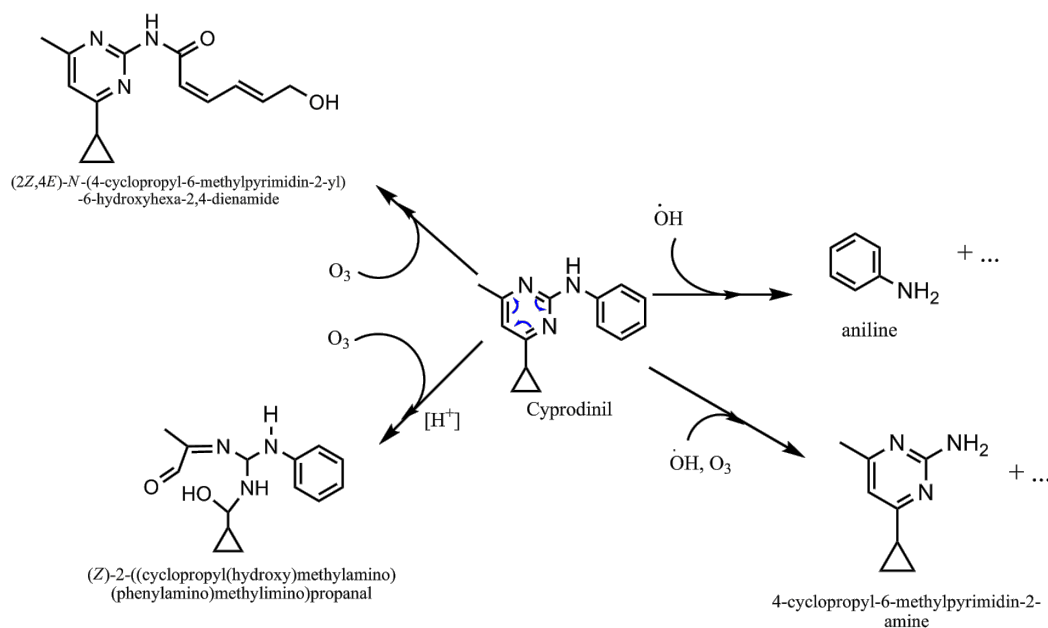


Figure 10.3: Proposed reaction products for Cyprodinil (based on [Walse and Karaca \[2011\]](#)).

fect on the degradation of azoxystrobin. [Bai et al. \[2010\]](#) have reported similar observations, where the effect of an increase in applied power to plasma has insignificant effect on the degradation of dichlorovos. The excited nitrogen species despite their short life-time can shield the action of ozone by forming local acidic environments, after the discharge is turned off. However, using optical absorption spectroscopy the presence of ozone in packages for up to 4-6 h was confirmed, even after the discharge is turned off. The degradation of azoxystrobin in alkaline environments over acidic is already reported in the literature [[Singh et al., 2010](#)]. Since azoxystrobin has several functional groups, this most likely provides several sites for the attack by the active chemical species of NTP. It has been suggested that the photodegradation of azoxystrobin proceeds via multiple, parallel reaction pathways including photo-isomerization, photo-hydrolysis of the methyl ester and of the nitrile group, cleavage of the acrylate double bond, photohydrolytic ether cleavage between the aromatic ring resulting in phenol, and oxidative cleavage of the acrylate double bond [[Boudina et al., 2007](#); [Rodrigues et al., 2013](#)]. Similarly, the degradation of pyriproxyfen most likely begins by the cleavage of central ether

linkage.

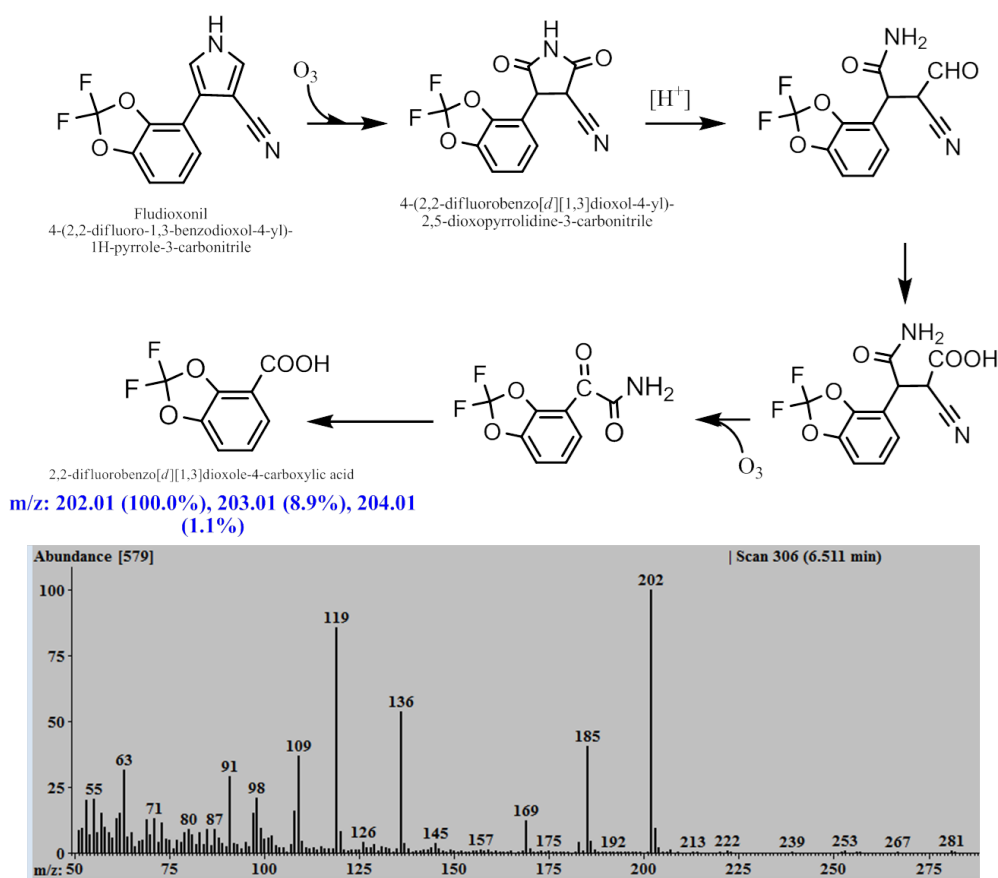


Figure 10.4: Proposed mechanisms for degradation of Fludioxonil (see c.f. [Roberts and Hutson \[1999\]](#)). On bottom is the mass spectrum of the peak obtained at 6.51 min which shows abundance in the 202 m/z peak.

In order to explore the possible degradation mechanisms of pesticides, it is important to identify the intermediates and by-products during plasma treatment [[Bai et al., 2010](#)]. However, it is worthwhile noting that the identification and toxicity determination of the degradation products is often quite difficult, considering the number of breakdown products that could form after exposure to various treatments [[Karaca et al., 2012](#)]. Unavailability of commercial standards of the degraded products also adds to the analytical problems. A total ion scan with an aim to identify the degradation reaction pathway was also performed. An unidentified peak at 6.51 min with abundance in 202 m/z ion fragment was observed.

Based on previous reports [Roberts and Hutson, 1999], the degradation pathway for fludioxinil shown in Figure 10.4 was proposed, whose end product was assigned to the peak at 6.51 min. Besides this there could be other unidentified free or conjugated degradation products. It is worth mentioning that it was difficult to make any conclusions or identify common degradation products reported in the literature for all other pesticides, with added complexities from the compounds of strawberry matrix. The large number of peaks observed in the chromatogram (Figure 10.1) correspond to non-polar metabolites of strawberries. Therefore, at this point the identification of degradation products using NMR spectroscopy is planned as a future work.

## 10.4 Conclusion

Pesticides are of concern to fresh both consumers and regulatory bodies as many fruits, including strawberries are often consumed without processing. Nonthermal plasma treatment inside a sealed package, using a dielectric barrier discharge successfully degraded pesticide residues on strawberries. In particular, the levels of azoxystrobin, cyprodinil, fludioxonil and pyriproxyfen decreased by a maximum of 69%, 45%, 71 and 46% respectively after 5 minute of treatment at 80 kV (RMS). The kinetics of degradation was modelled using a simple first-order differential rate equation.

The dissipating action of plasma on the pesticide residues was suspected to be an outcome of the direct attack of ozone and other active species. A reaction pathway for the degradation of fludioxonil was proposed based on the mass-spectrometry data. The proposed end product of degradation was far less toxic compared to fludioxonil.

These findings suggest the potential of nonthermal plasma treatment as a means to ensure chemical food safety, in addition to its proven microbicidal effects. Future studies must focus on identifying the degradation products, and unravelling the mechanism of degradation(s) using advanced methods and model systems. In addition, the safety of the end products of degradation should be assessed either using the data from literature or with the help of toxicity studies.

# Chapter 11

## Concluding Remarks & Future Recommendations

- In-package decontamination of fresh foods is desirable as this minimises the possibility of post-processing contamination. In order to achieve this, atmospheric cold plasma was generated inside a sealed package containing the food, using a dielectric barrier discharge.
- The electrical diagnostics revealed that the dielectric barrier discharge plasma source operates in a stable filamentary regime. The operation in a filamentary regime allows to generate very high concentrations of ozone in a very short duration.
- Within the typical operating conditions employed, the plasma source is efficient in generating high concentrations of ozone, the antimicrobial properties of which are well-established.
- The application of high voltages allows sustaining a stable discharge even at large gaps in the order of few centimetres. The operation at centimetre scale permits plasma treatment of most fruits and vegetables whose dimensions lie within these limits. However, it is practically impossible to plasma treat foods in-field with large dimensions. However, indirect (out-of-field) treatments could prove to be useful for such foods.
- The set-up allows transferring power to the gas typically in the order of 10-100 W, making it energy efficient. This points to the possible long term



sustainability of nonthermal plasma treatment as a food processing technology.

- The emission spectrum of the discharge revealed the generation of reactive oxygen and excited molecular nitrogen species. The low or negligible intensity of the OH peaks indicated the 'cold' or nonthermal nature of the plasma, which was also confirmed from infrared thermometry measurements. The operation within ambient temperature conditions also indicates that plasma technology is suitable for most heat sensitive biomaterials.
- The discolouration of methylene blue dye treated in the plasma, both in-field and out-of-field indicated that the reactive species diffused within the package and into the liquid. Gompertz and first-order kinetic models were evaluated to model dye discolouration and it was observed that the models exhibited a good fit within the exponential phase only. Thus, use of methylene blue dye as a chemical diagnostic tool is not ideal. In order to further explore the possibility for use of MB as an indicator for ozone levels, further studies are desirable with extensive experiments within short time scales.
- Methylene Blue is a potential environmental contaminant from textile industries and NTP can degrade it. This raises the possibility for another interesting application of plasma for the treatment of effluents from the food industries, especially with high phenolic content (e.g. waste water from olive mills).
- The out-of-field (or remote) plasma treatment of cherry tomatoes does not adversely affect the critical quality parameters of colour, firmness, pH and weight loss. The respiration rate of cherry tomatoes does not exhibit a rise following cold plasma treatments. However, the optimisation of packaging conditions for meeting the requirements of high barrier nature for in-package plasma, while relatively high permeability desired for respiring produce needs to be addressed in future studies.
- Of the three different gases explored, NTP treatment in air was found best for retention of quality of strawberries, followed by high oxygen environments

and then high nitrogen. A high nitrogen and low oxygen environment, although effective in background flora reduction, causes significant decrease in firmness and leads to unpleasant dark colour in strawberries. However, these results were specific for strawberries and other produce could behave differently.

- The results with modified atmosphere gases show that the discharge characteristics are affected by the presence of strawberries as the discharge becomes up to 20% more effective in terms of power transfer. While these results have to be further elaborated by rigorous studies under different conditions, they can be ascribed to the smaller gas volume leading to faster species accumulation and more efficient chemical kinetics in the closed container and are strongly dependent on the type of gas mixture.
- Fourier transform infrared spectroscopy and chemometric studies on the plasma treated strawberries indicated that there were differences among the control and treated groups. However, the exact nature of the change was not detectable using this methods.
- Further studies quantifying the changes in anthocyanin and ascorbic acid content using liquid chromatography indicated degradation at 80 kV treatment voltages. Head space gas analysis using solid-phase micro-extraction coupled with gas chromatography-mass spectrometry (GC-MS) revealed loss of some volatiles in the strawberries. However, the dominant esters responsible for strawberry aroma were retained. The effects on the loss of ascorbic acid indicated that the reactive species are capable of diffusing into the internal tissues of the fruit and that in-package nonthermal plasma is a volumetric treatment.
- The diffusivity of the reactive species from nonthermal plasma into foods is yet to be studied. The analytical challenge arises from the rapid recombination rates, escape from the package and lack of appropriate diagnostic methods to probe the individual reactive species. When treating solid foods, the properties such as surface-to-volume ratio, the gas permeability of the

cuticle (for plant foods), the porosity and susceptibility to oxidation are some important factors that should be considered.

- There is a good potential for treatment of liquid foods- either by allowing diffusion of the gas phase species into the liquid or using plasma generated inside the liquid itself.
- The NTP set-up employed is also capable of eliminating the residues of contemporary pesticide on fresh produce by significant levels. Thus, it contributes not only to microbiological, but also chemical safety. The degradation kinetics can be approximated to follow first-order mechanism. To unravel the mechanism of the degradation of pesticides, it is desirable to conduct experiments using nuclear magnetic resonance (NMR) spectroscopy with treatment of individual pesticides in liquid media.
- The fact that foods retain their quality following NTP treatments at 60 kV for up to 1 minute renders it an ideal and robust technology for decontamination of thermally sensitive or fragile solid foods.
- Apart from the results reported in this thesis, the author has also found several other interesting applications of this technology, especially for modification of food properties. For example, nonthermal plasma treatment can alter the surface of snack foods to enhance spread of oils and minimise seepage into the product. Similarly, plasma can modify the rheological properties of wheat flour. Such potential of NTP should be harnessed by extensive set of experiments.

# Publications

## Peer-reviewed Journal Articles

1. **Misra, NN**, Tiwari, BK, Raghavarao, KSMS & Cullen, PJ (2011) Nonthermal plasma inactivation of food-borne pathogens, *Food Engineering Reviews*, 3(3-4), 159-170. (IF: 2.81) DOI:10.1007/s12393-011-9041-9
2. **Misra, NN**, Ziuzina, D, Cullen, PJ & Keener, KM (2013) Characterization of a novel atmospheric air cold plasma system for treatment of biomaterials, *Transactions of the American Society of Agricultural and Biological Engineers*, 56(3):1-6. (IF: 0.97) DOI: 10.13031/trans.56.9939
3. **Misra, NN**, Patil, S, Moiseev, T, Bourke, P, Mosnier, JP, Keener, KM, & Cullen, PJ (2014) In-package atmospheric pressure cold plasma treatment of strawberries, *Journal of Food Engineering*, 125, 131-138. (IF: 2.27) DOI:10.1016/j.jfoodeng.2013.10.023.
4. **Misra, NN**, Pankaj, SK, Walsh, T, O Regan, F., Bourke, P, & Cullen, PJ (2014) In-package nonthermal plasma degradation of pesticides on fresh produce, *Journal of Hazardous Materials*, 271, 33-40. (IF: 3.93) DOI:10.1016/j.jhazmat.2014.02.005
5. **Misra, NN**, Keener, KM, Mosnier, JP, Bourke, P, & Cullen, PJ (2014) In-package atmospheric pressure cold plasma treatment of cherry tomatoes, *Journal of Bioscience and Bioengineering*, (in-press). (IF: 1.74) DOI:10.1016/j.jbiosc.2014.02.005

6. **Misra, NN**, Moiseev, T, Patil, S, Pankaj, SK, Keener, KM, Mosnier, JP, Bourke, P & Cullen, PJ (2014) In-package atmospheric pressure cold plasma treatment of strawberries using MAP gases. *Food & Bioprocess Technology*, (in-press). (IF: 4.12) DOI: 10.1007/s11947-014-1356-0
7. **Misra, NN**, et al. Evaluation of ozone generation within a sealed package from a dielectric barrier discharge using degradation of methylene blue. *Ozone: Science & Engineering*, (Under Review).
8. **Misra, NN**, Kaur, S, Tiwari, BK, Kaur, A, Singh, N & Cullen, PJ (2015) Atmospheric pressure cold plasma (ACP) treatment of wheat flour, *Food Hydrocolloids*, in-press. (IF: 4.28)
9. **Misra, NN**, Sullivan, C, Pankaj, SK, Alvarez-Jubete, L, Cama, R, Jacoby, F & Cullen, PJ (2014) Enhancement of oil spreadability of biscuit surface by nonthermal barrier discharge plasma, *Innovative Food Science & Emerging Technologies*, Accepted. (IF: 2.53)
10. Pankaj, SK, **Misra, NN** & Cullen, PJ (2013) Kinetics of tomato peroxidase inactivation by atmospheric pressure cold plasma based on dielectric barrier discharge, *Innovative Food Science & Emerging Technologies*, 19:153-157. (IF: 2.53) DOI: 10.1016/j.ifset.2013.03.001
11. Cullen, PJ, **Misra, NN**, Han, L, Bourke, P, Keener, KM, O'Donnell, CP, Moiseev, T, Mosnier, JP & Milosavljević, V (2014) Inducing a Dielectric Barrier Discharge Plasma within a Package, *IEEE Transactions on Plasma Science* (Accepted). (IF: 0.87) DOI: 10.1109/TPS.2014.2321568
12. Pankaj, SK, Bueno-Ferrer, C, **Misra, NN**, Milosavljević, V, O'Donnell, CP, Bourke, P, Keener, KM, & Cullen, PJ (2013) Applications of cold plasma technology in food packaging, *Trends in Food Science & Technology*, 35(1):5-17. (IF: 4.14) DOI: 10.1016/j.tifs.2013.10.009
13. Pankaj, SK, Bueno-Ferrer, C, **Misra, NN**, O'Neill, L, Jiménez, A, Bourke, P, & Cullen, PJ (2014) Characterization of polylactic acid films for food packaging as affected by dielectric barrier discharge atmospheric plasma,

---

*Innovative Food Science & Emerging Technologies*, 21:107-113. (IF: 2.53)  
DOI: 10.1016/j.ifset.2013.10.007.

14. Pankaj, SK, Bueno-Ferrer, C, **Misra, NN**, O'Neill, L, Jiménez, A, Bourke, P, & Cullen, PJ (2014) Surface, thermal and antimicrobial release properties of plasma treated zein films, *Journal of Renewable Materials*, 2(1):77-84. DOI: 10.7569/JRM.2013.634129
15. Pankaj, SK, Bueno-Ferrer, C, **Misra, NN**, Bourke, P, & Cullen, PJ (2014) Zein film: Effects of dielectric barrier discharge atmospheric cold plasma, *Journal of Applied Polymer Science* (Accepted). (IF: 1.39)  
DOI: 10.1002/app.40803
16. Moiseev, T, **Misra, NN**, Patil, S, Cullen, PJ, Bourke, P, Keener, KM & Mosnier, JP (2014) Post-discharge gas composition of a large-gap DBD in humid air by UV-Vis absorption spectroscopy, *Plasma Sources Science & Technology* (Accepted). (IF: 2.52)
17. Patil, S, Moiseev, T, **Misra, NN**, Cullen, PJ, Mosnier, JP, Keener, KM, & Bourke, P (2013) Influence of atmospheric cold plasma process parameters and role of relative humidity on inactivation of *Bacillus atrophaeus* spores inside a sealed package, *Journal of Hospital Infection* (Accepted). (IF: 2.86)

## Conference Publications

1. **Misra, NN**, Ziuzina, D, Keener, KM & Cullen PJ (2012) Characterization of a Novel Cold Atmospheric Air Plasma System for Treatment of Packaged Liquid Food Products, Paper # 121337629, in *ASABE Annual International Meeting*, Dallas, Texas, 29 Jul - 1 Aug, 2012.
2. **Misra, NN**, Pankaj, SK, Bourke, P & Cullen, PJ (2013) Kinetics of Tomato Peroxidase Activity Following Atmospheric Cold Plasma Treatments, in *42<sup>nd</sup> Annual Food Research Conference*, Teagasc Food Research Centre, Ashtown, Dublin, 27-28 June, 2013.

3. **Misra, NN**, Pankaj, SK, Walsh, T, O Regan, F., Bourke, P, & Cullen, PJ (2013) In-package nonthermal plasma treatment degrades contemporary pesticides on strawberries, in *International Conference on Plasma Science and Applications (ICPSA2013)*, Nanyang Technological University, Singapore, 4-6 December, 2013.
4. **Misra, NN**, Pankaj, SK, Bourke, P & Cullen, PJ (2013) Bioactive profiles of in-package nonthermal plasma treated strawberries, in *International Conference on Plasma Science and Applications (ICPSA2013)*, Nanyang Technological University, Singapore, 4-6 December, 2013.
5. Pankaj, SK, Bueno-Ferrer, C, **Misra, NN**, O'Neill, L, Jiménez, A, Bourke, P, & Cullen, PJ (2013) Effects of in-package dielectric barrier discharge atmospheric plasma on polylactic acid, in *4<sup>th</sup> International Conference on Biodegradable and Biobased Polymers (BIOPOL-2013)*, Rome, Italy, 1-3 October, 2013.
6. Moiseev, T, **Misra, NN**, Bourke, P, Cullen, PJ, & Mosnier, JP (2013) Non-thermal DBD plasma for in-pack sterilization: diagnostics on SAFE-BAG using electrical and optical methods, In: *11th UK Technological Plasma Workshop (TPW)*, York Plasma Institute, The University of York, UK, 16-17 December, 2013.
7. **Misra, NN**, NN, Milosavljević, V, Chapwanya, M, Pankaj, SK, Mosnier, JP, & Cullen, PJ (2013) A computational model of the nonthermal plasma discharge inside a sealed package, In: *International Food Convention (IFCON)*, Central Food Technological Research Institute, Mysore, 18-21 December, 2013.
8. Pankaj, SK, **Misra, NN**, Bourke, P, & Cullen, PJ (2013) Investigation of changes in cold plasma treated strawberries using spectroscopic and chemometric approaches, In: *International Food Convention (IFCON)*, Central Food Technological Research Institute, Mysore, 18-21 December, 2013.
9. **Misra, NN**, & Cullen, PJ (2014) Chemistry of nonthermal plasma treated foods- an untargeted metabolomics approach, In: *Gordon Research Conference-*

*Plasma Processing Science: Many Scales, Many Applications, One Discipline*, Bryant University, Rhode Island, USA, 27 July-1 August, 2014.

## Book Chapters

1. **Misra, NN**, Han, L, Tiwari, BK, Bourke, P & Cullen, PJ (2014) Nonthermal plasma technology for decontamination of foods, Chapter 6, pp 155-183, In: Bozariis, I.S. (Ed.), *Innovations in Food Microbiology*, CRC Press.
2. **Misra, NN**, Segat, A. & Cullen, PJ (2014) Atmospheric pressure nonthermal plasma decontamination of foods, In: Ravishankar, R.V. (Ed.), *Advances in Food Biotechnology*, Wiley-Blackwell (in-press).
3. **Misra, NN**, Cullen PJ, Jaeger, H, Lik, HC, Yoshida, H, & Barba, FJ (2014) Emerging macroscopic pre-treatment, In: Galanakis, Charis (Ed.), *Food Waste Recovery: Processing technologies and industrial techniques*, Elsevier Press (in-press).

## Patent

**Misra, NN**, Sullivan, C, & Cullen, PJ (2013) A method for reducing the oil in snacks by increasing spreadability, *UK1322387.0*, (filed).

## Awards

1. **2014:** Rain Bird Engineering Concept of the Year Award, conferred by American Society of Agricultural and Biological Engineers for *High Voltage Atmospheric Cold Plasma Process*.
2. **2011:** Irish Research Council- Embark Initiative Fellowship (Nov 2011- Nov 2014) for pursuing PhD research in the field of *In-Pack Decontamination of Fresh Produce using Nonthermal Plasma*.



# References

- Aaby, K., Mazur, S., Nes, A., and Skrede, G. (2012). Phenolic compounds in strawberry (*Fragaria x ananassa* Duch.) fruits: Composition in 27 cultivars and changes during ripening. *Food Chemistry*, 132:86–97. [115](#)
- Abramzon, N., Joaquin, J., Bray, J., and Brelles-Marino, G. (2006). Biofilm destruction by rf high-pressure cold plasma jet. *IEEE Transactions on Plasma Science*, 34(4):1304–1309. [30](#)
- Acree, T. and Arn, H. (2014). Flavornet and human odor space. [117](#)
- Adams, J. B. (1991). Review: Enzyme inactivation during heat processing of food-stuffs. *International Journal of Food Science & Technology*, 26:1–20. [97](#)
- Aday, M. S., Buyukcan, M. B., Temizkan, R., and Caner, C. (2014). Role of ozone concentrations and exposure times in extending shelf life of strawberry. *Ozone: Science & Engineering*, 36:43–56. [92](#), [94](#)
- Aguiló-Aguayo, I., Oms-Oliu, G., Soliva-Fortuny, R., and Martn-Belloso, O. (2009). Flavour retention and related enzyme activities during storage of strawberry juices processed by high-intensity pulsed electric fields or heat. *Food Chemistry*, 116:59–65. [120](#)
- Akbudak, B., Akbudak, N., Seniz, V., and Eris, A. (2007). Sequential treatments of hot water and modified atmosphere packaging in cherry tomatoes. *Journal of Food Quality*, 30(6):896–910. [9](#)
- Alonso, J., Garcia, J., Calleja, A., Ribas, J., and Cardesin, J. (2005). Analysis, design, and experimentation of a high-voltage power supply for ozone generation

- based on current-fed parallel-resonant push-pull inverter. *IEEE Transactions on Industry Applications*, 41(5):1364–1372. 70
- Amjad, M., Salam, Z., Facta, M., and Ishaque, K. (2012). A simple and effective method to estimate the model parameters of dielectric barrier discharge ozone chamber. *IEEE Transactions on Instrumentation and Measurement*, 61:1676–1683. 70
- Anfossi, L., Sales, P., and Vanni, A. (2006). Degradation of anilinopyrimidine fungicides photoinduced by iron(III)-polycarboxylate complexes. *Pest Management Science*, 62:872–879. 128
- AOAC (1998). *Official methods of analysis of the Association of Official Analytical Chemists*. Association of Official Analytical Chemists. 50
- Arias, R., Lee, T.-C., Logendra, L., and Janes, H. (2000). Correlation of lycopene measured by HPLC with the  $L^*$ ,  $a^*$ ,  $b^*$  color readings of a hydroponic tomato and the relationship of maturity with color and lycopene content. *J. Agric. Food Chem.*, 48:1697–1702. 52
- Azharonok, V., Kratáko, L., Nekrashevich, Y., Filatova, I., Meľnikova, L., Dudchik, N., Yanetskaya, S., and Bologa, M. (2009). Bactericidal action of the plasma of high-frequency capacitive and barrier discharges on microorganisms. *Journal of Engineering Physics & Thermophysics*, 82(3):419–426. 28
- Bai, Y., Chen, J., Mu, H., Zhang, C., and Li, B. (2009). Reduction of dichlorvos and omethoate residues by  $O_2$  plasma treatment. *Journal of Agricultural & Food Chemistry*, 57(14). 42
- Bai, Y., Chen, J., Yang, Y., Guo, L., and Zhang, C. (2010). Degradation of organophosphorus pesticide induced by oxygen plasma: Effects of operating parameters and reaction mechanisms. *Chemosphere*, 81:408–414. 42, 129, 130
- Baier, M., Foerster, J., Schnabel, U., Knorr, D., Ehlbeck, J., Herppich, W., and Schlüter, O. (2013). Direct non-thermal plasma treatment for the sanitation of fresh corn salad leaves: Evaluation of physical and physiological effects and antimicrobial efficacy. *Postharvest Biology & Technology*, 84(0):81 – 87. 5

- Bárdoš, L. and Baránková, H. (2008). Plasma processes at atmospheric and low pressures. *Vacuum*, 83(3):522–527. [20](#)
- Bárdoš, L. and Baránková, H. (2010). Cold atmospheric plasma: Sources, processes, and applications. *Thin Solid Films*, 518:6705–6713. [18](#), [20](#)
- Basaran, P., Basaran-Akgul, N., and Oksuz, L. (2008). Elimination of *Aspergillus parasiticus* from nut surface with low pressure cold plasma (LPCP) treatment. *Food Microbiology*, 25:626–32. [2](#), [29](#), [33](#), [37](#)
- Bellan, P. (2006). *Fundamentals of plasma physics*. Cambridge University Press. [13](#)
- Berchieri Jr, A., Wigley, P., Page, K., Murphy, C., and Barrow, P. (2001). Further studies on vertical transmission and persistence of *Salmonella enterica* serovar Enteritidis phage type 4 in chickens. *Avian pathology*, 30:297–310. [34](#)
- Bermúdez-Aguirre, D., Wemlinger, E., Pedrow, P., Barbosa-Cánovas, G., and Garcia-Perez, M. (2013). Effect of atmospheric pressure cold plasma (APCP) on the inactivation of *Escherichia coli* in fresh produce. *Food Control*, 34:149–157. [5](#), [84](#)
- Bernard, C., Leduc, A., Barbeau, J., Saoudi, B., Yahia, L., and Crescenzo, G. D. (2006). Validation of cold plasma treatment for protein inactivation: a surface plasmon resonance-based biosensor study. *Journal of Physics D: Applied Physics*, 39:3470–3478. [100](#)
- Berzins, A., Hellstrom, S., Silins, I., and Korkeala, H. (2010). Contamination patterns of *Listeria monocytogenes* in cold-smoked pork processing. *Journal of Food Protection*, 73(11). [35](#)
- Bhande, S., Ravindra, M., and Goswami, T. (2008). Respiration rate of banana fruit under aerobic conditions at different storage temperatures. *Journal of Food Engineering*, 87:116–123. [79](#)
- Boudam, M., Moisan, M., Saoudi, B., Popovici, C., Gherardi, N., and Massines, F. (2006). Bacterial spore inactivation by atmospheric-pressure plasmas in the

- presence or absence of UV photons as obtained with the same gas mixture. *Journal of Physics D: Applied Physics*, 39:3494. 21
- Boudina, A., Emmelin, C., Baaliouamer, A., Päissé, O., and Chovelon, J. (2007). Photochemical transformation of azoxystrobin in aqueous solutions. *Chemosphere*, 68:1280 – 1288. 129
- Cameron, A. C., Boylan-Pett, W., and Lee, J. (1989). Design of modified atmosphere packaging systems: Modeling oxygen concentrations within sealed packages of tomato fruits. *Journal of Food Science*, 54:1413–1416. 79
- Cano, M. P., Hernandez, A., and De Ancos, B. (1997). High pressure and temperature effects on enzyme inactivation in strawberry and orange products. *Journal of Food Science*, 62:85–88. 55
- Cao, W., Zhu, Z., Shi, Z., Wang, C., and Li, B. (2009). Efficiency of slightly acidic electrolyzed water for inactivation of *Salmonella enteritidis* and its contaminated shell eggs. *International Journal of Food Microbiology*, 130:88–93. 34
- Capocasa, F., Scalzo, J., Mezzetti, B., and Battino, M. (2008). Combining quality and antioxidant attributes in the strawberry: The role of genotype. *Food Chemistry*, 111:872–878. 115
- Casariego, García, M., Díaz, R., and Roblejo, L. (2014). Effect of edible chitosan/zeolite coating on tomatoes quality during refrigerated storage. *Emirates Journal of Food and Agriculture*, 26:238–246. 85
- Céline, A., Gonçalves, O., Jacquemin, F., and Fréour, S. (2014). Qualitative and quantitative assessment of water sorption in natural fibres using ATR-FTIR spectroscopy. *Carbohydrate Polymers*, 101:163–170. 58
- Cerdán-Calero, M., Sendra, J. M., and Sentandreu, E. (2012). Gas chromatography coupled to mass spectrometry analysis of volatiles, sugars, organic acids and aminoacids in valencia late orange juice and reliability of the automated mass spectral deconvolution and identification system for their automatic identification and quantification. *Journal of Chromatography A*, 1241:84–95. 117

- Cerezo, A. B., Cuevas, E., Winterhalter, P., Garcia-Parrilla, M., and Troncoso, A. (2010). Isolation, identification, and antioxidant activity of anthocyanin compounds in Camarosa strawberry. *Food Chemistry*, 123:574–582. [115](#)
- Cerrutti, P. and Alzamora, S. (1996). Inhibitory effects of vanillin on some food spoilage yeasts in laboratory media and fruit purees. *International Journal of Food Microbiology*, 29:379–386. [37](#)
- Chen, J., Yang, J., Pan, H., Su, Q., Liu, Y., and Shi, Y. (2010). Abatement of malodorants from pesticide factory in dielectric barrier discharges. *Journal of Hazardous Materials*, 177:908–913. [120](#)
- Chen, L. C. (2000). Effects of factors and interacted factors on the optimal decolorization process of methyl orange by ozone. *Water Research*, 34:974–982. [66](#)
- Chiper, A. S., Anita, V., Agheorghiesei, C., Pohoata, V., Anita, M., and Popa, G. (2004). Spectroscopic diagnostics for a DBD plasma in He/Air and He/N<sub>2</sub> gas mixtures. *Plasma Processes & Polymers*, 1:57–62. [71](#)
- Chiper, A. S., Chen, W., Mejlholm, O., Dalgaard, P., and Stamate, E. (2011). Atmospheric pressure plasma produced inside a closed package by a dielectric barrier discharge in Ar/CO<sub>2</sub> for bacterial inactivation of biological samples. *Plasma Sources Science & Technology*, 20:10. [24](#), [36](#)
- Clydesdale, F. M. (1993). Color as a factor in food choice. *Critical Reviews in Food Science and Nutrition*, 33:83–101. [10](#), [93](#)
- Connolly, J., Mosnier, J., V.P., V., Byrne, E., Cullen, P., and Keener, K. (2010). Diagnostic of reactive species in a dielectric barrier discharge air/helium plasma for the treatment of a pre-packed food simulant. In *Proceedings of the 37th EPS Conference on Plasma Physics*, volume 34A, page P4.317. [32](#)
- Connolly, J., Valdramidis, V., Byrne, E., Karatzas, K., Cullen, P. J., K.M., K., and J.P., M. (2013). Characterization and antimicrobial efficacy against *E. coli* of a helium/air plasma at atmospheric pressure created in a plastic package. *Journal of Physics D: Applied Physics*, 46:035401. [46](#)

- Cooper, M., Fridman, G., Staack, D., Gutsol, A., Vasilets, V., Anandan, S., Cho, Y., Fridman, A., and Tsapin, A. (2009). Decontamination of surfaces from extremophile organisms using nonthermal atmospheric-pressure plasmas. *IEEE Transactions on Plasma Science*, 37:866–871. [28](#)
- Critzer, F., Kelly-Wintenberg, K., South, S., and Golden, D. (2007). Atmospheric plasma inactivation of foodborne pathogens on fresh produce surfaces. *Journal of food protection*, 70:2290. [2](#), [5](#), [29](#), [39](#)
- Cruz-Rus, E., Amaya, I., Sanchez-Sevilla, J. F., Botella, M. A., and Valpuesta, V. (2011). Regulation of l-ascorbic acid content in strawberry fruits. *Journal of Experimental Botany*, 62:4191–4201. [113](#)
- Davies, R. and Breslin, M. (2003). Investigations into possible alternative decontamination methods for salmonella enteritidis on the surface of table eggs. *Journal of Veterinary Medicine, Series B*, 50(1):38–41. [34](#)
- Day, B. (1996). High oxygen modified atmosphere packaging for fresh prepared produce. *Postharvest News and Information*, 7:1N–34N. [92](#)
- De Luca, M., Terouzi, W., Ioele, G., Kzaiber, F., Oussama, A., Oliverio, F., Tauler, R., and Ragno, G. (2011). Derivative FTIR spectroscopy for cluster analysis and classification of morocco olive oils. *Food Chemistry*, 124:1113–1118. [103](#)
- Deilmann, M., Halfmann, H., Bibinov, N., Wunderlich, J., and Awakowicz, P. (2008). Low-pressure microwave plasma sterilization of polyethylene terephthalate bottles. *Journal of Food Protection*, 71:2119–2123. [26](#)
- Del-Valle, V., Hernández-Muñoz, P., Guarda, A., and Galotto, M. (2005). Development of a cactus-mucilage edible coating (*Opuntia ficus indica*) and its application to extend strawberry (*Fragaria ananassa*) shelf-life. *Food Chemistry*, 91:751–756. [93](#)
- Deng, S., Ruan, R., Mok, C. K., Huang, G., Lin, X., and Chen, P. (2007). Inactivation of *Escherichia coli* on almonds using nonthermal plasma. *Journal of Food Science*, 72(2):M62–6. [33](#), [100](#)

- Deng, X., Shi, J., and Kong, M. (2006). Physical mechanisms of inactivation of *Bacillus subtilis* spores using cold atmospheric plasmas. *IEEE Transactions on Plasma Science*, 34(4):1310–1316. 31
- Deng, X., Shi, J., and Kong, M. (2009). Protein destruction by a helium atmospheric pressure glow discharge: Capability and mechanisms. *Journal of Applied Physics*, 101(7):074701. 29
- Dirks, B. P., Dobrynin, D., Fridman, G., Mukhin, Y., Fridman, A., and Quinlan, J. J. (2012). Treatment of raw poultry with nonthermal dielectric barrier discharge plasma to reduce *Campylobacter jejuni* and *Salmonella enterica*. *Journal of Food Protection*, 75:22–28. 36
- Dojcinovic, B. P., Roglic, G. M., Obradovic, B. M., Kuraica, M. M., Kostic, M. M., Nestic, J., and Manojlovic, D. D. (2011). Decolorization of reactive textile dyes using water falling film dielectric barrier discharge. *Journal of Hazardous Materials*, 192(2):763–771. 67, 71
- Donner, A. and Keener, K. (2011). Investigation of in-package ionisation. *Journal of purdue undergraduate research*, 1:10–15. 34
- Doyle, M. and Erickson, M. (2006). Reducing the carriage of foodborne pathogens in livestock and poultry. *Poultry science*, 85(6):960–973. 34
- DrLange (2000). *Fundamentals of colorimetry- Application report No. 10e*. DrLange. 84
- Elez-Martínez, P., Soliva-Fortuny, R., and Martín-Belloso, O. (2006). Comparative study on shelf life of orange juice processed by high intensity pulsed electric fields or heat treatment. *European Food Research and Technology*, 222:321–329. 56
- Elhadi, M. (2009). Introduction. In *Modified and Controlled Atmospheres for the Storage, Transportation, and Packaging of Horticultural Commodities*, chapter 1. CRC Press. 5
- Ercan, S. d. and Soysal, c. (2011). Effect of ultrasound and temperature on tomato peroxidase. *Ultrasonics Sonochemistry*, 18:689–695. 54

- Eskin, M. (1990). Biochemical changes in raw foods: fruits and vegetables. In Eskin, M., editor, *Biochemistry of foods*, pages 70–78. Academic Press, Inc. [90](#)
- Espie, S., Marsili, L., MacGregor, S., and Anderson, J. (2001). Investigation of dissolved ozone production using plasma discharge in liquid. *Pulsed power plasma science, Digest of Technical Papers*, 1:616–619. [38](#)
- Falkenstein, Z. and Coogan, J. J. (1997). Microdischarge behaviour in the silent discharge of nitrogen-oxygen and water-air mixtures. *Journal of Physics D: Applied Physics*, 30:817. [24](#), [45](#), [69](#)
- Fang, Z., Qiu, Y., Sun, Y., Wang, H., and Edmund, K. (2008). Experimental study on discharge characteristics and ozone generation of dielectric barrier discharge in a cylinder-cylinder reactor and a wire-cylinder reactor. *Journal of Electrostatics*, 66:421–426. [89](#)
- FDA (2012). Information on the recalled jensen farms whole cantaloupes. [1](#)
- Fernandez, A., Noriega, E., and Thompson, A. (2013). Inactivation of *Salmonella enterica* serovar typhimurium on fresh produce by cold atmospheric gas plasma technology. *Food Microbiology*, 33(1):24–9. [5](#)
- Fernández-Gutierrez, S., Pedrow, P., Pitts, M., and Powers, J. (2010). Cold atmospheric-pressure plasmas applied to active packaging of apples. *IEEE Transactions on Plasma Science*, 38(4):957–965. [37](#)
- Ferrando, M. and Spiess, W. (2003). Mass transfer in strawberry tissue during osmotic treatment II: Structure-function relationships. *Journal of Food Science*, 68:1356–1364. [50](#)
- Fitzgerald, D., Stratford, M., Gasson, M., Ueckert, J., Bos, A., and Narbad, A. (2004). Mode of antimicrobial action of vanillin against *Escherichia coli*, *Lactobacillus plantarum* and *Listeria innocua*. *Journal of Applied Microbiology*, 97:104–113. [37](#)
- Forina, M., Oliveri, P., Lanteri, S., and Casale, M. (2008). Class-modeling techniques, classic and new, for old and new problems. *Chemometrics and Intelligent Laboratory Systems*, 93:132–148. [103](#)



- Fuhrmann, H., Rupp, N., Behner, A., and Braun, P. (2010). The effect of gaseous ozone treatment on egg components. *Journal of the Science of Food and Agriculture*, 90:593–598. [34](#)
- GARA (2014). Glomerular activity response archive. [117](#)
- Garau, V. L., Angioni, A., Del Real, A. A., Russo, M., and Cabras, P. (2002). Disappearance of azoxystrobin, pyrimethanil, cyprodinil, and fludioxonil on tomatoes in a greenhouse. *Journal of Agricultural and Food Chemistry*, 50:1929–1932. [41](#)
- Gaydon, A. and Pearse, R. (1976). *The identification of molecular spectra*. The identification of Molecular Spectra. Chapman and Hall, London. [25](#), [71](#)
- Giampieri, F., Tulipani, S., Alvarez-Suarez, J. M., Quiles, J. L., Mezzetti, B., and Battino, M. (2012). The strawberry: Composition, nutritional quality, and impact on human health. *Nutrition*, 28:9–19. [104](#)
- Gomez-Lopez, V. M., Ragaert, P., Debevere, J., and Devlieghere, F. (2007). Pulsed light for food decontamination: a review. *Trends in Food Science & Technology*, 18:464–473. [2](#)
- Gordillo-Vazquez, F. J. (2008). Air plasma kinetics under the influence of sprites. *Journal of Physics D: Applied Physics*, 41(23):234016. [22](#), [23](#)
- Gössinger, M., Moritz, S., Hermes, M., Wendelin, S., Scherbichler, H., Halbwirth, H., Stich, K., and Berghofer, E. (2009). Effects of processing parameters on colour stability of strawberry nectar from puree. *Journal of Food Engineering*, 90:171–178. [49](#)
- Gottscho, R. A. and Miller, T. A. (1984). Optical techniques in plasma diagnostics. *Pure and Applied Chemistry*, 56:189–208. [24](#), [25](#)
- Gould, G. W. (2001). New processing technologies: an overview. *Proceedings of the Nutrition Society*, 60(04):463–474. [1](#)

- Grabowski, L. R., Veldhuizen, E. M. v., Pemen, A. J. M., and Rutgers, W. R. (2007). Breakdown of methylene blue and methyl orange by pulsed corona discharge. *Plasma Sources Science and Technology*, 16:226–232. [74](#), [76](#)
- Grzegorzewski, F. (2010). *Influence of Non-Thermal Plasma Species on the Structure and Functionality of Isolated and Plant-based 1, 4-Benzopyrone Derivatives and Phenolic Acids*. Phd thesis, Technische Universität, Berlin. [39](#)
- Grzegorzewski, F., Rohn, S., Kroh, L. W., Geyer, M., and Schlüter, O. (2010). Surface morphology and chemical composition of lamb's lettuce (*Valerianella locusta*) after exposure to a low-pressure oxygen plasma. *Food Chemistry*, 122(4):1145–1152. [39](#)
- Gülec, H. A., Sarioğlu, K., and Mutlu, M. (2006). Modification of food contacting surfaces by plasma polymerisation technique. Part I: Determination of hydrophilicity, hydrophobicity and surface free energy by contact angle method. *Journal of Food Engineering*, 75:187–195. [26](#)
- Gurol, C., Ekinçi, F. Y., Aslan, N., and Korachi, M. (2012). Low temperature plasma for decontamination of *E. coli* in milk. *International Journal of Food Microbiology*, 167. [38](#)
- Hannum, S. M. (2004). Potential impact of strawberries on human health: A review of the science. *Critical Reviews in Food Science and Nutrition*, 44:1–17. [113](#)
- Havelaar, A. H., Brul, S., de Jong, A., de Jonge, R., Zwietering, M. H., and Ter Kuile, B. H. (2010). Future challenges to microbial food safety. *International Journal of Food Microbiology*, 139 Suppl 1:S79–94. [1](#)
- Hayashi, N., Akiyoshi, Y., Kobayashi, Y., Kanda, K., Ohshima, K., and Goto, M. (2013). Inactivation characteristics of *Bacillus thuringiensis* spore in liquid using atmospheric torch plasma using oxygen. *Vacuum*, 88:173–176. [101](#)
- Hemeda, H. and Klein, B. (1990). Effects of naturally occurring antioxidants on peroxidase activity of vegetable extracts. *Journal of Food Science*, 55:184–185. [54](#)

- Heredia, A., Barrera, C., and Andrés, A. (2007). Drying of cherry tomato by a combination of different dehydration techniques. Comparison of kinetics and other related properties. *Journal of Food Engineering*, 80:111–118. [53](#)
- Herman, I. P. (2003). Optical diagnostics for thin film processing. *Annual Review of Physical Chemistry*, 54:277–305. [24](#)
- Hernández-Muñoz, P., Almenar, E., Ocio, M. J., and Gavara, R. (2006). Effect of calcium dips and chitosan coatings on postharvest life of strawberries (*Fragaria × ananassa*). *Postharvest Biology & Technology*, 39:247–253. [94](#)
- Herron, J. and Green, D. (2001). Chemical kinetics database and predictive schemes for nonthermal humid air plasma chemistry. Part II. Neutral species reactions. *Plasma Chemistry and Plasma Processing*, 21:459–481. [23](#), [46](#)
- Hershkowitz, N. and Breun, R. A. (1997). Diagnostics for plasma processing (etching plasmas) (invited). *Review of Scientific Instruments*, 68:880. [24](#)
- Hierro, E., Manzano, S., Ordóñez, J. A., de la Hoz, L., and Fernández, M. (2009). Inactivation of *Salmonella enterica* serovar Enteritidis on shell eggs by pulsed light technology. *International Journal of Food Microbiology*, 135(2):125–130. [34](#)
- Hong, Y. F., Kang, J. G., Lee, H. Y., Uhm, H. S., Moon, E., and Park, Y. H. (2009). Sterilization effect of atmospheric plasma on *Escherichia coli* and *Bacillus subtilis* endospores. *Letters in Applied Microbiology*, 48:33–7. [28](#)
- Huang, F., Chen, L., Wang, H., and Yan, Z. (2010). Analysis of the degradation mechanism of methylene blue by atmospheric pressure dielectric barrier discharge plasma. *Chemical Engineering Journal*, 162:250–256. [73](#), [76](#)
- Hury, S., Vidal, D. R., Desor, F., Pelletier, J., and Lagarde, T. (1998). A parametric study of the destruction efficiency of *Bacillus* spores in low pressure oxygen-based plasmas. *Letters in Applied Microbiology*, 26:417–21. [21](#)
- Hwang, E.-S., Cash, J. N., and Zabik, M. J. (2001). Postharvest treatments for the reduction of mancozeb in fresh apples. *Journal of Agricultural and Food Chemistry*, 49:3127–3132. [127](#)

- Iizuka, T., Maeda, S., and Shimizu, A. (2013). Removal of pesticide residue in cherry tomato by hydrostatic pressure. *Journal of Food Engineering*, 116:796–800. [41](#)
- Innawong, B., Mallikarjunan, P., Irudayaraj, J., and Marcy, J. E. (2004). The determination of frying oil quality using Fourier transform infrared attenuated total reflectance. *LWT - Food Science and Technology*, 37:23 – 28. [108](#)
- Javanmardi, J. and Kubota, C. (2006). Variation of lycopene, antioxidant activity, total soluble solids and weight loss of tomato during postharvest storage. *Postharvest Biology and Technology*, 41:151–155. [81](#)
- Jewison, T., Knox, C., Neveu, V., Djoumbou, Y., Guo, A. C., Lee, J., Liu, P., Mandal, R., Krishnamurthy, R., Sinelnikov, I., and et al. (2012). YMDB: the yeast metabolome database. *Nucleic Acids Research*, 40:D815–D820. [117](#)
- Jiménez, M., Mateo, R., Querol, A., Huerta, T., and Hernández, E. (1991). Mycotoxins and mycotoxigenic moulds in nuts and sunflower seeds for human consumption. *Mycopathologia*, 115:121–127. [32](#)
- José, J. F. B. S. o. and Vanetti, M. C. D. (2012). Effect of ultrasound and commercial sanitizers in removing natural contaminants and *Salmonella enterica* Typhimurium on cherry tomatoes. *Food Control*, 24:95–99. [32](#)
- Kader, A. and Saltveit, M. (2003). Respiration and gas exchange. In Bartz, J. and Brecht, J., editors, *Postharvest physiology and pathology of vegetables*, pages 229–246. Marcel Dekker, Inc. [9](#)
- Kader, A. A. and Ben-Yehoshua, S. (2000). Effects of superatmospheric oxygen levels on postharvest physiology and quality of fresh fruits and vegetables. *Postharvest Biology and Technology*, 20:1–13. [92](#)
- Karaca, H., Walse, S. S., and Smilanick, J. L. (2012). Effect of continuous 0.3 $\mu$ L/L gaseous ozone exposure on fungicide residues on table grape berries. *Postharvest Biology and Technology*, 64:154–159. [128](#), [130](#)
- Kennedy, M. (2012). E coli outbreak: Who says bacterium is a new strain, guardian, uk. [1](#)

- Khadre, M. A., Yousef, A. E., and Kim, J. G. (2001). Microbiological aspects of ozone applications in food: A review. *Journal of food science*, 66:1242–1252. [32](#)
- Kim, B., Yun, H., Jung, S., Jung, Y., Jung, H., Choe, W., and Jo, C. (2011). Effect of atmospheric pressure plasma on inactivation of pathogens inoculated onto bacon using two different gas compositions. *Food Microbiology*, 28:9–13. [17](#), [35](#), [36](#), [40](#)
- Kim, S. H., Kim, J. H., and Kang, B.-K. (2007). Decomposition reaction of organophosphorus nerve agents on solid surfaces with atmospheric radio frequency plasma generated gaseous species. *Langmuir*, 23:8074–8078. [42](#)
- Kim, S. W., Min, S. R., Kim, J., Park, S. K., Kim, T. I., and Liu, J. R. (2009). Rapid discrimination of commercial strawberry cultivars using Fourier transform infrared spectroscopy data combined by multivariate analysis. *Plant Biotechnol Rep*, 3:87–93. [103](#)
- Klockow, P. A. and Keener, K. M. (2009). Safety and quality assessment of packaged spinach treated with a novel ozone-generation system. *LWT - Food Science and Technology*, 42:1047–1053. [5](#), [19](#)
- Kogelschatz, U. (2002). Filamentary, patterned, and diffuse barrier discharges. *IEEE Transactions on Plasma Science*, 30:1400–1408. [19](#)
- Kogelschatz, U. (2003). Dielectric-barrier discharges: Their history, discharge physics, and industrial applications. *Plasma Chemistry & Plasma Processing*, 23(1):1–46. [23](#), [70](#)
- Kogelschatz, U., Eliasson, B., and Egli, W. (1997). Dielectric-barrier discharges-Principle & Applications. *Journal de physique. IV*, 7:47–66. [70](#)
- Konuma, M. (1992). Plasma diagnostics. In Konuma, M., editor, *Film Deposition by Plasma Techniques*, volume 10 of *Springer Series on Atoms+Plasmas*, chapter 4, pages 74–106. Springer Berlin Heidelberg. [24](#)
- Korachi, M., Gurol, C., and Aslan, N. (2010). Atmospheric plasma discharge sterilization effects on whole cell fatty acid profiles of *Escherichia coli* and *Staphylococcus aureus*. *Journal of Electrostatics*, 68:508–512. [27](#)

- Kossyi, I. A., Kostinsky, A. Y., Matveyev, A. A., and Silakov, V. P. (1992). Kinetic scheme of the non-equilibrium discharge in nitrogen-oxygen mixtures. *Plasma Sources Science and Technology*, 1:207. [128](#)
- Kruk, Z. A., Yun, H., Rutley, D. L., Lee, E. J., Kim, Y. J., and Jo, C. (2011). The effect of high pressure on microbial population, meat quality and sensory characteristics of chicken breast fillet. *Food Control*, 22:6–12. [2](#)
- Kudra, T. and Mujumdar, A. (2009). *Advanced drying technologies*. CRC Press. [13](#)
- Kumar, A., Ghuman, B., and Gupta, A. (1999). Non-refrigerated storage of tomatoes: Effect of HDPE film wrapping. *Journal of food science & technology*, 36:438–440. [82](#)
- Kute, K., Zhou, C., and Barth, M. (1995). The effect of ozone exposure on total ascorbic acid activity and soluble solids contents in strawberry tissue. In *Proceedings of the IFT Annual Meeting*, page 82. IFT Press. [106](#)
- Laroussi, M. (2005). Low temperature plasma-based sterilization: Overview and state-of-the-art. *Plasma Processes and Polymers*, 2(5):391–400. [21](#)
- Laroussi, M. (2009). Low-temperature plasmas for medicine? *IEEE Transactions on Plasma Science*, 37(6):714–725. [74](#)
- Laties, G. (1978). The development and control of respiratory pathways in slices of plant storage organs. In Günter, K., editor, *Biochemistry of wounded plant tissues*, pages 421–466. Walter de Gruyter. [90](#)
- Laux, C., Spence, T., Kruger, C., and Zare, R. (2003). Optical diagnostics of atmospheric pressure air plasmas. *Plasma Sources Science & Technology*, 12:125. [25](#)
- Lê, S., Josse, J., and Husson, F. (2008). Factominer: An r package for multivariate analysis. *Journal of Statistical Software*, 25. [59](#)
- Lee, H., Chang, M., and Wei, T. (2004). Kinetic modeling of ozone generation via dielectric barrier discharges. *Ozone: Science & Engineering*, 26(6):551–562. [23](#)

- Lee, H. J., Jung, H., Choe, W., Ham, J. S., Lee, J. H., and Jo, C. (2011). Inactivation of *Listeria monocytogenes* on agar and processed meat surfaces by atmospheric pressure plasma jets. *Food Microbiology*, 28:1468–1471. [36](#)
- Lee, K., Paek, K., Ju, W., and Lee, Y. (2006). Sterilization of bacteria, yeast, and bacterial endospores by atmospheric-pressure cold plasma using helium and oxygen. *Journal of Microbiology*, 44(3):269–275. [2](#)
- Li, H.-P., Wang, L.-Y., Li, G., Jin, L.-H., Le, P.-S., Zhao, H.-X., Xing, X.-H., and Bao, C.-Y. (2011). Manipulation of lipase activity by the helium radio-frequency, atmospheric-pressure glow discharge plasma jet. *Plasma Processes & Polymers*, 8(3):224–229. [100](#), [121](#)
- Li Yoon, W., D. Jee, R., C. Moffat, A., D. Blackler, P., Yeung, K., and C. Lee, D. (1999). Construction and transferability of a spectral library for the identification of common solvents by near-infrared transreflectance spectroscopy. *The Analyst*, 124:1197. [59](#), [107](#)
- Likas, D., Tsiropoulos, N., and Miliadis, G. (2007). Rapid gas chromatographic method for the determination of famoxadone, trifloxystrobin and fenhexamid residues in tomato, grape and wine samples. *Journal of Chromatography A*, 1150(1-2):208 – 214. [63](#)
- Liu, F. X., Sun, P., Bai, N., Tian, Y., Zhou, H. X., Wei, S. C., Zhou, Y. H., Zhang, J., Zhu, W. D., Becker, K., and Fang, J. (2010). Inactivation of bacteria in an aqueous environment by a direct-current, cold-atmospheric-pressure air plasma microjet. *Plasma Processes & Polymers*, 7(3-4):231–236. [27](#)
- Liu, Y.-X., Jiang, W., Li, X.-S., Lu, W.-Q., and Wang, Y.-N. (2012). An overview of diagnostic methods of low-pressure capacitively coupled plasmas. *Thin Solid Films*, 521:141–145. [24](#), [25](#)
- Mahajan, P. and Goswami, T. (2001). Postharvest technology: Enzyme kinetics based modelling of respiration rate for apple. *Journal of Agricultural Engineering Research*, 79(4):399–406. [79](#)

- Maleki, M., Mouazen, A., Ramon, H., and De Baerdemaeker, J. (2007). Multiplicative scatter correction during on-line measurement with near infrared spectroscopy. *Biosystems Engineering*, 96:427–433. [104](#)
- Manley, T. (1943). The electric characteristics of the ozonator discharge. *Transactions of the Electrochemical Society*, 84(1):83–96. [24](#), [45](#), [69](#)
- Meiners, A. (2010). Optical emission spectroscopy for plasma diagnostics- Application note. *Andor Technologies*. [25](#), [46](#)
- Min, S. and Zhang, Q. (2005). Packaging for non-thermal food processing. In Han, J., editor, *Innovations in food packaging*, pages 482–500. Elsevier Academic Press. [12](#)
- Misra, N., Patil, S., Moiseev, T., Bourke, P., Mosnier, J., Keener, K., and Cullen, P. (2014). In-package atmospheric pressure cold plasma treatment of strawberries. *Journal of Food Engineering*, 125:131–138. [84](#), [108](#), [116](#)
- Mittendorfer, J., Bierbaumer, H., Gratzl, F., and Kellauer, E. (2002). Decontamination of food packaging using electron beamstatus and prospects. *Radiation Physics & Chemistry*, 63(3):833–836. [36](#)
- Moisan, M., Barbeau, J., Moreau, S., Pelletier, J., Tabrizian, M., and Yahia, L. H. (2001). Low-temperature sterilization using gas plasmas: a review of the experiments and an analysis of the inactivation mechanisms. *International journal of Pharmaceutics*, 226(1-2):1–21. [21](#)
- Montenegro, J., Ruan, R., Ma, H., and Chen, P. (2002). Inactivation of *E. coli* O157:H7 using a pulsed nonthermal plasma system. *Journal of Food Science*, 67:646–648. [37](#)
- Moon, S. Y., Kim, D. B., Gweon, B., Choe, W., Song, H. P., and Jo, C. (2009). Feasibility study of the sterilization of pork and human skin surfaces by atmospheric pressure plasmas. *Thin Solid Films*, 517(14):4272–4275. [35](#), [40](#)
- Muranyi, P., Wunderlich, J., and Heise, M. (2007). Sterilization efficiency of a cascaded dielectric barrier discharge. *Journal of Applied Microbiology*, 103(5):1535–44. [30](#)



- Murphy, R., Osaili, T., Duncan, L., and Marcy, J. (2004). Thermal inactivation of *Salmonella* and *Listeria monocytogenes* in ground chicken thigh/leg meat and skin. *Poultry science*, 83(7):1218–1225. [36](#)
- Newell, D. and Fearnley, C. (2003). Sources of *Campylobacter* colonization in broiler chickens. *Applied & Environmental Microbiology*, 69(8):4343–4351. [34](#)
- Nguyen-the, C. and Carlin, F. (1994). The microbiology of minimally processed fresh fruits and vegetables. *Critical Reviews in Food Science and Nutrition*, 34(4):371–401. [32](#)
- Nielsen, T. and Leufven, A. (2008). The effect of modified atmosphere packaging on the quality of honeoye and korona strawberries. *Food Chemistry*, 107(3):1053–1063. [11](#)
- Niemira, B. and Sites, J. (2008). Cold plasma inactivates *Salmonella stanley* and *Escherichia coli* O157:H7 inoculated on golden delicious apples. *Journal of Food Protection*, 71(7):1357–1365. [2](#), [5](#), [22](#), [29](#), [32](#), [38](#)
- Niemira, B. A. (2012). Cold plasma reduction of *Salmonella* and *Escherichia coli* O157:H7 on almonds using ambient pressure gases. *Journal of Food Science*, 77:M171–M175. [20](#), [34](#)
- NIST (2012). National institute of standards and technology: Atomic spectra database. [46](#)
- Noriega, E., Shama, G., Laca, A., Daz, M., and Kong, M. (2011). Cold atmospheric gas plasma disinfection of chicken meat and chicken skin contaminated with *Listeria innocua*. *Food Microbiology*. [26](#), [36](#)
- Nunes, M. C. N., Brecht, J. K., Morais, A. M., and Sargent, S. A. (2005). Physicochemical changes during strawberry development in the field compared with those that occur in harvested fruit during storage. *J. Sci. Food Agric.*, 86:180–190. [53](#)
- Oehmigen, K., Hähnel, M., Brandenburg, R., Wilke, C., Weltmann, K.-D., and von Woedtke, T. (2010). The role of acidification for antimicrobial activity of

- atmospheric pressure plasma in liquids. *Plasma Processes & Polymers*, 7(3-4):250–257. [76](#)
- Ong, K., Cash, J., Zabik, M., Siddiq, M., and Jones, A. (1996). Chlorine and ozone washes for pesticide removal from apples and processed apple sauce. *Food Chemistry*, 55:153 – 160. [127](#)
- Ophuis, P. A. O. and Trijp, H. C. V. (1995). Perceived quality: A market driven and consumer oriented approach. *Food Quality & Preference*, 6(3):177 – 183. [8](#)
- Ozdemir, M., Yurteri, C. U., and Sadikoglu, H. (1999). Surface treatment of food packaging polymers by plasmas. *Food Technology*, 53:54–58. [26](#)
- Palgan, I., Caminiti, I. M., Muoz, A., Noci, F., Whyte, P., Morgan, D. J., Cronin, D. A., and Lyng, J. G. (2011). Effectiveness of high intensity light pulses (hilp) treatments for the control of *Escherichia coli* and *Listeria innocua* in apple juice, orange juice and milk. *Food Microbiology*, 28(1):14–20. [37](#)
- Pankaj, S., Misra, N., and Cullen, P. (2013). Kinetics of tomato peroxidase inactivation by atmospheric pressure cold plasma based on dielectric barrier discharge. *Innovative Food Science & Emerging Technologies*, 19:153–157. [121](#)
- Pelayo, C., Ebeler, S., and Kader, A. (2003). Postharvest life and flavor quality of three strawberry cultivars kept at 5 °C in air or air + 20 kPa CO<sub>2</sub>. *Postharvest Biology and Technology*, 27(2):171–183. [11](#)
- Perez, A. G., Sanz, C., and Olias, J. M. (1993). Partial purification and some properties of alcohol acyltransferase from strawberry fruits. *Journal of Agricultural and Food Chemistry*, 41:1462–1466. [120](#)
- Pérez, A. G., Sanz, C., Ríos, J. J., Olas, R., and Olías, J. M. (1999). Effects of ozone treatment on postharvest strawberry quality. *Journal of Agricultural and Food Chemistry*, 47:1652–1656. [114](#), [116](#)
- Perni, S., Shama, G., and Kong, M. G. (2008a). Cold atmospheric plasma disinfection of cut fruit surfaces contaminated with migrating microorganisms. *Journal of Food Protection*, 71(8):1619–1625. [28](#)

- Perni, S., Shama, G., and Kong, M. G. (2008b). Cold atmospheric plasma disinfection of cut fruit surfaces contaminated with migrating microorganisms. *Journal of Food Protection*, 71:1619–1625. [29](#)
- Petasch, W., Ruchle, E., Muegge, H., and Muegge, K. (1997). Duo-plasmaline- a linearly extended homogeneous low pressure plasma source. *Surface & Coatings Technology*, 93(1):112–118. [18](#)
- Pokorný, P., Novotný, M., Musil, J., Fitl, P., Bulíř, J., and Lančok, J. (2013). Mass spectrometric characterizations of ions generated in RF magnetron discharges during sputtering of silver in Ne, Ar, Kr and Xe gases. *Plasma Processes & Polymers*, 10:593–602. [25](#)
- Ragni, L., Berardinelli, A., Vannini, L., Montanari, C., Sirri, F., Guerzoni, M. E., and Guarnieri, A. (2010). Non-thermal atmospheric gas plasma device for surface decontamination of shell eggs. *Journal of Food Engineering*, 100:125–132. [24](#), [34](#), [40](#)
- Raso, J. and Barbosa-Cánovas, G. V. (2003). Nonthermal preservation of foods using combined processing techniques. *Critical Reviews in Food Science and Nutrition*, 43(3):265–285. [13](#)
- Rastogi, N., Raghavarao, K., Balasubramaniam, V., Niranjana, K., and Knorr, D. (2007). Opportunities and challenges in high pressure processing of foods. *Critical Reviews in Food Science and Nutrition*, 47(1):69–112. [2](#)
- Reynolds, G., Graham, N., Perry, R., and Rice, R. (1989). Aqueous ozonation of pesticides: A review. *Ozone: Science & Engineering*, 11:339–382. [127](#)
- Rico, D., Martín-Diana, A., Barat, J., and Barry-Ryan, C. (2007). Extending and measuring the quality of fresh-cut fruit and vegetables: a review. *Trends in Food Science & Technology*, 18(7):373 – 386. [10](#), [32](#), [90](#)
- Rinnan, A., Berg, F. v. d., and Engelsen, S. B. (2009). Review of the most common pre-processing techniques for near-infrared spectra. *TrAC Trends in Analytical Chemistry*, 28:1201–1222. [57](#)

- Roberts, T. R. and Hutson, D. H. (1999). *Fludioxonil*, In: *Metabolic pathways of agrochemicals: insecticides and fungicides*. Royal Society of Chemistry. 130, 131
- Robertson, G. L. (2012). *Food Packaging: Principles and Practice*. CRC Press, third edition. 9, 82
- Rød, S. K., Hansen, F., Leipold, F., and Knchel, S. (2012). Cold atmospheric pressure plasma treatment of ready-to-eat meat: Inactivation of *Listeria innocua* and changes in product quality. *Food Microbiology*, 30(1):233–238. 35, 40
- Rodrigues, E. T., Lopes, I., and Ângelo Pardal, M. (2013). Occurrence, fate and effects of azoxystrobin in aquatic ecosystems: A review. *Environment International*, 53:18 – 28. 129
- Rodriguez-Lafuente, A., Nerin, C., and Batlle, R. (2010). Active paraffin-based paper packaging for extending the shelf life of cherry tomatoes. *Journal of Agricultural and Food Chemistry*, 58:6780–6786. 85
- Rodriguez-Romoand, L. and Yousef, A. (2005). Inactivation of *Salmonella enterica* serovar Enteritidis on shell eggs by ozone and uv radiation. *Journal of Food Protection*, 68(4):711–717. 34
- Rohman, A. and Man, Y. C. (2010). Fourier transform infrared (FTIR) spectroscopy for analysis of extra virgin olive oil adulterated with palm oil. *Food Research International*, 43:886–892. 104
- Roth, S., Feichtinger, J., and Hertel, C. (2010). Characterization of *Bacillus subtilis* spore inactivation in low-pressure, low-temperature gas plasma sterilization processes. *Journal of Applied Microbiology*, 108(2):521–31. 27
- Rowan, N., Espie, S., Harrower, J., Anderson, J., Marsili, L., and MacGregor, S. (2007). Pulsed-plasma gas-discharge inactivation of microbial pathogens in chilled poultry wash water. *Journal of Food Protection*, 70(12):2805–2810. 30
- Sampedro, F., Rodrigo, M., Martinez, A., Rodrigo, D., and Barbosa-Cánovas, G. (2005). Quality and safety aspects of pef application in milk and milk products. *Critical Reviews in Food Science and Nutrition*, 45(1):25–47. 2, 38

- Schneider, J., Baumgärtner, K. M., Feichtinger, J., Krüger, J., Muranyi, P., Schulz, A., Walker, M., Wunderlich, J., and Schumacher, U. (2005). Investigation of the practicability of low-pressure microwave plasmas in the sterilisation of food packaging materials at industrial level. *Surface and Coatings Technology*, 200(1-4):962–966. [37](#)
- Schram, D. C. (2002). Plasma processing and chemistry. *Pure and applied chemistry*, 74:369–380. [22](#)
- Schulz, A., Feichtinger, J., Krüger, J., Walker, M., and Schumacher, U. (2003). Spectroscopic investigations on silicon nitride deposition with the Plasmodul. *Surface and Coatings Technology*, 174-175:947–951. [18](#)
- Selcuk, M., Oksuz, L., and Basaran, P. (2008). Decontamination of grains and legumes infected with *Aspergillus* spp. and *Penicillium* spp. by cold plasma treatment. *Bioresource Technology*, 99(11):5104–5109. [2](#), [33](#)
- SenseLab (2014). SenseLab- Odor Molecules Database. [117](#)
- Shankar, M., Nélieu, S., Kerhoas, L., and Einhorn, J. (2007). Photo-induced degradation of diuron in aqueous solution by nitrites and nitrates: Kinetics and pathways. *Chemosphere*, 66:767 – 774. [128](#)
- Shi, X.-M., Zhang, G.-J., Wu, X.-L., Li, Y.-X., Ma, Y., and Shao, X.-J. (2011). Effect of low-temperature plasma on microorganism inactivation and quality of freshly squeezed orange juice. *IEEE Transactions on Plasma Science*, 39(7):1591–1597. [37](#)
- Sieck, L., Heron, J., and Green, D. (2000). Chemical kinetics database and predictive schemes for humid air plasma chemistry. Part I: Positive ion-molecule reactions. *Plasma Chemistry and Plasma Processing*, 20(2):235–258. [23](#)
- Singh, N., Singh, S. B., Mukerjee, I., Gupta, S., Gajbhiye, V. T., Sharma, P. K., Goel, M., and Dureja, P. (2010). Metabolism of 14c-azoxystrobin in water at different ph. *Journal of Environmental Science and Health, Part B*, 45:123–127. [129](#)

- Snelling, W., McKenna, J., Lecky, D., and Dooley, J. (2005). Survival of *Campylobacter jejuni* in waterborne protozoa. *Applied & Environmental Microbiology*, 71(9):5560–5571. [34](#)
- Sobrino-López, A. and Martín-Belloso, O. (2010). Review: potential of high-intensity pulsed electric field technology for milk processing. *Food Engineering Reviews*, 2(1):17–27. [38](#)
- Song, H. P., Kim, B., Choe, J. H., Jung, S., Moon, S. Y., Choe, W., and Jo, C. (2009). Evaluation of atmospheric pressure plasma to improve the safety of sliced cheese and ham inoculated by 3-strain cocktail *Listeria monocytogenes*. *Food Microbiology*, 26(4):432–436. [38](#)
- Stertz, S. C., Espírito Santo, A. P. d., Bona, C., and Freitas, R. J. a. S. d. (2005). Comparative morphological analysis of cherry tomato fruits from three cropping systems. *Scientia Agricola*, 62:296–298. [50](#), [78](#)
- Stillahn, J. M., Trevino, K. J., and Fisher, E. R. (2008). Plasma diagnostics for unraveling process chemistry. *Annual Reviews in Analytical Chemistry*, 1:261–91. [25](#)
- Sung, W. S., Jung, H. J., Park, K., Kim, H. S., Lee, I.-S., and Lee, D. G. (2007). 2,5-dimethyl-4-hydroxy-3(2h)-furanone (DMHF): antimicrobial compound with cell cycle arrest in nosocomial pathogens. *Life Sciences*, 80:586–591. [120](#)
- Surowsky, B., Fischer, A., Schlueter, O., and Knorr, D. (2013). Cold plasma effects on enzyme activity in a model food system. *Innovative Food Science & Emerging Technologies*, 19:146–152. [101](#), [121](#)
- Suutarinen, J., Änäkäinen, L., and Autio, K. (1998). Comparison of light microscopy and spatially resolved fourier transform infrared (FT-IR) microscopy in the examination of cell wall components of strawberries. *LWT - Food Science and Technology*, 31:595 – 601. [104](#)
- Sykes, G. (1965). *Disinfection and sterilisation*. E. & F.N. Spon., Ltd., London, 2nd edition. [32](#)

- Takai, E., Kitano, K., Kuwabara, J., and Shiraki, K. (2012). Protein inactivation by low-temperature atmospheric pressure plasma in aqueous solution. *Plasma Processes and Polymers*, 9(1):77–82. [100](#)
- Tappi, S., Berardinelli, A., Ragni, L., Dalla Rosa, M., Guarnieri, A., and Rocculi, P. (2014). Atmospheric gas plasma treatment of fresh-cut apples. *Innovative Food Science & Emerging Technologies*, 21:114–122. [80](#), [85](#)
- Terefe, N. S., Yang, Y. H., Knoerzer, K., Buckow, R., and Versteeg, C. (2010). High pressure and thermal inactivation kinetics of polyphenol oxidase and peroxidase in strawberry puree. *Innovative Food Science & Emerging Technologies*, 11:52–60. [54](#)
- Terrier, O., Essere, B., Yver, M., Barthelemy, M., Bouscambert-Duchamp, M., Kurtz, P., VanMechelen, D., Morfin, F., Billaud, G., Ferraris, O., Lina, B., Rosa-Calatrava, M., and Moules, V. (2009). Cold oxygen plasma technology efficiency against different airborne respiratory viruses. *Journal of Clinical Virology*, 45(2):119–24. [20](#), [28](#)
- Tiwari, B., O'Donnell, C., Patras, A., Brunton, N., and Cullen, P. (2009a). Effect of ozone processing on anthocyanins and ascorbic acid degradation of strawberry juice. *Food Chemistry*, 113:1119–1126. [114](#), [116](#)
- Tiwari, B. K., O'Donnell, C. P., and Cullen, P. J. (2009b). Effect of non thermal processing technologies on the anthocyanin content of fruit juices. *Trends in Food Science & Technology*, 20(3-4):137–145. [2](#)
- Tzortzakis, N. G. (2007). Maintaining postharvest quality of fresh produce with volatile compounds. *Innovative Food Science & Emerging Technologies*, 8(1):111–116. [10](#), [85](#)
- Uckoo, R. M., Jayaprakasha, G. K., Somerville, J. A., Balasubramaniam, V., Pinarte, M., and Patil, B. S. (2013). High pressure processing controls microbial growth and minimally alters the levels of health promoting compounds in grapefruit (*Citrus paradisi* macfad) juice. *Innovative Food Science & Emerging Technologies*, 18:7–14. [59](#)

- Vandendriessche, T., Nicolai, B. M., and Hertog, M. L. A. T. M. (2013a). Optimization of hs spme fast gc-MS for high-throughput analysis of strawberry aroma. *Food Analytical Methods*, 6:512–520. [61](#)
- Vandendriessche, T., Vermeir, S., Mayayo Martinez, C., Hendrickx, Y., Lammer-tyn, J., Nicolaï, B., and Hertog, M. (2013b). Effect of ripening and inter-cultivar differences on strawberry quality. *LWT - Food Science and Technology*, 52(2):62–70. [11](#)
- Venta, M. B., Broche, S. S. C., Torres, I. F., Pérez, M. G., Lorenzo, E. V., Ro-driguez, Y. R., and Cepero, S. M. (2010). Ozone application for postharvest disinfection of tomatoes. *Ozone: Science & Engineering*, 32:361–371. [81](#), [82](#)
- Vleugels, M., Shama, G., Deng, X., Greenacre, E., Brocklehurst, T., and Kong, M. (2005). Atmospheric plasma inactivation of biofilm-forming bacteria for food safety control. *Plasma Science, IEEE Transactions on*, 33:824–828. [2](#), [39](#)
- Von Keudell, A., Awakowicz, P., Benedikt, J., Raballand, V., Yanguas Gil, A., Opretzka, J., Flötgen, C., Reuter, R., Byelykh, L., and Halfmann, H. (2010). Inactivation of bacteria and biomolecules by low pressure plasma discharges. *Plasma Processes and Polymers*, 7:327–352. [27](#)
- Walse, S. S. and Karaca, H. (2011). Remediation of fungicide residues on fresh produce by use of gaseous ozone. *Environmental Science & Technology*, 45:6961–6969. [127](#), [129](#)
- Walsh, J. L., Liu, D. X., Iza, F., Rong, M. Z., and Kong, M. G. (2010). Contrast-ing characteristics of sub-microsecond pulsed atmospheric air and atmospheric pressure helium-oxygen glow discharges. *Journal of Physics D: Applied Physics*, 43:032001. [72](#)
- Wszelaki, A. and Mitcham, E. (2000). Effects of superatmospheric oxygen on strawberry fruit quality and decay. *Postharvest Biology and Technology*, 20:125–133. [92](#), [94](#)
- Yamaguchi, Y. (2006). Environmental and food hygiene approach to pesticide. *Journal of Urban Living Health Association*, 50:283–290. [41](#)



- Yoon, Y. and Ryu, K. (2007). Atmospheric plasma surface treatment equipment. *News Information Chemical Engineering*, 25:268–271. [17](#)
- Yu, H., Perni, S., Shi, J. J., Wang, D. Z., Kong, M. G., and Shama, G. (2006). Effects of cell surface loading and phase of growth in cold atmospheric gas plasma inactivation of *Escherichia coli* K12. *Journal of applied microbiology*, 101:1323–30. [26](#), [31](#)
- Yun, H., Kim, B., Jung, S., Kruk, Z., Kim, D., Choe, W., and Jo, C. (2010). Inactivation of *Listeria monocytogenes* inoculated on disposable plastictray, aluminum foil, and paper cup by atmospheric pressure plasma. *Food Control*, 21:1182–1186. [17](#)
- Zabetakis, I. and Holden, M. A. (1997). Strawberry flavour: Analysis and biosynthesis. *Journal of the Science of Food and Agriculture*, 74:421–434. [120](#)
- Zhang, C., Shao, T., Yu, Y., Niu, Z., Yan, P., and Zhou, Y. (2010). Comparison of experiment and simulation on dielectric barrier discharge driven by 50hz ac power in atmospheric air. *Journal of Electrostatics*, 68(5):445–452. [24](#), [45](#), [68](#)
- Zhang, X., Zhang, Z., Wang, L., Zhang, Z., Li, J., and Zhao, C. (2011). Impact of ozone on quality of strawberry during cold storage. *Frontiers of Agriculture in China*, 5(3):356–360. [11](#), [94](#)
- Zhu, X., Li, S., Shan, Y., Zhang, Z., Li, G., Su, D., and Liu, F. (2010). Detection of adulterants such as sweeteners materials in honey using near-infrared spectroscopy and chemometrics. *Journal of Food Engineering*, 101:92–97. [103](#)
- Ziuzina, D., Patil, S., Cullen, P., Keener, K., and Bourke, P. (2014). Atmospheric cold plasma inactivation of escherichia coli, salmonella enterica serovar typhimurium and listeria monocytogenes inoculated on fresh produce. *Food Microbiology*, 42:109–116. [82](#)